CHALMERS
UNIVERSITY OF TECHNOLOGY



Complex Adaptive Systems as Theoretical Lenses on Digital Behavior

An Exploratory Evaluation of Eight Model Families Across Heterogeneous Digital Trace Data

Master's Thesis in Physics

Svea Victoria Strassburger

DEPARTMENT OF PHYSICS AND ASTRONOMY
CHALMERS UNIVERSITY OF TECHNOLOGY
Gothenburg, Sweden 2026
www.chalmers.se

Master's thesis 2026

Complex Adaptive Systems as Theoretical Lenses on Digital Behavior

An Exploratory Evaluation of Eight Model Families Across Heterogeneous Digital Trace Data

Svea Victoria Strassburger







Chalmers University of Technology
Gothenburg, Sweden 2026

in collaboration with

Stanford School of Medicine
Division of Computational Medicine
Schmiedmayer Lab
Stanford University
Stanford, CA, USA 2026

and

Center for Adaptive Rationality
Max Planck Institute for Human Development
Berlin, Germany 2026

Complex Adaptive Systems as Theoretical Lenses on Digital Behavior
An Exploratory Evaluation of Eight Model Families Across Heterogeneous Digital Trace Data
Svea Victoria Strassburger

© Svea Victoria Strassburger, 2026.

Supervisor: David J. Grüning
Max Planck Institute for Human Development, Berlin, Germany;
University of Cambridge, Cambridge, UK;
Stanford University, Stanford, CA, USA
Supervisor: Paul Schmiedmayer
Stanford University, Stanford, CA, USA
Examiner: Torbjörn Lundh
Applied Mathematics and Statistics — Chalmers University of Technology, Gothenburg, Sweden

Master's Thesis 2026
Department of Physics and Astronomy
Chalmers University of Technology
SE-412 96 Gothenburg
Telephone +46 31 772 1000

Complex Adaptive Systems as Theoretical Lenses on Digital Behavior
An Exploratory Evaluation of Eight Model Families Across Heterogeneous Digital Trace Data

Svea Victoria Strassburger
Department of Physics and Astronomy
Chalmers University of Technology, Sweden
Division of Computational Medicine at Stanford School of Medicine
Stanford University, USA
Center for Adaptive Rationality,
Max Planck Institute for Human Development, Berlin, Germany.

Abstract

Digital behavior consists of repeated, context-dependent interactions with digital tools and platforms. It may be habitual or intentional, and it varies between individuals and within the same individual over time. Smartphone app use is one important example: a brief delay before app access can interrupt an automatic action, but people may respond differently. Describing such variation is relevant to behavioral phenotyping, understood here as the non-diagnostic characterization of multidimensional patterns in digital traces. A central methodological challenge is to derive interpretable measures from partial event logs without treating those logs as complete explanations of behavior.

This thesis examines whether concepts from complex adaptive systems (CAS) can be systematically translated into theoretically guided descriptions of digital behavior. It conducts an exploratory feasibility study of eight CAS-inspired model families: statistical mechanics, dynamical systems, stochastic processes, network theory, information theory, game-theory-motivated proxies, individual-based simulation, and system dynamics. It asks to what extent these families can be operationalized as valid, non-redundant descriptions of heterogeneous digital trace data, and what low-dimensional profile structure, if any, they recover.

The empirical work uses four behavioral datasets: a randomized smartphone-friction trial, a long-horizon naturalistic One Sec cohort, a baseline–intervention One Sec cohort with repeated psychosocial measures, and task-planning traces from the Structured application. Each model family is translated from a theoretical construct to an observable quantity, evaluated against the structure and limits of the relevant data, and included in cross-family profile analyses where eligible.

The findings support a qualified conclusion. Descriptive summaries of stochastic variation, entropy, and app-state or task-state concentration were more readily operationalized across datasets than strategic, generative, nonlinear-dynamical, or causal feedback mechanisms. Several nominally distinct features were exact transforms or re-binnings of the same upstream estimates; others were sensitive to event volume, window length, censoring, or classifier construction. The recoverable profile structure was low-dimensional and dataset-specific. It described patterns of intervention response and digital-tool use, but did not establish universal or temporally stable user types.

A systematic correctness audit materially narrowed several claims by identifying

measurement artifacts, dependent evidence, and analyses that were not identifiable from the available data. The thesis therefore finds that CAS-inspired families are most useful here as a disciplined vocabulary for theory-guided feature derivation and model criticism, not as proof that digital behavior is a CAS or that eight independent mechanisms have been recovered. The exploratory path contributes an explicit account of what can be measured, what remains ambiguous, and which data and validation steps would be required for stronger mechanistic claims.

Keywords: complex adaptive systems, digital behavior, exploratory modeling, digital traces, friction interventions, behavioral profiles, individual differences, model validation.

Acknowledgements

What an adventure! Who would have thought that this would be how I would end my physics studies - with a project bursting with interdisciplinarity, a thesis that brings mathematical and physical perspectives into dialogue with digital behavioral science?
Studying physics has definitely taken me places: Zurich, Switzerland; Heidelberg, Germany; New Delhi, India; Gothenburg, Sweden; Guanajuato, Mexico; Longyearbyen, Svalbard; Berlin, Germany; and now Palo Alto, California.
After exploring environmental physics, biomedical physics, quantum computing and nanotechnology, Arctic research, and finally computational physics and computational digital medicine — combined, in the latter case, with the field of digital behavioral science - I cannot wait to see where physics will take me next.
Thank you to my supervisors, Dr. David J. Grüning and Dr. Paul Schmiedmayer. I can say with complete sincerity that I could never have imagined better supervisors. You care, you are honest, you are supportive, and, above all, you share your excitement about your research — as well as the very valid frustrations that come with it.
Who would have thought that a "Digital Health Implementation" course taken in late spring 2025 in Sweden would lead to such an interesting research project?
I can only thank you, Torbjörn Lundh - my examiner - for being there from the very beginning, during the course in Sweden and our study visit to Stanford. Thank you for your ease, enthusiasm, and willingness to make everything possible.
Thank you to One Sec and Structured for providing access to the datasets.
Thank you to Timon for being there during those first months - and for talking me through everything I did not know about psychology as best as you could.
Thank you to the Kaufmänner for giving me a home and, ultimately, a new extended family. This is, in all honesty, one of the greatest things to have come out of this entire endeavor.
Thank you to everyone at Stanford: my lab, my friends (old and new), and all the people I met along the way, for the little and big moments of joy - cheers to the frozen popsicles (we thought you were never-ending), the bags of chips from B2B (you actually never ended), the longboard that carried me miles and miles, my Sunday swims with Crush the subrobot, and the 1,001 new ideas that were planted in my head — oh boy, world, you better get ready!
Thank you, Katrin (and subsequently Marian), for giving me a home in Palo Alto, even though I was out every single day from dawn till dusk, and for sharing that craziness for and about life.
Thank you, Mama and Papa, for always making sure I know that I have a home base to return to after all my journeys.
Thank you to my Sara for being there every single second - my partner in crime and my personal rock in the surf. Thank you for caring, for actively and sincerely thinking about the challenges I was facing as if they were yours, and for your utterly deep trust that whatever I do will be good.
And last of all, thank you to Australian Home Affairs and the Mexican medical health centers for taking months to approve my visa. Without you, I would never

have had to cancel my thesis in Sydney and search for a new one, and hence would never have found David - by far the best and most caring supervisor to work alongside (and the worst at taking compliments), or joined Paul in his lab at Stanford. Thank you, Paul, for having my back to 100% and for all those lessons and your trust that went far beyond the scope of my thesis. I am so happy to keep working with both of you. You will not get rid of me that quickly, I can tell you that!
Let us see where this journey takes me next - ah yes, UTS, Sydney: microbiological physics research. For the next few months, you will find me playing around with bacterial infections and antibiotics!

Svea Victoria Strassburger, Porto Valtravaglia, Italy, August 2026

Contents

Abstract v

Acknowledgements ix

List of Figures xv

List of Tables xvii

List of Acronyms xix

Nomenclature xxi

1 Introduction 1
- 1.1 Research Question and Contributions . . . 3
- 1.2 Scope and Boundaries . . . 4

2 Conceptual-Theoretical Foundations 5
- 2.1 Complex Adaptive Systems as a Frame for Digital Behavior . . . 5
- 2.2 The Eight CAS-Inspired Model Families . . . 6
- 2.3 Translating the Families Across Two Digital Domains . . . 8
- 2.4 From Model Lenses to Behavioral Phenotypes . . . 12

3 Methodology 13
- 3.1 Study Design and Analytical Status . . . 13
- 3.2 Analytical Workflow and Development Order . . . 13
- 3.3 Datasets . . . 14
  - 3.3.1 DS5 — Randomized Friction Trial . . . 15
  - 3.3.2 DS4 — Long-Horizon Naturalistic Use . . . 15
  - 3.3.3 DS6 — Baseline–Intervention Structure . . . 15
  - 3.3.4 Structured — Task-Planning Behavior . . . 16
- 3.4 Preprocessing, Eligibility, and Measurement Controls . . . 16
- 3.5 Operationalization and Validity Criteria . . . 17
- 3.6 Statistical Analysis . . . 18
- 3.7 Profile Construction . . . 18
- 3.8 Data Governance, Ethics, and Use of Artificial Intelligence . . . 19

4 Exploratory Results and Analysis 21
- 4.1 Statistical Mechanics (StM) . . . 22

4.2 Dynamical Systems (DyS) . . . 24
4.3 Stochastic Processes (StoP) . . . 28
4.4 Network Theory (NeT) . . . 31
4.5 Information Theory (InT) . . . 33
4.6 Game-Theory-Motivated Commitment Proxy (GaT) . . . 36
4.7 Individual-Based Simulations (ABM) . . . 37
4.8 System-Dynamics-Motivated Stock and Loop Analysis (SyD) . . . 38
4.9 Cross-Family Profiles and Redundancy . . . 39

5 Overall Discussion and Conclusion 47
5.1 Answer to the Research Question . . . 47
5.2 What Was Learned From the Four Subquestions . . . 49
5.2.1 Operationalization Requires Dataset-Specific Validity Conditions . . . 49
5.2.2 Cross-Domain Transfer Was Partial Rather Than Literal . . . 49
5.2.3 Person-Level Structure Is Low-Dimensional and Conditional . 50
5.2.4 Non-Redundancy and Identifiability Are Part of the Result . . 51
5.3 Limitations . . . 51
5.4 Which Data Fit This Framework Best? . . . 52
5.5 Priorities for Future Work . . . 54
5.6 Conclusion . . . 56
5.7 Code and Website Availability . . . 56

Bibliography 57

A Statistical Reading Guide 63
A.1 Statistical Evidence . . . 63
A.2 Model-Specific Scales and Reference Points . . . 65

B Detailed Results and Diagnostics 71
B.1 Consolidated Statistical Results . . . 71
B.2 Statistical-Mechanics Distribution Diagnostic . . . 77
B.3 Dynamical-Systems Diagnostics . . . 78
B.4 Stochastic-Process Diagnostics . . . 79
B.5 System-Dynamics Statistical Tables . . . 80
B.6 Profile-Sensitivity Table . . . 81

C CAS Model-Family Foundations 83
C.1 Statistical Mechanics (StM) . . . 83
C.2 Dynamical Systems (DyS) . . . 86
C.3 Stochastic Processes (StoP) . . . 88
C.4 Network Theory (NeT) . . . 89
C.5 Information Theory (InT) . . . 92
C.6 Game Theory (GaT) . . . 94
C.7 Agent-Based Modeling (ABM) . . . 96
C.8 System Dynamics (SyD) . . . 97

List of Figures

1.1 Individual trajectories and conditional group means 2

2.1 CAS lens architecture for One Sec 10
2.2 CAS model architecture for Structured planning behavior 11

4.1 DS5 condition-level behavioral landscape 23
4.2 DS6 configuration change by condition cohort 24
4.3 Structured time-valid path-dependence diagnostic 25
4.4 DS5 low-noise and low-entropy overlap 26
4.5 DS6 regime labels under unequal and matched windows 27
4.6 DS5 raw and sampling-adjusted stochastic-process summaries 29
4.7 DS6 stochastic-process parameters by period 30
4.8 DS5 multi-app network metrics by condition 32
4.9 Pooled Structured task-state network 33
4.10 DS5 entropy dimensions by condition 35
4.11 Structured weekly backlog trajectories 39
4.12 DS5 blended profile summaries 41
4.13 DS4 blended profile summaries 42
4.14 DS4 behavioral and network partition cross-tabulation 42
4.15 DS6 profile summaries 43
4.16 Structured profile summaries 44

B.1 DS6 pooled configuration-change distribution 77
B.2 DS4 model-implied fixed-point check 78
B.3 DS4 relaxation estimates at daily and weekly resolution 79
B.4 Structured planning-count dispersion 79

C.1 Graphic illustration of hubs, degree centrality, betweenness centrality, closeness centrality, eigenvector centrality, PageRank, and participation coefficient in a hypothetical network sequence. Reproduced from Farahani et al., 2019, Figure 5 (CC BY 4.0). 90

List of Tables

2.1 Theoretical foundations of the eight CAS-inspired model families . . . 7
2.2 CAS model families translated across two digital domains 9

3.1 Dataset designs and inferential roles 14
3.2 Model-family operationalizations and validity conditions 17

4.1 Recoverable profile structure in the four behavioral datasets. 45

5.1 Final empirical role and claim boundary of each model family. 48
5.2 Dataset-specific conclusions and inferential boundaries. 50
5.3 Family-by-dataset coverage and outcome type 53

A.1 Plain-language guide to statistical quantities 63
A.2 Plain-language guide to model-specific quantities 66
A.3 Plain-language guide to derived and profile quantities 68

B.1 Consolidated statistical results 71
B.2 DS6 original-window regime transitions 78
B.3 DS6 exploratory loop-association tests 80
B.4 Structured feedback loops, pooled versus within-participant 80
B.5 DS5 profile feature-sensitivity checks 81

List of Acronyms

The acronyms used throughout this thesis are listed below in alphabetical order:

ABM	Agent-Based Modeling (conceptual family; implemented here as individual-based simulation)
ANOVA	Analysis of Variance
ARI	Adjusted Rand Index
AR(1)	First-Order Autoregressive Process
CAS	Complex Adaptive Systems
DyS	Dynamical Systems
GaT	Game Theory
HHI	Herfindahl–Hirschman Index (concentration measure)
InT	Information Theory
JSD	Jensen–Shannon Divergence
KL	Kullback–Leibler (divergence)
MI	Mutual Information
NeT	Network Theory
OU	Ornstein–Uhlenbeck (process)
SD	Standard Deviation
SDE	Stochastic Differential Equation
SE	Standard Error
StM	Statistical Mechanics
StoP	Stochastic Processes
SyD	System Dynamics

Nomenclature

The following tables define the indices, state variables, fitted parameters, and derived quantities used throughout this thesis. Quantities carrying a hat ($\hat{\cdot}$) are estimated from data rather than observed directly.

Indices and Sets

t	Index for a day, or for a week where a weekly resolution is stated
w	Index for a calendar week
i, j	Indices for states in a transition network (apps, or task-lifecycle states)
T	Number of observed time steps for a participant
N	Number of participants

State Variables

X_t	Daily override rate: opened attempts divided by outcome-bearing attempts on day t, bounded in $[0, 1]$
x_{mean}	Participant-level mean of X_t over the observation window
N_t	Daily count state: app-opening attempts in DS6 or task creations or completions in Structured; bounded below at zero
B_w	Backlog stock: open, unresolved tasks standing at the end of week w

Fitted Process Parameters

$\hat{\mu}$	Estimated drift; mean increment of the state variable per time step
$\hat{\sigma}$	Estimated diffusion; standard deviation of the increments

$\hat{\theta}$	Mean-reversion rate of an Ornstein–Uhlenbeck process
$\hat{\tau}$	Relaxation time, $\hat{\tau} = 1/\hat{\theta}$
$\hat{\varphi}$	Autoregressive coefficient of a first-order autoregressive fit
σ_μ	Ratio $\hat{\sigma}/\lvert\hat{\mu}\rvert$; dominance of variability over directed drift
h_{period}	Within-participant drift difference, $\hat{\mu}^{\text{intervention}} - \hat{\mu}^{\text{baseline}}$; a period contrast, not a condition effect
σ_{thr}	Per-period diffusion threshold used to split participants into deterministic and stochastic regimes
F	Fano factor, $\text{Var}(N_t)/\mathbb{E}[N_t]$; equals one for a Poisson process

Information-Theoretic and Thermodynamic Quantities

H_{out}	Shannon entropy of the outcome distribution
$H_{\text{out,resid}}$	Outcome entropy residualized on condition, to remove the confound of H_{out} being condition-dependent by construction
H_{app}	Shannon entropy of the target-app distribution
H_{hour}	Shannon entropy of the hour-of-day distribution
H_{emp}	Empirical entropy of the binned daily state series
H_{trans}	Source-weighted conditional entropy of the transition network
H_{SDE}	Differential entropy of a Gaussian, $\frac{1}{2}\log_2(2\pi e\,\hat{\sigma}^2)$
I_{consec}	Mutual information between consecutive states, $H_{\text{source}} - H_{\text{trans}}$, using the source-state marginal of the same transition population
β	Behavioral inverse temperature; degree of ordering of the state distribution
T_{behav}	Behavioral temperature, $1/\beta$
χ_{DS5}	Thermodynamic susceptibility proxy, $\beta_{\text{behav}}p(1-p)$; a function of the fitted variability and state occupation
χ_{DS6}	Configuration-shift measure: Jensen–Shannon divergence between baseline and intervention app–time distributions
$V(x)$	Scaled negative log-density used for the DS5 landscape display, $-(\bar{\sigma}^2/2)\log\hat{P}(x)$; minima mark modes of the pooled distribution

Network and Phenotype Quantities

$\mathrm{HHI}_{\mathrm{net}}$	Concentration measure used for app-transition flow
$\mathrm{HHI}_{\mathrm{source}}$	Concentration of transition flow across source states, $\sum_i (s_i^{\mathrm{out}}/M)^2$; not edge-level concentration
ρ_{self}	Self-transition share; repetition of the same state
π	Stationary distribution of the transition matrix
W_{ij}	Weight of the directed edge from state i to state j
M	Total transition flow, $\sum_{ij} W_{ij}$
J	Bootstrap Jaccard index; stability of a cluster under resampling
ARI	Adjusted Rand Index; agreement between two partitions, not a test of statistical independence
d	Cohen's d; standardized difference between two group means
η_p^2	Partial eta squared; proportion of variance attributable to an effect

1
Introduction

Research problem. Digital behavior encompasses repeated interactions with applications, platforms, and other digital tools. It includes brief actions such as opening or switching apps as well as longer processes such as creating, revising, and completing a task. These actions can be habitual or intentional, depend on context and prior activity, and vary between people and within the same person over time (Böhmer et al., 2011; Heino et al., 2021; Wood et al., 2002). Understanding this variation is difficult because digital traces record selected actions and timestamps, but not the full psychological, social, or platform context in which they occur.

Smartphone use is a prominent application of this broader problem. App access can follow automatic patterns that do not always match a user's prior intentions. Design-friction tools such as One Sec introduce a brief pause before a selected app opens, creating an opportunity to reconsider the action (Cox et al., 2016; Grüning et al., 2023; Haliburton et al., 2024). Such an intervention does not remove behavioral heterogeneity: people may differ in their exposure to the prompt, their immediate response, and how their behavior changes over time. Smartphone friction is therefore a useful empirical case in this thesis, but it is not its complete subject.

The Structured planning data provide a second domain in which behavior unfolds without an app-opening intervention. Structured is a digital planning application in which users create, schedule, revise, and complete tasks, allowing behavior to be observed through the resulting task lifecycles rather than through app-opening decisions.

Characterizing this variation is also a behavioral-phenotyping problem. Digital phenotyping uses data from personal digital devices to describe patterns relevant to behavior and health (Bufano et al., 2023; Jain et al., 2015; Onnela & Rauch, 2016). Here, a phenotype is used more narrowly as a descriptive, multidimensional profile of observed digital behavior, not as a diagnosis or fixed psychological type. The methodological question is how to derive such profiles from theory rather than selecting isolated metrics only because they are readily available.

Average treatment effects and single usage measures remain useful, but they do not fully describe person-level variation (Bryan et al., 2021; Szaszi et al., 2025). A framework that relates temporal change, variability, uncertainty, transition structure, and intervention response could ultimately inform more targeted hypotheses. Before explanation or prediction is attempted, however, it is necessary to establish which quantities are computable, interpretable, and non-redundant in the available traces. The traces alone cannot establish why a person uses a digital tool or why an intervention changes behavior for one person but not another. They can show whether candidate descriptions distinguish people and survive checks for sampling

and design artifacts. Related person-specific research likewise cautions that a population mean need not represent any one individual (Beyens et al., 2020; Fisher et al., 2018; Molenaar, 2004; Turner, Dalmaijer, et al., 2026).
Figure 1.1 makes this motivation visible using the final DS5 state definition: on each active day, X_t is the proportion of opened decisions among opened and dismissed outcomes. Panel A displays the orderly randomized-condition means. Panel B adds the 379 underlying participant trajectories (control $n = 124$, default friction $n = 128$, reintervention $n = 127$), each smoothed with a seven-day rolling mean. The difference between the panels is not a contradiction: the group contrast and the person-level heterogeneity coexist. The trajectories motivate the person-level analysis that follows; on their own, smoothed curves like these do not yet establish stable phenotypes or causal individual effects, a stronger claim evaluated only once the phenotyping methodology of Chapter 3 is in place.

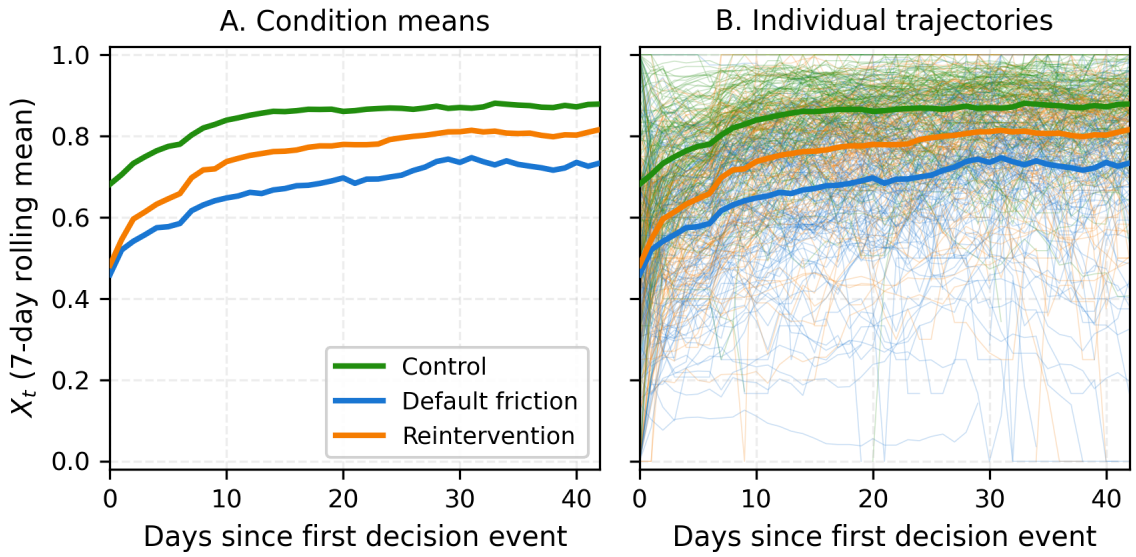


Figure 1.1: Group-level (A) and person-level (B) views of opening decisions in the DS5 smartphone-friction data ($N = 379$ participants with at least 14 active days). The state variable is the daily override proportion $X_t = n_{\text{opened},t}/(n_{\text{opened},t} + n_{\text{dismissed},t})$, the share of resolved opening decisions on day t in which the app was opened rather than dismissed; the plotted values are its 7-day rolling mean over the first 42 days since each participant's first decision event.

Complex adaptive systems (CAS) are systems of interacting, adaptive components whose local and history-dependent interactions can generate nonlinear, emergent macroscopic patterns (Holland, 1992; Mitchell, 2009). This thesis considers the coupled person–digital-tool process over time. In the smartphone datasets, that process may include an app and an intervention; in Structured, it concerns a person and a planning tool. Logged micro-decisions are observations of these processes, not themselves interacting components. This distinction is essential: applying a CAS-inspired measure to a log does not prove that the observed process is a CAS. The thesis therefore treats eight CAS-inspired model families from complex-systems research as candidate analytical lenses. A stochastic- process lens can summarize

drift and variability; a network lens can describe the organization of app or task-state transitions; an information-theoretic lens can quantify uncertainty. Other families require stronger ingredients, such as observed payoffs, interacting agents, nonlinear dynamics, or causal feedback. Whether those ingredients exist in the data is part of the question, not something assumed in advance.
The eight families form a structured stress test of the available traces. The central contribution is a systematic assessment of when complex-systems quantities provide defensible, non-redundant descriptions and when the mathematical language exceeds what the data can support. Negative and corrective results are part of this intended outcome.

1.1 Research Question and Contributions

This thesis asks:

> *To what extent can eight CAS-inspired model families be operationalized as valid, non-redundant descriptions of heterogeneous digital trace data across behavioral domains, and what low-dimensional phenotype structure, if any, do they recover?*

The main question is addressed through four subquestions:

1. How can each model family be translated into observables in each dataset, and which validity and identifiability conditions does that translation require?
2. Which translations remain meaningful across the smartphone-intervention and task-planning domains, and where is dataset-specific re-grounding necessary?
3. Do the derived features reveal person-level structure beyond group averages and combine into low-dimensional behavioral profiles?
4. Under which conditions do the features provide non-redundant information rather than reflecting algebraic dependence, sampling variation, censoring, unequal observation windows, or analytical construction?

The first contribution is an explicit translation from theoretical construct to observable trace for each family, together with the point at which the translation ceases to be defensible (Chapters 2 and 3; Appendix C provides the fuller original-domain foundations). The second is an empirical feasibility comparison across four behavioral datasets of differing design: a randomized friction trial, a long-horizon naturalistic cohort, a baseline–intervention cohort with repeated psychosocial measures, and a planning application without a friction event (Chapter 3). Results are organized by model family so that transfer, re-grounding, and failure conditions can be compared directly (Chapter 4).
The third contribution is a cross-family assessment of redundancy and person-level profile structure. Here, *phenotype* denotes a descriptive position in a multidimensional feature space, not a diagnosis, latent psychological trait, or proven stable user type. A fourth contribution emerged during the work: a systematic correctness audit reclassified several initially positive findings as null, dependent, or artifactual. These corrections are integrated into the final results. A modeling toolbox is only useful if it also specifies how to recognize when an output is not interpretable.

1.2 Scope and Boundaries

The study is exploratory, and its breadth is deliberate. The eight-family selection is theory-guided but neither systematic nor exhaustive; operationalizations evolved with the available data, and the analyses were not preregistered as confirmatory tests. The aim is to screen a wide theoretical search space, including unconventional candidates, rather than maximize depth within a few already plausible families. Reported p-values and effect sizes therefore summarize exploratory contrasts, not a prespecified test of a unified CAS theory. Uneven empirical depth is an acknowledged trade-off: the design allows unexpected uses to emerge and unsupported translations to be ruled out or assigned clearer data requirements, but it does not imply equal implementation or definitive validation across families. Complex-systems terminology alone establishes neither nonlinearity, emergence, adaptation, nor psychological mechanism.

Only DS5's randomized comparisons support causal claims. A causal claim states that a condition or intervention produced an outcome rather than merely co-occurring with it, a distinction that random assignment is designed to support. DS4 and Structured contain no experimental condition, while DS6's three-level condition was assigned at cohort level; its within-person period contrast is therefore distinct from its quasi-experimental condition associations. Even in DS5, the descriptive profiles are constructed after assignment and cannot be treated as pre-existing traits, treatment moderators, or individual causal effects.

Several families remain partial operationalizations. The conceptual suitability of a framework is distinct from its empirical feasibility. Without observed utility or payoffs, the game-theory analysis is a commitment proxy, not a formal game or equilibrium. The independently parameterized simulations contain no agent interaction and use fitted inputs, making them individual-based Monte Carlo checks rather than conventional agent-based emergence or independent validation. System-dynamics analyses provide stock summaries and loop-motivated associations, not identified causal feedback. These limits do not show that the source theories are unsuitable or simply that the data are poor; they expose mismatches between theoretical requirements and the variables, temporal resolution, system boundaries, and observation processes in datasets collected for other purposes. Identifying those mismatches and the measurements needed to resolve them is an intended output of the framework, whose role is to state what each family requires, how it maps to observable traces, and where a mechanistic interpretation ceases to be defensible.

Measurement structure bounds every inference. Observation windows differ across and within datasets, daily proportions inherit event-counting variance, Structured lifecycles are left- and right-censored, and several derived quantities share fitted inputs. No dataset records content viewed inside target platforms, so the analyses concern access attempts, intervention responses, and task lifecycles rather than content exposure or recommendation dynamics. These limits are evaluated with each result and define what the present data identify; they are not negative findings about digital behavior in general. No analysis establishes a nonlinear attractor, temporally stable phenotype, or universal user taxonomy.

2

Conceptual-Theoretical Foundations

2.1 Complex Adaptive Systems as a Frame for Digital Behavior

Complex adaptive systems are collections of interacting, adaptive components whose local and history-dependent rules can generate emergent macroscopic behavior such as pattern formation, regime shifts, and adaptation. Their dynamics are often nonlinear, and the structure they produce can span several levels at once. Ecosystems, economies, neural circuits, the climate system, immune systems, and financial markets are the standard examples (Holland, 1992; Levin, 1998; Rahmstorf, 2006). What unites them is not a shared subject matter but a shared difficulty: the aggregate cannot be read off any single component, and the system's present state depends on the path by which it arrived there (Carmichael & Hadžikadić, 2019; Mitchell, 2009).

Digital behavior motivates, but does not automatically satisfy, this description. Smartphone use is repeated, context-dependent, partly habitual, and shaped by recent history. In the working system boundary used here, the components are the person, the digital tool, and, where present, the intervention; their coupling unfolds over time. Logged attempts and task events are partial observations of that coupled process. The purpose of the CAS framing is to generate candidate questions about feedback, state transitions, and person-specific variation, not to assert before analysis that the traces demonstrate emergence, nonlinearity, or adaptation (Heino et al., 2021; Molenaar, 2004; Nahum-Shani et al., 2018; Wang & Miller, 2020).

The frame adopted here is therefore not a single model. It is a set of eight established methodological traditions — statistical mechanics, dynamical systems, stochastic processes, network theory, information theory, game theory, agent-based modeling, and system dynamics — applied as parallel lenses on the same behavior (Heino et al., 2021). The aim is explicitly not to select a universally best family. It is to explore which aspects of digital behavior each family can describe, and to keep two things apart that are easy to conflate: whether a family is *conceptually* suited to a behavior, and whether it can actually be *operationalized* on the data at hand. The empirical chapters show that these two judgments diverge sharply.

2.2 The Eight CAS-Inspired Model Families

The eight model families draw on mathematical, physical, and computational traditions. They differ in both formal logic and explanatory focus. The concise overview below introduces these differences, while Appendix C provides the fuller theoretical foundations and original-domain examples for each family.

The families were selected as a broad, theory-guided set of prominent approaches in complex-systems research. The selection is intentionally exploratory rather than systematic and does not assume that one family is sufficient or superior for understanding digital behavior. The selected families span complementary perspectives on distributional organization, temporal dynamics, relational structure, uncertainty, strategic decision-making, generative simulation, and feedback. Several approaches also have precedent in adjacent behavioral research: dynamical-systems concepts have been applied in social and personality psychology (Richardson et al., 2014), and information-theoretic measures to dynamical social networks (Zhao et al., 2011). Considering this deliberately broad set provides an exploratory basis for testing which lenses can be translated meaningfully to digital behavior, where their limits lie, and whether complementary perspectives contribute to a more general framework.

All eight families can contribute to the study of a complex adaptive system, but they differ in their primary unit of analysis and in what they treat as explanatory. Statistical mechanics emphasizes collective states and how macroscopic order emerges from many microscopic configurations (Netz, 2016). Dynamical systems and stochastic processes both emphasize temporal evolution, with the latter extending the former by making randomness explicit rather than incidental (Gunesch, 2005; Øksendal, 2003). Network theory emphasizes relational structure (Newman, 2010); information theory emphasizes uncertainty and statistical dependence (Cover & Thomas, 2006); game theory emphasizes strategic interaction under competing incentives (Hotz, 2006); agent-based modeling emphasizes bottom-up emergence from heterogeneous local rules (Borrill & Tesfatsion, 2011; Macal & North, 2010); and system dynamics emphasizes aggregate feedback and accumulation (Roy, 2007). Table 2.1 sets the eight side by side.

Two structural relationships in that table matter later. First, the families are not mutually exclusive descriptions of different things; several are formal relatives. Stochastic differential equations combine a dynamical rule with stochastic terms; agent-based modeling often represents processes from the bottom up, whereas system dynamics commonly uses an aggregate stock–flow representation; and entropy appears in both statistical mechanics and information theory. These are conceptual relationships, not mathematical equivalences. Second, and as a consequence, conceptual parallelism does not guarantee measurement independence. Two lenses that ask different questions can still end up computing functions of the same estimated number — a possibility that has to be checked rather than assumed, and one that the results chapters return to repeatedly.

Table 2.1: Overview of the theoretical foundations of the eight CAS-inspired model families. Adapted from the conceptual framework underlying this thesis (Strassburger et al., 2026).

Model family	Theoretical perspective	Central elements	Primary explanatory focus
Statistical Mechanics	Explains how macroscopic regularities emerge from many interacting microscopic components and probabilistic system states.	Microstates, ensembles, energy landscapes, entropy, temperature, phase transitions, susceptibility, and hysteresis.	Collective order, state probabilities, sensitivity to perturbations, critical transitions, and path-dependent system behavior.
Dynamical Systems	Represents a system as a state that evolves over time according to deterministic or stochastic update rules.	State space, trajectories, fixed points, attractors, stability, control parameters, bifurcations, and chaos.	Temporal development, stable regimes, transitions between regimes, and sensitivity to initial conditions or parameter changes.
Stochastic Processes	Extends dynamical models by explicitly incorporating uncertainty and random fluctuations.	Random variables, drift, diffusion, Brownian motion, Markov processes, stochastic differential equations, and probability distributions.	Variability between trajectories, noise-driven behavior, probabilistic transitions, and the interaction between systematic tendencies and randomness.
Network Theory	Describes a system through the relations among its components rather than through isolated component properties.	Nodes, edges, adjacency matrices, centrality, clustering, communities, paths, hubs, and network topology.	Relational organization, structural importance, connectivity, behavioral flow, and the emergence of global structure from local links.

Continued on the next page.

Table 2.1 continued from the previous page.

Model family	Theoretical perspective	Central elements	Primary explanatory focus
Information Theory	Quantifies uncertainty, predictability, dependence, and information exchange within and between variables or processes.	Shannon entropy, joint entropy, conditional entropy, mutual information, KL divergence, transfer entropy, and information gain.	Behavioral uncertainty, predictability, shared information, statistical dependence, and directed information transfer.
Game Theory	Models decisions in situations in which outcomes depend on the strategies and actions of interacting actors.	Players, strategies, payoffs, utility, Nash equilibria, mixed strategies, evolutionary stability, and strategic adaptation.	Strategic choice, competing incentives, cooperation, conflict, equilibrium behavior, and adaptation of strategies over time.
Agent-Based Modeling	Uses bottom-up simulations to examine how system-level patterns emerge from heterogeneous autonomous agents following local rules.	Agents, attributes, environments, interaction rules, bounded rationality, heterogeneity, stochastic updates, and emergence.	How simple local behaviors and interactions generate complex, unintended, or nonlinear collective outcomes.
System Dynamics	Uses a top-down representation of aggregate stocks, flows, delays, and feedback structures to explain system-wide change.	Stocks, inflows, outflows, reinforcing loops, balancing loops, delays, causal-loop diagrams, and stock-and-flow models.	Endogenous feedback, accumulation, growth, stabilization, oscillation, saturation, and system-level responses to interventions.

2.3 Translating the Families Across Two Digital Domains

The framework is applied to two different behavioral episodes. In One Sec, a user attempts to open a target app, encounters friction, and then opens, dismisses, or redirects. In Structured, a user creates a task, assigns more or less temporal structure, and may later move, complete, reopen, delete, or leave it unresolved. Holding each episode fixed across the eight lenses makes their complementarity concrete: the observed episode does not change from family to family, but the unit treated as explanatory does — a configuration, trajectory, increment, edge, distribution,

commitment proxy, simulated individual, or accumulating stock. Table 2.2 provides a compact cross-domain reference.

Table 2.2: Compact conceptual translation of the eight CAS-inspired model families into the One Sec smartphone-intervention and Structured planning domains. The entries state the behavioral object supplied to each lens, not an empirical finding. Adapted from the conceptual framework underlying this thesis (Strassburger et al., 2026).

Model family	One Sec smartphone-intervention object	Structured planning object
Statistical mechanics	Event and daily-state distributions describe friction-response configurations and their reorganization.	Task-feature configurations and weekly dominant states describe planning regimes and their persistence.
Dynamical systems	Daily or weekly attempt and override trajectories are examined for stable, drifting, or noise-dominated regions.	Weekly vectors of task volume, temporal structure, completion, and complexity describe movement through planning-state space.
Stochastic processes	Daily override proportions or attempt counts are summarized through drift, increment variability, relaxation, and burstiness.	Daily task-creation and completion counts are summarized through drift, increment variability, and count dispersion.
Network theory	Target apps are nodes and temporally successive attempts are directed edges, exposing concentration, repetition, and possible switching.	Task-lifecycle states are nodes and recorded state changes are edges, exposing dominant completion paths and rescheduling loops.
Information theory	Entropy and mutual information quantify uncertainty in outcomes, apps, hours, and daily states.	Entropy and mutual information quantify diversity and dependence in task type, timing, recurrence, and terminal status.
Game theory	Opening versus dismissing motivates a post-assignment commitment proxy; utilities, opponents, and equilibrium are unobserved.	Encoded task structure forms an ordinal commitment proxy; it does not measure payoff, utility, or strategic interaction.

Table 2.2 continued from the previous page.

Model family	One Sec smartphone-intervention object	Structured planning object
Individual-based simulation	Participant-specific fitted processes generate synthetic response trajectories and test whether the specification reproduces observed summaries.	Static and episodic participant-level activity rules test which ingredients are required to reproduce planning-count dispersion.
System dynamics	Candidate stocks and flows require repeated measurement; only DS6 supplies two survey waves for exploratory loop associations.	The open-ended lifecycle supplies an observable backlog stock, with task creation, completion, and rescheduling as flows.

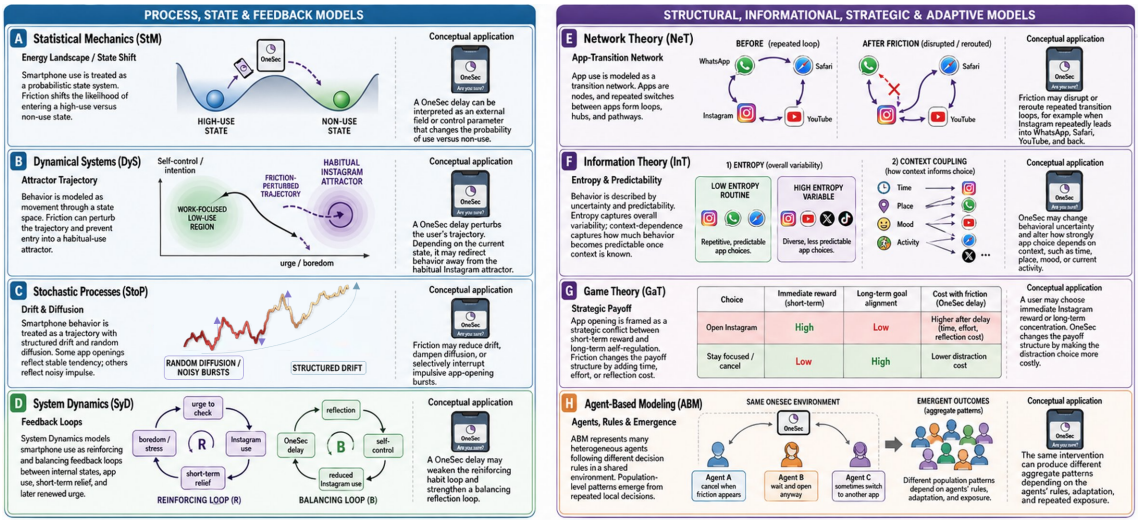


Figure 2.1: Eight CAS-inspired model families translated to smartphone use and One Sec intervention response. The map records the conceptual questions preceding empirical evaluation; its application statements are hypotheses, not findings.

Figure 2.1 holds the One Sec episode constant and changes only the explanatory unit. Its apparent symmetry is conceptual rather than empirical: several quantities later turn out to share inputs or to be exact transformations of one another. The figure therefore explains why multiple lenses were attempted, while Chapter 4 determines how much independent information each lens actually contributes.

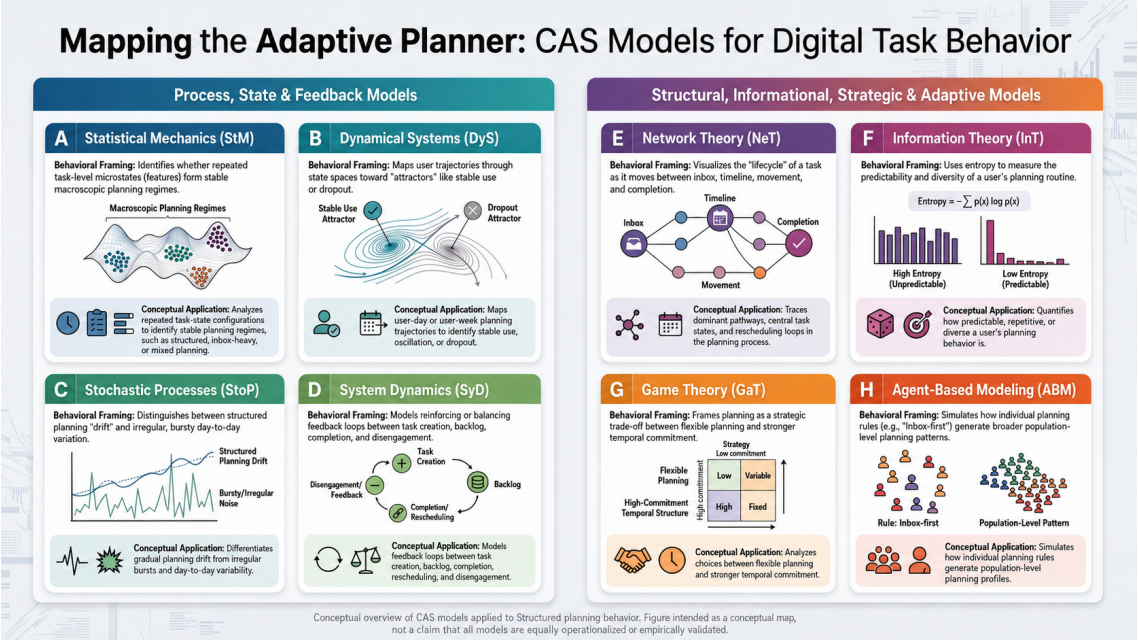


Figure 2.2: Eight CAS-inspired model families translated to the task-planning lifecycle. The map is a conceptual transfer to a domain without a friction prompt, binary response, or closed behavioral episode.

Figure 2.2 applies the same organizing device to a genuinely different behavioral object. The task lifecycle has no intervention moment, so the One Sec estimators cannot simply be relabeled: states, clocks, transitions, and the available stock must be re-grounded in planning behavior. The equal visual weight of the eight cards does not claim that all families are equally identifiable. It establishes the conceptual questions against which empirical feasibility, null results, and failed operationalizations are later judged.

The translations aim to make every lens return an observable or derived quantity rather than remain a metaphor. They also make the limits visible. Payoffs and strategic opponents are never observed; simulated individuals do not interact; a system-dynamics stock is available only where the design supplies repeated measurement or an open-ended lifecycle; and several apparent cross-family quantities prove to be algebraically dependent. The full conceptual reasoning is therefore contained in Table 2.2 and Figures 2.1–2.2; Appendix C retains the model families' fuller original-domain foundations.

The participant-level outputs from the eight lenses feed the later phenotyping analysis, but phenotyping is a downstream synthesis rather than a ninth model family. Nor does placing several features in one profile make them independent: exact transforms, shared inputs, and feature-dominance are screened explicitly in Methodology and reported in Section 4.9.

2.4 From Model Lenses to Behavioral Phenotypes

The purpose of deriving these quantities is to move from simple individual usage metrics — screen time, morning use, evening use — toward theory-derived behavioral phenotypes (Jain et al., 2015; Onnela & Rauch, 2016; Torous et al., 2016). Two things change in that move. First, the metrics are not chosen because they are intuitive; they are chosen because a theory says they should matter, so drift comes from stochastic processes, entropy from information theory, centralization from network theory, feedback dominance from system dynamics, and adaptation rules from agent-based modeling. Second, those metrics can then be combined, so a user is characterized by a profile across several behavioral dimensions rather than by one number.

This thesis treats phenotypes as *multidimensional profiles rather than fixed categories*. A participant is a position in a continuous feature space, and any cluster label assigned afterwards is a summary of that space, not a replacement for it. The distinction is not cosmetic. Static categories invite the assumption that a user *is* a type; a profile keeps visible that the same person may be extreme on one dimension, unremarkable on another, and possibly different again under a different context or intervention. Where grouped phenotypes are reported in the following chapters, the underlying continuous dimensions are reported alongside them, and the stability of each grouping is diagnosed rather than presumed.

The framework began with an exploratory, non-preregistered inventory of roughly eight to ten candidate dimensions, including friction sensitivity, habitual stability, impulsivity or noise dominance, context and threshold dependence, adaptation, override and substitution tendencies, network centralization, and feedback dominance. The inventory made possible constructs explicit so that redundancy and identifiability could be tested; it did not predict one independent dimension per family. The empirical chapters recover fewer dimensions because some constructs are non-equivalent despite sharing a name, some are not identifiable in the available windows, and others collapse onto shared inputs. Chapter 5 reports what survives. Thus the eight lenses generate and audit candidate features; they do not imply a fixed eight-dimensional structure of digital behavior.

3

Methodology

This chapter describes the study design, datasets, preprocessing decisions, model-family operationalizations, and cross-family profile analysis. Because the project is exploratory, the method is organized around feasibility: for each proposed quantity, the analysis asks whether the required variables and temporal structure exist, whether the quantity is identifiable, and whether it contributes information beyond its inputs.

3.1 Study Design and Analytical Status

This secondary analysis is exploratory and was not preregistered as a confirmatory test. The theory-guided operationalizations developed iteratively as each dataset was examined. Inferential statistics therefore describe uncertainty and screen candidate relationships; they do not certify a unified CAS mechanism. Null and failed operationalizations remain relevant to the feasibility question.

The primary unit for most models is the participant. Event logs are aggregated to daily or weekly series where a temporal model requires regular steps, with zero-activity intervals included when the absence of an event is meaningful and observable. Event-level or participant-period analyses are used where explicitly stated. The four behavioral datasets are analyzed separately; no pooled cross-dataset model is fitted because their state variables, populations, observation windows, and designs differ.

Final claims were classified into four practical categories: (1) descriptive results supported by the implemented estimator and sensitivity checks; (2) condition associations or randomized contrasts, distinguished by design; (3) provisional results sensitive to measurement or modeling choices; and (4) unidentifiable or invalid constructions, reported as methodological lessons rather than empirical findings. This classification governs the wording in Chapters 4 and 5.

The correctness audit was an iterative verification process rather than a prespecified formal audit. It systematically checked estimator definitions, algebraic dependencies, observation processes, eligibility criteria, and robustness to alternative analytical choices.

3.2 Analytical Workflow and Development Order

Each dataset was carried through the same development sequence: data cleaning, preprocessing and harmonization, feature extraction aligned to the model families

in Chapter 2, per-family model implementation, and, where the dataset was eligible, cross-family phenotyping. The analysis was first developed most extensively for DS5. This established the sequence, which was then reapplied to DS4, DS6, and Structured, in each case re-grounding the family-specific operationalizations in that dataset's own state variables and structure rather than porting DS5's estimators directly (Sections 3.3.2–3.3.4). Where a direct port failed — most visibly DS6's structurally constant outcome (Section 3.3.3) and Structured's complete absence of a friction episode (Section 3.3.4) — the model family was re-derived from its own theoretical requirement rather than adapted from DS5's implementation, a distinction Chapter 4 states explicitly wherever it applies. This iterative re-grounding creates researcher degrees of freedom and is part of the study's exploratory status. A confirmatory extension should define features, transformations, thresholds, and eligibility rules in one development dataset or time window, lock them, and then apply them without refitting to another dataset or later window.

3.3 Datasets

Three datasets record One Sec app-opening traces, although they differ substantially in design and available outcomes. Structured records task-planning lifecycles and therefore provides a transfer test to another behavioral domain. Table 3.1 summarizes their analytical roles.

Table 3.1: Dataset designs, primary analytical units, and inferential roles.

Dataset	Design and sample	Logged episode	Primary state or structure	Inferential role
DS5	Randomized friction trial; $N = 573$ (568 with valid events; 414 at ≥ 7 days)	Target-app attempt and resolution	Daily override proportion X_t; app sequence	Only randomized condition contrasts in the thesis
DS4	Naturalistic long-horizon One Sec cohort; $N = 1{,}039$	Target-app attempt and resolution	Daily override proportion; app sequence	Temporal-resolution and long-window feasibility; no causal contrast
DS6	Baseline–intervention cohort; $N = 243$	Target-app attempt; outcome structurally constant	Daily attempt count N_t; app sequence; repeated surveys	Within-person period description and quasi-experimental condition associations

Dataset	Design and sample	Logged episode	Primary state or structure	Inferential role
Structured	Retrospective planning-app export; $N = 61$	Task creation, revision, and terminal state	Daily/weekly counts; task-state transitions; backlog	Cross-domain transfer without a friction event or intervention

3.3.1 DS5 — Randomized Friction Trial

DS5 contains German adolescents assigned to control, default friction, or reintervention conditions ($N = 573$; 414 meet the minimum of seven observed days). After excluding missing and non-target outcomes, the analysis table contains 285,112 events and 14,565 participant-days from 568 participants. The control condition is not equivalent to an opening rate of one; observed app-opening attempts can resolve without an opening. The daily state is therefore

$$n_{\text{outcome-bearing},t} = n_{\text{opened},t} + n_{\text{dismissed},t}, \qquad X_t = \frac{n_{\text{opened},t}}{n_{\text{outcome-bearing},t}}, \qquad X_t \in [0,1]. \tag{3.1}$$

X_t is the daily override rate: the number of opened attempts divided by the number of attempts with a valid opening-or-dismissal outcome on day t, bounded in $[0,1]$. Here X_t is an override-behavior proxy, not a measurement of urge, self-control, habit, or dependence (Jain et al., 2015; Oudin et al., 2023). Every transformation of X_t inherits that limitation. Network analyses instead use the ordered target-app sequence, allowing them to contribute information not constructed from the outcome proportion. Because assignment is randomized, between-arm contrasts can estimate condition effects, subject to the observation and eligibility rules of each analysis.

3.3.2 DS4 — Long-Horizon Naturalistic Use

DS4 contains 1,039 One Sec users and approximately 2.49 million events, with observation windows extending to 897 days. A 30-day minimum leaves 786 participants for analyses requiring long series; particular fits impose additional criteria. The cohort is self-selected into using One Sec and remaining observed, and it has no experimental condition. It therefore supports no causal claim about friction. Its main purpose is to test whether temporal conclusions drawn at a daily resolution survive longer windows and alternative time aggregation. Survey coverage is limited (283/1,039, one wave), so psychosocial change and system-dynamics analyses are not identified.

3.3.3 DS6 — Baseline–Intervention Structure

DS6 contains Danish adolescents ($N = 243$) and 353,796 events, with native baseline (158,889 events) and intervention (194,907) period labels. The median baseline

window is 15 days and the intervention window 29 days. A three-level condition variable is assigned at the cohort rather than the individual level and is treated as quasi-experimental. Period and condition are therefore distinct: a within-participant period difference is not itself an estimated condition effect, and a between-condition contrast is an association rather than a randomized comparison.
The recorded outcome is *opened* for every event, making Equation 3.1 constant and uninformative. DS6 models are re-grounded on the daily attempt count N_t, not ported from DS5. Candidate session and next-app fields were checked against the raw log and excluded after they proved to be logging artifacts. Zero-activity days within each designed period are included in the count grid. The unequal period lengths are carried into sensitivity checks because they alter slope, variance, and classification precision.

3.3.4 Structured — Task-Planning Behavior

Structured contains 61 participants and 26,729 tasks, represented by 10,529 creation, 40,718 update, and 2,439 deletion events. The episode is a task lifecycle rather than an intervention response. A last-transition-wins reconstruction yields 70.2% completed, 20.7% unresolved, and 9.1% deleted tasks.
Left-censoring is substantial: 16,213 tasks (60.7%) first appear as an update or deletion rather than a creation. Entry-state, creation-channel, and backlog analyses are therefore restricted to the 10,516 distinct tasks whose creation is observed. The two creation counts have different units: 10,529 counts creation-event rows, whereas 10,516 counts distinct tasks with at least one observed creation event. Right-censoring also means that an unresolved task cannot be distinguished from one completed after observation ended. Eligibility varies with the required feature: analyses use between 36 complete-case participants in the cross-family profile and 53 participants for configurational summaries; the pooled transition graph uses all 61. Task energy, alert, and category variables named in early conceptual documentation are absent from the export and are not treated as observed features.

3.4 Preprocessing, Eligibility, and Measurement Controls

Participant identifiers were canonicalized before linkage, timestamps were placed on a common time basis, duplicate records and impossible values were screened, and outcome codes were mapped to analysis-specific categories. The eligible denominator is reported separately for each result, because requirements differ across event, time-series, transition, survey, and complete-case analyses. Missing observations are not imputed. For regular count series, observable zero-activity days are filled with zero; for proportion series, days without an outcome-bearing event remain missing rather than being assigned zero.
Three measurement controls recur throughout the thesis. First, the sampling variance of a daily proportion is compared with $p(1-p)/n_t$, because low event counts can mimic behavioral diffusion. Second, analyses based on unequal windows are

repeated on matched or truncated windows where possible. Third, every bridge between families is checked for exact algebraic dependence, valid support, and required identities such as entropy non-negativity. Structured creation-based features are restricted to non-left-censored tasks, and conclusions concerning unresolved tasks retain the right-censoring caveat.

3.5 Operationalization and Validity Criteria

Table 3.2 distinguishes a full descriptive implementation from a proxy, simulation, or loop-motivated association. The labels describe what was actually estimated, not the conceptual reach of the source theory.

Table 3.2: Empirical operationalization and principal validity condition by model family.

Family	Empirical object	Implementation status	Principal validity or interpretation condition
Statistical mechanics	State distributions, persistence, thermodynamic analogies, JSD	Descriptive configurations; proxy analogies	Temperature and susceptibility derived from $\hat{\sigma}$ are not independent thermodynamic evidence
Dynamical systems	State trajectories and low-drift/noise regimes	Descriptive state-space summaries	No nonlinear equation, stability test, or attractor is identified from a constant-drift fit
Stochastic processes	Increment mean and standard deviation; OU approximation; Fano factor	Method-of-moments or AR(1) summaries	Boundary behavior, observation noise, Gaussianity, and time resolution must be checked
Network theory	Ordered app or task-state transitions	First-order descriptive transition networks	Edges encode temporal succession, not interaction or causality; session boundaries may be unknown
Information theory	Entropy and mutual information	Descriptive distributional summaries	Estimates depend on discretization, support, sample size, and the correct marginal population
Game theory	Ordinal commitment score	Game-theory-motivated proxy only	No payoff, utility, opponent, or equilibrium is observed

Family	Empirical object	Implementation status	Principal validity or interpretation condition
Agent-based modeling	Forward simulations of parameterized individuals	Individual-based Monte Carlo simulation	Agents do not interact; fitted inputs and in-sample targets preclude independent validation
System dynamics	Backlog stock, change scores, loop-motivated correlations	Stock descriptions and exploratory panel associations	Two-wave or observational correlations do not identify causal feedback loops

3.6 Statistical Analysis

Linear and monotonic relationships are summarized with Pearson's r and Spearman's ρ, respectively; both describe association rather than causation. Differences among group means are tested with analysis of variance (ANOVA), whose F-statistic compares between-group with within-group variation, while Mann–Whitney and Wilcoxon tests provide rank-based alternatives where distributional or pairing considerations make them more appropriate. Associations between categorical variables are assessed with χ^2 or Fisher's exact tests. Within-person or baseline-adjusted analyses are preferred when pooled estimates could mix variation within people with variation between people, and confidence intervals, eligible sample sizes, group summaries, and p-values are reported where available. No thesis-wide multiplicity correction is applied across all model-family–dataset analyses because they address heterogeneous exploratory questions, not one prespecified confirmatory family. Corrections are applied only within explicitly defined local test batteries. All other p-values are nominal exploratory summaries and are not interpreted as confirmatory evidence.

The model-family analyses additionally use drift and diffusion summaries, Fano factors, entropy, Jensen–Shannon divergence, network concentration and persistence, mutual information, and clustering diagnostics. These quantities have different scales and no shared "good" or "bad" direction. Appendix A explains where each value comes from, its range or reference point, and how to interpret it, including a worked example for $F = 5.06$, $p = 0.0071$. Chapter 4 therefore emphasizes each finding's direction, magnitude, behavioral meaning, and dataset-specific limitation rather than interpreting a test statistic in isolation.

3.7 Profile Construction

For phenotyping, candidate participant-level features were curated from the family-specific analyses, standardized, screened for near-zero variance, and checked for exact or near-exact redundancy before clustering. k-means solutions over small candidate ranges were compared using silhouette separation, minimum-cell rules, and bootstrap reassignment stability. Alternative behavior-only and network-only

feature sets were used to determine whether a solution was driven by one feature family. Cluster labels summarize the observed feature space. No temporal train/test stability or independent-cohort replication was available, so they are reported as dataset-specific behavioral profiles rather than stable types.

3.8 Data Governance, Ethics, and Use of Artificial Intelligence

The analyses use pseudonymous secondary datasets supplied within the project workspace. They do not attempt to re-identify participants and do not inspect the content viewed inside target apps. Only the minimum participant-level linkage required for longitudinal aggregation is used in the models. Consent-related eligibility available in the processed sources is preserved, and Structured's behavioral-linked sample contains only participants recorded as consenting.

Use of artificial intelligence. Artificial-intelligence tools, including ChatGPT, Claude, and NotebookLM, were used as supporting aids during the exploratory development and writing process. ChatGPT and Claude assisted with reflecting on emerging analytical observations, planning subsequent analyses, organizing initially unstructured material, supporting code development and debugging, and revising paragraph wording. NotebookLM was used to navigate and organize collected source material. These tools were not treated as empirical or scholarly sources and did not independently determine the study design, operationalizations, statistical interpretations, arguments, or conclusions. Suggested code, claims, and formulations were critically reviewed against the underlying data, executed outputs, and original sources before inclusion. The substantive logic, critical judgments, and final decisions are those of the author, who takes full responsibility for the accuracy, integrity, and final wording of the thesis.

4

Exploratory Results and Analysis

The chapter is organized by model family to compare successful translations, regroundings, and failure conditions across datasets. Conceptual diagrams explain the intended mappings. The main text retains the figures needed to explain a concept or carry a substantive finding; displaced diagnostic figures, detailed tables, and exact test statistics are preserved in Appendix B. Numerical results are retained only with the evidential status and limitations established by the audit described in Chapter 3.

Reading convention. Appendix A explains where the reported quantities come from, their possible ranges or reference values, and how to interpret F, p, r, ρ, entropy, JSD, Fano factors, profile diagnostics, and the other recurring statistics. Each dataset paragraph below should therefore be read in four steps: the observations and unit used, the relevant scale or reference, the observed comparison, and the narrow claim that comparison supports. In particular, an ANOVA F-statistic is a between-group/within-group variance ratio, whereas the Fano factor is a count variance/mean ratio; neither is a universal performance score. Each model–dataset paragraph selects one headline outcome and reports only the value or comparison needed to establish its magnitude. The consolidated statistical record, including secondary results, exact tests, and p-values, is Table B.1.

Shared claim boundaries. Generic safeguards are stated once here. Only DS5 supplies individually randomized condition contrasts; DS4 and Structured are observational, DS6's condition is cohort-level and quasi-experimental. A model-family name does not establish its corresponding physical, psychological, strategic, or feedback mechanism. Exact transformations and thresholded labels are not independent evidence, a small p-value is not an effect size, and failure to detect a difference is not proof of equality. Later cautions are retained only where a particular dataset, estimator, window, or measurement process adds something specific to these shared boundaries.

The cross-domain conceptual maps and compact translation table are given in Section 2.3. Each family below retains its complete concept and mathematical definition. The short translation paragraph then serves only as a reminder of the actual behavioral object used in One Sec and Structured before the findings are compared across datasets.

4.1 Statistical Mechanics (StM)

Concept

Statistical mechanics explains how macroscopic regularities emerge from many microscopic configurations (Netz, 2016). A system's state s occurs with probability $P(s) = e^{-\beta H(s)}/Z$, where H is an energy function, $\beta = 1/k_B T$ an inverse temperature, and Z the partition function normalizing over all states; the susceptibility $\chi = (\partial M/\partial H)_T$ measures how strongly the system responds to a small perturbation. Chapter 2 and Appendix C give the full formal apparatus, including the canonical Ising-model example of how a coupling parameter and an external field jointly select an ordered state.

Translation into the Two Domains

As summarized in Table 2.2, One Sec configurations combine app, time, condition, and response, whereas Structured configurations combine task type and task features into planning states. In both domains, temperature, energy, and equilibrium are behavioral proxies rather than observed physical quantities and may reuse the stochastic-process fit.

Results Across Datasets

DS5: order, temperature, susceptibility, landscape. Diffusion was translated into behavioral thermodynamic analogs,

$$\beta_{\text{behav}} = \frac{2}{\hat{\sigma}^2}, \qquad T_{\text{behav}} = \frac{\hat{\sigma}^2}{2}, \qquad \chi_{\text{behav}} = \beta_{\text{behav}}\, p\,(1-p), \tag{4.1}$$

with p defined as the Laplace-smoothed share of observed days on which $X_t > 0.5$ (Netz, 2016). The main result is an ordering on this constructed scale: control has the lowest mean temperature (0.0196), default the highest (0.0398), and reintervention lies between them. Lower T means less observed day-to-day fluctuation, not healthier behavior. Because T and β are exact transforms of $\hat{\sigma}$, this result restates the stochastic-process estimate rather than independently corroborating it. Susceptibility does not distinguish the arms; all supporting values are in Table B.1. Figure 4.1 is retained to make the statistical-mechanics translation visible. All three observed densities have their mode at the upper boundary, so the transformed landscapes share one boundary minimum rather than showing separate basins or a phase transition. The "potential" is therefore an explanatory display, not a literal physical energy landscape.

DS6: a condition-associated configuration shift. No inverse-temperature apparatus was built for DS6, since its unbounded daily count makes the DS5 bridge inapplicable even as a loose analogy. The microstate is instead the joint configuration of target app and hour-of-day, and configuration change is summarized by

$$\chi_i = \mathrm{JSD}\Big(P_i^{\text{baseline}}(\text{app}, \text{hour}) \,\|\, P_i^{\text{intervention}}(\text{app}, \text{hour})\Big) \in [0, 1] \text{ bit}. \tag{4.2}$$

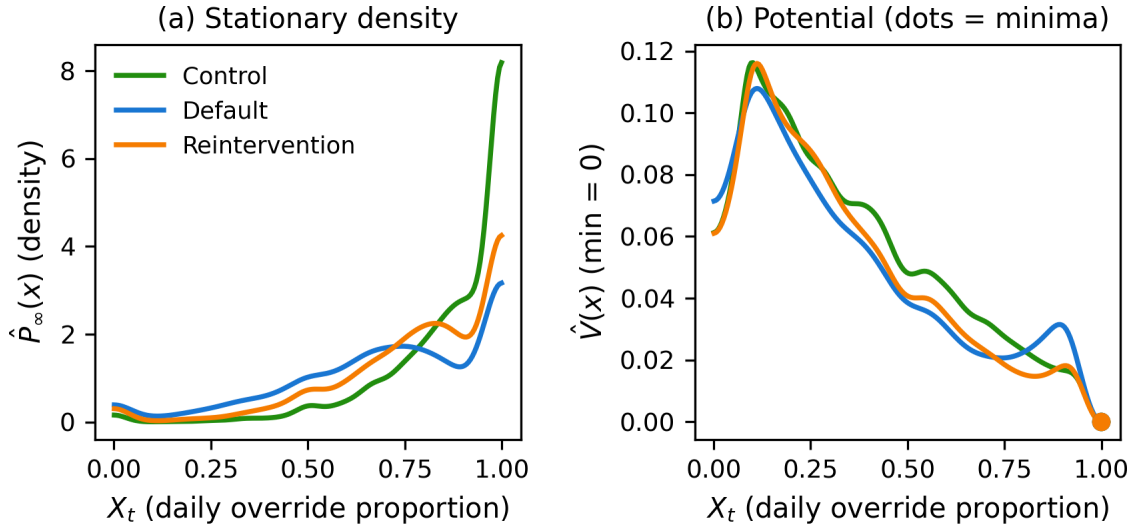


Figure 4.1: Boundary-reflected condition-level densities of the daily override proportion $X_t \in [0, 1]$ (the share of resolved opening decisions in which the app was opened) and their approximate potential transformation, by randomized condition ($N = 414$). Panel (a): estimated stationary density $\hat{P}_\infty(x)$, a reflection-corrected kernel density estimate of all daily X_t values pooled within a condition. Panel (b): behavioral potential $\hat{V}(x) = -\frac{1}{2}\bar{\sigma}^2 \log \hat{P}_\infty(x)$, where $\bar{\sigma}$ is the condition-mean increment variability, shifted so that its minimum is zero; dots mark each condition's potential minimum.

The main result is that the friction cohorts show roughly twice the reorganization of control (0.052–0.070 versus 0.028 bits). These values remain small relative to the one-bit maximum, but the cohort separation survives participant-specific finite-sampling correction. Figure 4.2 shows this comparison directly; Appendix A explains the exact test and Table B.1 retains the full statistics. Because condition is assigned at cohort level, the result is an association rather than an individually randomized effect.

Structured: no detected time-valid path dependence. Dominant weekly configurations are highly persistent, although this partly reflects the prevalence of timed tasks. The main result comes from correcting the original future-information leak: after comparing tasks within person, the association between a prior unresolved streak and added structure is practically zero ($r = 0.003$). Figure 4.3 shows the corrected pattern; descriptive configuration summaries and full tests are in Table B.1.

DS4: an identity arising from shared inputs. The statistical-mechanics entropy is numerically identical to the stochastic-process entropy H_{SDE}. It is the same measurement under a second family name, so no independent DS4 statistical-mechanics finding is claimed.

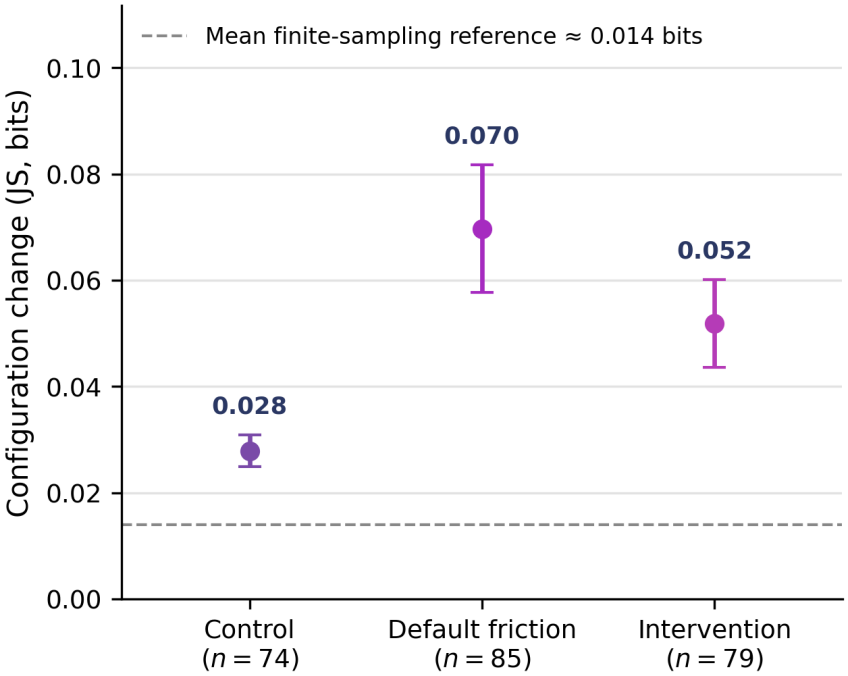


Figure 4.2: App-by-time reorganization across the DS6 condition cohorts ($n = 74$, 85 and 79 participants in the control, default-friction and intervention cohorts). The participant-level configuration change χ_i of Equation 4.2 is the baseline-to-intervention Jensen–Shannon divergence, in bits, between a participant's joint (app, hour-of-day) distributions in the two periods; points are cohort means with standard-error bars. The dashed line is the approximate mean finite-sampling reference ($\approx$ 0.014 bits). The condition comparison is cohort-level and does not estimate an individually randomized effect.

Suitability

The supported role of statistical mechanics here is distributional description. Configuration summaries such as DS6's JSD are useful, but temperature-like quantities derived from $\hat{\sigma}$ must not be counted as independent evidence. The analogy ends where the state and fitted process do not support the required occupation or potential interpretation.

4.2 Dynamical Systems (DyS)

Concept

Dynamical systems describe how a state evolves over time, deterministically or stochastically, through fixed points, attractors and bifurcations (Gunesch, 2005). A continuous system is written $\dot{x} = f(x, \mu)$ for state x and control parameter μ; a fixed point x^* satisfies $f(x^*, \mu) = 0$, and its stability is set by the sign of $f'(x^*, \mu)$. Throughout this thesis the family is implemented as the noise-free, $\sigma \to 0$ skeleton of an already-fitted stochastic process (Section 4.3) rather than as an independently

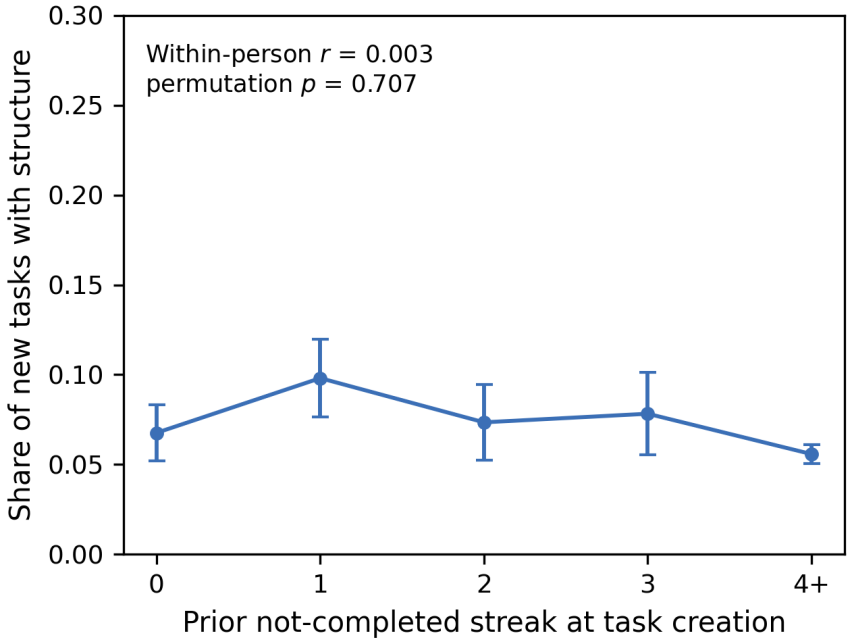


Figure 4.3: Share of newly created tasks carrying structure (recurring, having notes, or having subtasks), by the number of consecutive tasks created immediately before the current one (within participant) that were not completed at creation time; 4+ pools four or more. Error bars are 95% normal-approximation intervals; the annotation is the within-person (person-demeaned) correlation with its within-participant permutation p-value.

estimated nonlinear model, which is what makes its claims depend so strongly on how that process's state variable is bounded.

Translation into the Two Domains

One Sec trajectories use daily or weekly attempt and response states; Structured trajectories use weekly task volume, temporal structure, completion, and complexity. The reminder that matters for the results is that any fixed point or regime claim is licensed by the fitted equation and its state boundaries, not by the family name alone.

Results Across Datasets

DS5: a low-noise regime, not attractor dynamics. The family was implemented as the $\sigma \to 0$ limit of Equation 4.5. The main outcome is that the median-defined low-noise regime is more common in control than default (67.2% versus 29.6%), with reintervention between them. Figure 4.4 also shows that lower diffusion tends to accompany lower empirical entropy. Because the split is defined from $\hat{\sigma}$, it is a descriptive low-noise classification, not evidence of a fixed point, attractor, or independent four-model convergence. Full group and entropy results are in Table B.1.

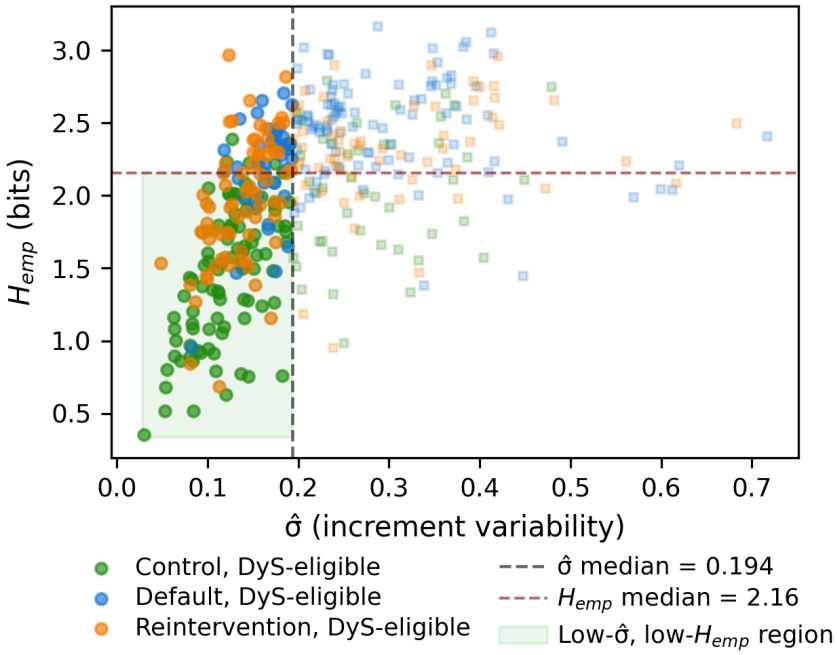


Figure 4.4: DS5 increment variability against empirical daily-state entropy ($N = 414$), combining the stochastic-process, dynamical-systems and information-theory views: $\hat{\sigma}$ is the fitted increment variability and H_{emp} the empirical entropy, in bits, of the participant's daily override proportion (ten bins on $[0, 1]$). Filled circles meet the median low-noise rule ($\hat{\sigma}$ below its sample median); the shaded quadrant, which also falls below median entropy, marks the low-noise, low-entropy region.

DS4: a model-implied equilibrium, not attractor evidence. The fitted long-run and empirical means agree almost perfectly ($r = 0.9925$), but this is the expected algebraic property of the selected AR(1) fit. The same agreement survives time shuffling, so the result checks arithmetic rather than validating a nonlinear attractor.
The diagnostic scatter plot is retained as Figure B.2 in Appendix B, where it is explicitly presented as an arithmetic check rather than attractor validation.

DS6: a descriptive low-drift classification. DS6's state variable is the daily attempt count N_t (Equation 4.10), bounded below at zero with no ceiling. The following rule partitions the two fitted increment summaries; it does not identify fixed points:

$$\text{regime} = \begin{cases} \text{stochastic} & \hat{\sigma}^{(p)} \geq \sigma_{\text{thr}}^{(p)} \\ \text{declining} & \hat{\mu} < -0.5 \quad \text{(drifts to the floor at } N = 0\text{)} \\ \text{growing} & \hat{\mu} > +0.5 \quad \text{(drifts upward, no ceiling to reach)} \\ \text{low-drift} & |\hat{\mu}| \leq 0.5 \quad \text{(approximately flat over the fitted window).} \end{cases} \tag{4.3}$$

The main result is the label's sensitivity to observation windows: after matching period lengths, the intervention low-drift count changes from 92 to 61. Figure 4.5

makes this instability visible. The labels are deterministic re-binnings of the drift and diffusion estimates, so they describe those estimates rather than independently identifying behavioral regimes. The complete matrix and sensitivity tests are in Table B.2 and Table B.1.

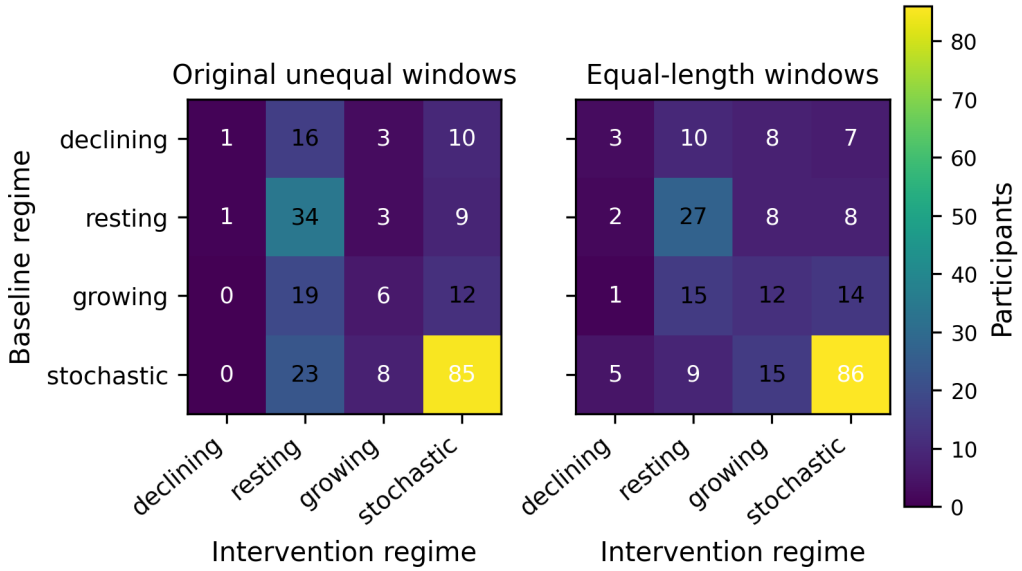


Figure 4.5: DS6 baseline-to-intervention regime transitions and their sensitivity to the observation window ($N = 230$): the original unequal windows (left) against matched participant-specific local-day windows (right). Regimes follow Equation 4.3, using the drift $\hat{\mu}$ and increment variability $\hat{\sigma}$ of the daily attempt count: "stochastic" ($\hat{\sigma}$ above the period-specific threshold), "declining" ($\hat{\mu} < -0.5$), "growing" ($\hat{\mu} > +0.5$) and "resting" ($|\hat{\mu}| \leq 0.5$), the low-drift label of that equation.

Structured: no sample-level trajectory. The median weekly volume slope is nearly zero (-0.026), so the data show no common increasing or decreasing trajectory. Apparent rarity of the "high-structure" region depends on classifier order, while volatility partly reflects gaps between observed weeks. The state labels therefore do not establish stable planner types; full sensitivity results are in Table B.1.

Suitability

State-space geometry and the fitted equation determine which dynamical claim is available. In this thesis the family mainly exposes arithmetic, classifier, and window dependencies; it does not provide independent evidence of nonlinear attractors or stable behavioral regimes.

4.3 Stochastic Processes (StoP)

Concept

Stochastic processes model randomness explicitly within a dynamical description. The notation used here follows Øksendal (2003). A state variable X_t follows

$$dX_t = \mu(X_t)\,dt + \sigma(X_t)\,dW_t, \tag{4.4}$$

where μ is the drift, σ the diffusion, and dW_t a Brownian increment. At a one-day step, the Euler–Maruyama update is $X_{n+1} = X_n + \mu + \sigma Z_n$, with $Z_n \sim \mathcal{N}(0,1)$. Most implementations below estimate the mean and standard deviation of daily increments by method of moments. These are simple process summaries compatible with the approximation; without residual, boundary, and observation-model checks they are not evidence that the full stochastic differential equation generated the data.

Translation into the Two Domains

One Sec uses daily override proportions or attempt counts; Structured uses daily task-creation and completion counts. Drift describes average direction, while diffusion or count dispersion describes how evenly or burstily activity varies around that direction.

Results Across Datasets

DS5: no identified drift or excess-variability contrast. Daily override behavior was summarized with a constant-drift approximation,

$$dX_t = \mu\,dt + \sigma\,dW_t, \tag{4.5}$$

estimated by method of moments (Øksendal, 2003). Two drift summaries are shown:

$$\hat{\mu}_{\text{end}} = \frac{X_T - X_1}{T-1}, \qquad \hat{\mu}_{\text{OLS}} = \text{slope}(X_t, t). \tag{4.6}$$

The endpoint estimate telescopes, whereas the all-days slope is less sensitive to two observations; neither detects a condition difference in direction.
The raw increment spread is

$$\hat{\sigma}_{\text{raw}} = \text{SD}(X_{t+1} - X_t). \tag{4.7}$$

Raw variability is about 0.085 higher in default than control, but daily proportions also contain binomial variation from finite decision counts. The sampling-floor comparison therefore determines whether this is excess behavioral variability.
For participant mean $\bar{X}$, the expected sampling contribution to adjacent-day increments is approximated by

$$\hat{\sigma}^2_{\text{bin}} = \frac{1}{T-1}\sum_{t=1}^{T-1} \bar{X}(1-\bar{X})\left(\frac{1}{n_t} + \frac{1}{n_{t+1}}\right), \qquad R_\sigma = \frac{\hat{\sigma}_{\text{raw}}}{\hat{\sigma}_{\text{bin}}}. \tag{4.8}$$

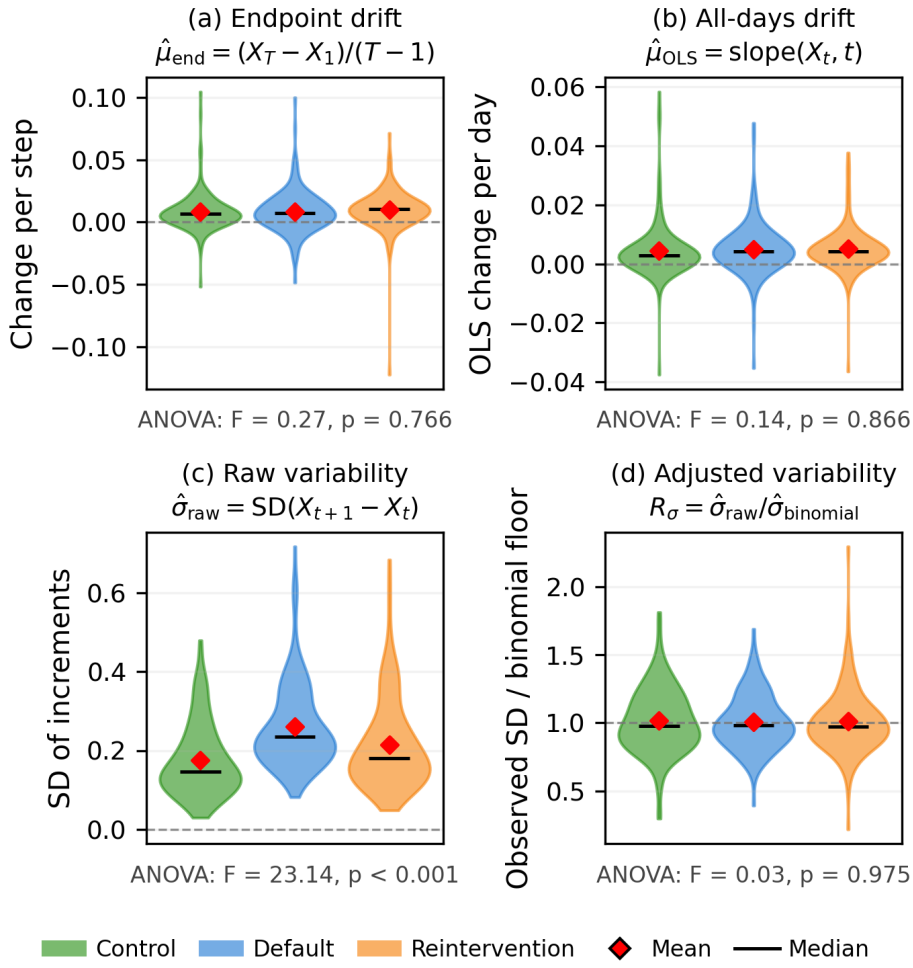


Figure 4.6: DS5 stochastic-process summaries by randomized condition ($N = 414$), computed per participant from the daily override proportion $X_t = n_{\text{opened},t}/(n_{\text{opened},t} + n_{\text{dismissed},t})$. The two drift estimators and the raw increment variability $\hat{\sigma}_{\text{raw}}$ are defined in Equations 4.6–4.8; panel (d) relates $\hat{\sigma}_{\text{raw}}$ to the binomial sampling floor $\hat{\sigma}_{\text{bin}}$ implied by the daily event counts. Dashed lines mark zero in (a)–(c) and the finite-count reference $R_\sigma = 1$ in (d); the annotation is the across-condition ANOVA statistic F and its p-value.

Here $R_\sigma = 1$ is the finite-count reference. The main result is that the raw between-arm variability difference disappears on this adjusted scale. The adjustment does not remove variability within participants; it shows that neither drift nor excess variability differs detectably between conditions. Figure 4.6 shows the raw and adjusted views together; exact statistics are in Table B.1.

DS4: a measurement artifact. DS4's long windows support a mean-reverting specification,

$$dX_t \;=\; \theta\left(\mu - X_t\right) dt \;+\; \sigma\, dW_t, \tag{4.9}$$

estimated as an AR(1) regression (Øksendal, 2003). The main result is that accounting for finite-count observation noise changes the median relaxation time from

0.63 to about 2.2 days. A single latent timescale observed at daily and weekly resolution reproduces the apparent discrepancy, so it is measurement structure rather than evidence of two behavioral timescales.
The daily-versus-weekly diagnostic scatter is retained as Figure B.3 in Appendix B; the observed-versus-simulated values are consolidated in Table B.1.

DS6: a change in activity level without a corresponding change in trend. With no dismiss/close outcome available (Section 3.3.3), the state variable is the daily attempt count on a zero-filled grid,

$$N_t^{(i,p)} = \#\{\text{app-opening events for } i \text{ on day } t\}, \qquad p \in \{\text{baseline},\ \text{intervention}\}. \tag{4.10}$$

The main result is a level change: mean daily volume falls from 45.1 to 29.1 events/-day, with larger reductions in the friction cohorts than control. The within-period drift does not change detectably, so Figure 4.7 should not be read as a steady downward trajectory. Unequal windows and cohort-level assignment limit the comparison; complete group and trend results are in Table B.1.

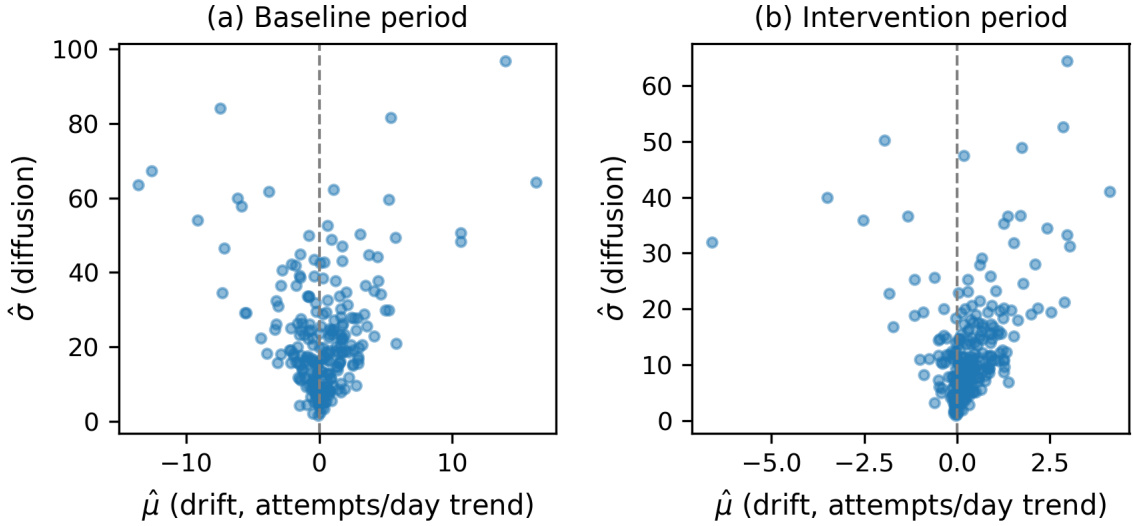


Figure 4.7: DS6 endpoint drift and increment variability, by period: (a) baseline, (b) intervention. The drift $\hat{\mu}$ is the mean daily change in attempt count and the diffusion $\hat{\sigma}$ the standard deviation of those daily changes; the state variable is the daily attempt count N_t (Equation 4.10), a behavioral proxy.

Structured: planning is overwhelmingly bursty. Two daily counts were built per participant on the zero-filled calendar grid,

$$\hat{\mu} = \tfrac{1}{T}\textstyle\sum_{t=1}^{T} \Delta N_t, \qquad \hat{\sigma} = \mathrm{sd}(\Delta N_t), \qquad F = \tfrac{\mathrm{Var}(N_t)}{\mathbb{E}[N_t]}, \tag{4.11}$$

with $F \approx 1$ Poisson-like and $F > 1$ overdispersed (Øksendal, 2003). Here F denotes the Fano factor, not the ANOVA statistic used for group comparisons.
The main result is strong overdispersion: median Fano factors lie between 3.83 and 4.96, well above the Poisson reference of 1. Planning activity is therefore episodic or

bursty. Endpoint drift and the derived "stable" label are too sensitive to endpoint and classifier choices to support a separate trend conclusion.
The full participant-level dispersion distributions are retained as Figure B.4 in Appendix B.

Suitability

Stochastic-process summaries are broadly computable and feed several later families. That makes an explicit observation model and resolution check essential: otherwise the same fitted variability can appear repeatedly as different evidence.

4.4 Network Theory (NeT)

Concept

Network theory describes a system through the relations among its components rather than their isolated properties (Newman, 2010). A network is a graph $G = (V, E)$ encoded in an adjacency matrix A, with node degree $k_i = \sum_j A_{ij}$; concentration of flow across a node's edges and the share of flow that returns to the same node are the two descriptors used throughout this thesis, alongside transition entropy (Section 4.5) as a measure of how predictable the next step is.
The general illustrated guide to hubs and centrality measures is retained in the theoretical foundations in Appendix C. The empirical analyses below use transition concentration, self-loop share, and transition entropy rather than every centrality shown there.

Translation into the Two Domains

One Sec networks connect successive target-app attempts; Structured networks connect recorded task-lifecycle states. Edges represent temporal succession, so concentration and repeated loops are descriptive structures rather than evidence of interaction, strategy, or causation.

Results Across Datasets

DS5: concentrated app-transition structure after removing one-app ceilings. Directed weighted transition graphs were built from temporally ordered events (Newman, 2010). Participants observed using only one app were excluded because their concentration is fixed mechanically. In the eligible multi-app graphs, the main result is a self-loop share of about 0.82: roughly four in five transitions repeat the same app. There is no clear condition ordering. These short, session-free event sequences describe repetition, not a switching strategy; full eligibility and group results are in Table B.1.

DS6: no robust repertoire narrowing. The apparent association between reduced volume and increased app concentration is weak ($r = -0.213$) and disappears

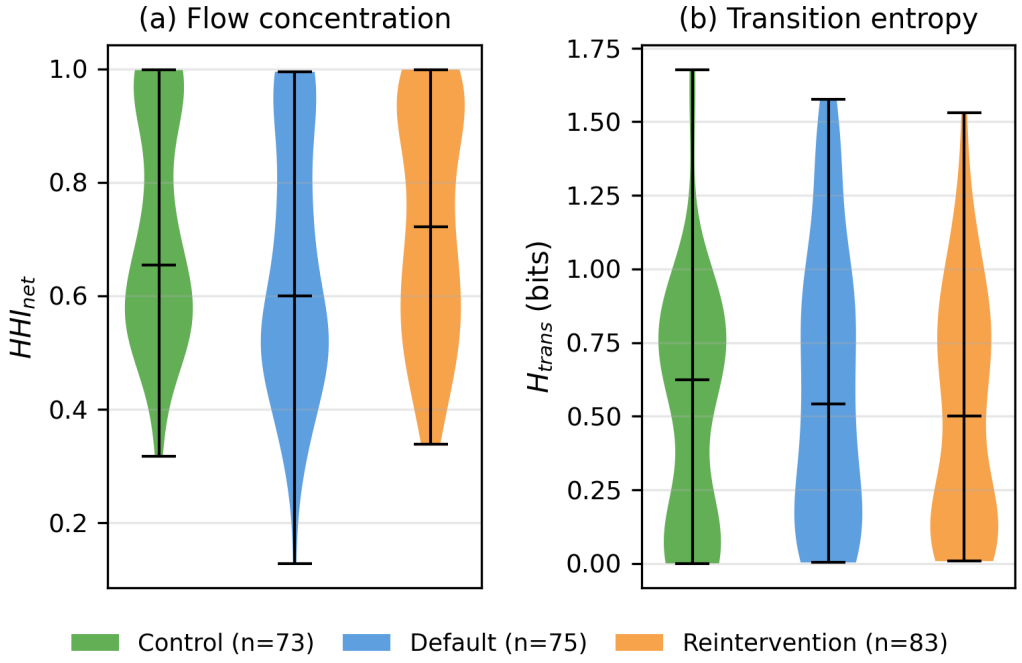


Figure 4.8: Flow concentration and transition entropy for the 231 eligible multi-app DS5 graphs, by randomized condition ($n = 73$ control, 75 default, 83 reintervention). Panel (a): $\mathrm{HHI}_{\mathrm{net}}$, the Herfindahl concentration $\sum_i (s_i^{\mathrm{out}}/M)^2$ of a participant's app-transition flow (Equation 4.12); it equals 1 when all flow leaves a single app. Panel (b): H_{trans}, the transition entropy in bits, i.e. the average uncertainty about the next app given the current one.

under rank and outlier-resistant checks. The dataset therefore does not establish that cutting back narrows use toward favorite apps. Full sensitivity results are in Table B.1.

Structured: a completion-dominated lifecycle with recurring rescheduling. Nodes are a seven-state lifecycle vocabulary, with descriptors computed over the 7×7 edge-weight matrix:

$$\mathrm{HHI}_{\mathrm{source}} = \sum_i \left(\frac{s_i^{\mathrm{out}}}{M} \right)^2, \tag{4.12}$$

$$\rho_{\mathrm{self}} = \frac{1}{M} \sum_i W_{ii}, \tag{4.13}$$

$$H_{\mathrm{trans}} = -\sum_i \frac{s_i^{\mathrm{out}}}{M} \sum_j \frac{W_{ij}}{s_i^{\mathrm{out}}} \log_2 \frac{W_{ij}}{s_i^{\mathrm{out}}}. \tag{4.14}$$

The main result is that timed→completed is the largest transition, correcting the expected timed→moved→completed pathway. Self-transitions account for 39.3% of flow, so recurrence is also prominent. Figure 4.9 shows this completion-dominated lifecycle; near-absorbing deletion limits stationary interpretation, and temporal succession does not reveal the cause of rescheduling.

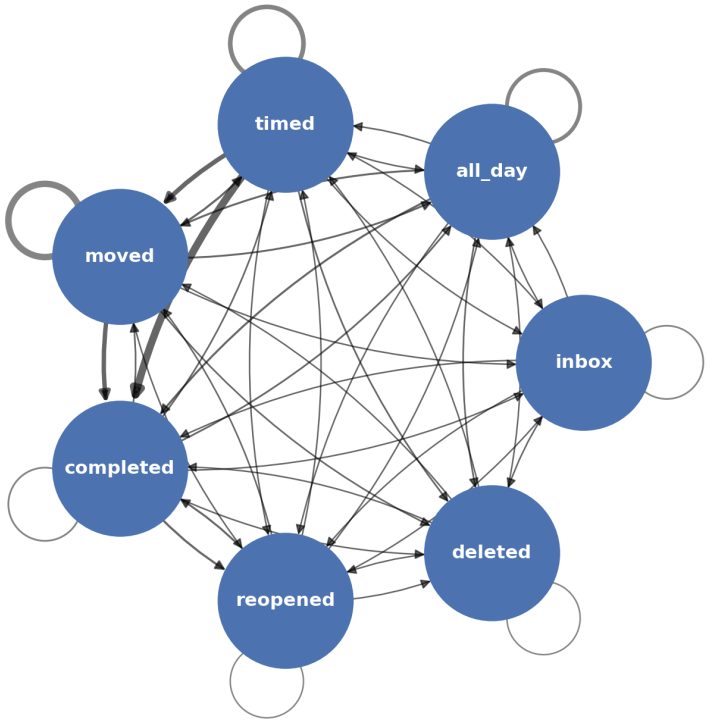


Figure 4.9: Pooled Structured task-state transition network over all 61 participants and 26,957 directed transitions between the seven lifecycle states. An arrow from state i to state j is the pooled count W_{ij} of observed transitions; edge width is proportional to flow and self-transitions are drawn as loops.

Suitability

Network measures add a genuinely different description of event order, with Structured's corrected completion pathway as the clearest contribution. In the app datasets, short windows, small vocabularies, and missing session boundaries sharply limit switching interpretations.

4.5 Information Theory (InT)

Concept

Information theory quantifies uncertainty and statistical dependence. Following Cover and Thomas (2006), Shannon entropy $H(X) = -\sum_x p(x) \log_2 p(x)$ measures how unpredictable a distribution is; mutual information $I(X;Y) = H(X) + H(Y) - H(X,Y)$ measures how much knowing one variable reduces uncertainty about another. A recurring bridge throughout this thesis converts a fitted diffusion estimate (Section 4.3) directly into an entropy,

$$H_{\mathrm{SDE}} = \tfrac{1}{2} \log_2\left(2\pi e\, \hat{\sigma}^2\right), \tag{4.15}$$

the differential entropy of a Gaussian with variance $\hat{\sigma}^2$ (Cover & Thomas, 2006). Because H_{SDE} is a strictly increasing function of $\hat{\sigma}$ alone, it never adds information beyond the increment-variability estimate. Agreement with an empirical entropy of *levels* can show consistency in the ordering of spread, but it cannot test whether increments are Gaussian; that requires direct residual or increment diagnostics.

Translation into the Two Domains

One Sec entropy describes uncertainty in outcomes, apps, hours, and daily states; Structured entropy describes diversity in task type, timing, recurrence, and terminal status. Mutual information asks whether knowing one recorded variable reduces uncertainty about another, while bridge identities provide mechanical consistency checks across families.

Results Across Datasets

DS5: uncertainty is multidimensional. Shannon entropy was computed for outcome, app, hour and the daily state series. The headline outcome is that empirical daily-state entropy rises from 1.652 bits in control to 2.387 in default, with reintervention between them. Higher entropy means less concentrated daily states, not better behavior. The other dimensions do not follow one common ordering, and the Gaussian bridge repeats the variability estimate rather than validating it independently. Full values are in Table B.1.

How to read the five panels. Entropy is easiest to understand here as a measure of how concentrated or mixed an observed distribution is. Low entropy means that one outcome, app, hour, or daily-state bin dominates and is therefore relatively predictable; high entropy means that observations are spread more evenly and are less predictable. A rise in entropy can consequently be consistent with an intervention disrupting or mixing an established behavioral pattern, but it is not automatically beneficial or harmful. That judgment requires the behavioral context and, where possible, additional outcomes.
The first panel concerns friction *outcomes*: control is lower than the two friction-exposed conditions, so observed outcomes are less diverse in control and more mixed after friction is introduced. This comparison is descriptive because the available outcome categories themselves differ by condition. The second panel concerns *apps*; the strongly overlapping distributions, large mass near zero, and long upper tails show little direct condition separation in app diversity. The third concerns *local hour*; all conditions are concentrated at similarly high values, so behavior is distributed over many hours and this temporal spread changes little across conditions. The fourth concerns the *daily override-rate distribution*; control is lowest, default highest, and reintervention intermediate, meaning that day-to-day states are less concentrated and less predictable in the friction-exposed conditions on this binning. The fifth converts the stochastic increment spread into Gaussian differential entropy and therefore mirrors its ordering. It provides a mathematical bridge between the stochastic-process and information-theory descriptions, but not an independent fifth

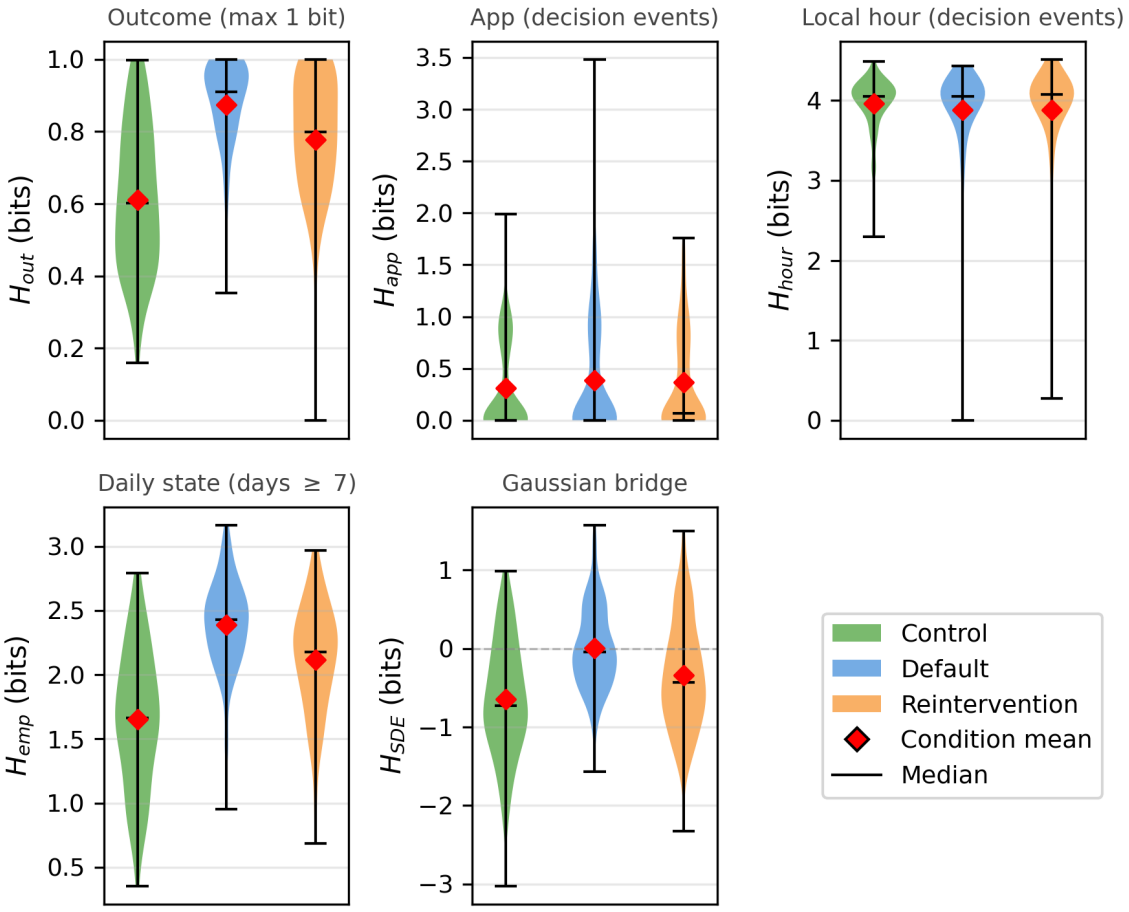


Figure 4.10: Five DS5 entropy summaries by randomized condition, per participant and in bits: outcome entropy H_{out} (opened versus dismissed; maximum 1 bit), app entropy H_{app} and local-hour entropy H_{hour} on the decision-event subset ($N = 478$), and empirical state entropy H_{emp} of the daily override proportion X_t (ten bins on $[0, 1]$, at least seven observed days) and the Gaussian differential-entropy bridge H_{SDE} (Equation 4.15, which can be negative) on the daily-series subset ($N = 414$).

finding. Taken together, the panels show why "uncertainty" is not a single quantity: some behavioral dimensions are condition-sensitive, while others show little difference across conditions.

DS4: an algebraic identity rather than independent evidence. H_{SDE} is the differential entropy of the fitted stationary distribution and is identical to the quantity reported under statistical mechanics. The outcome is a dependency check, not a second empirical finding.

DS6: period does not predict app identity. The main result is a pooled mutual information of only 0.0003 bits: knowing the period removes virtually none of the uncertainty about which app appears. Participant-level spread measures still order people similarly, but that bridge is not independent evidence and does not

contradict individual users narrowing toward different favorite apps. Full bridge and diagnostic values are in Table B.1.

Structured: concentrated task types, diverse timing. Task type at creation has only 0.200 bits of entropy, whereas creation time is much more diverse. In other words, the recorded task types are highly concentrated, whereas task-creation times are considerably more diverse. Class imbalance invalidates the largest-looking mutual-information value, and the network bridge works only with the correct destination-state marginal. Detailed scales and bridge checks are in Table B.1.

Suitability

Information theory is portable and useful as an audit layer. Its strongest contribution is the ability to compare uncertainty on explicit scales and to catch invalid cross-family bridges through support, marginal, and non-negativity checks.

4.6 Game-Theory-Motivated Commitment Proxy (GaT)

Concept and Empirical Status

Game theory models decisions whose outcomes depend on the strategies of interacting actors (Hotz, 2006). A formal game requires players, strategies, and payoffs; equilibrium analysis additionally requires a specified payoff structure. None of the datasets observes a payoff, utility, or strategic opponent. This section therefore does not implement a game-theoretic model. It evaluates an ordinal commitment proxy motivated by a tension between immediate flexibility and longer-term commitment. For One Sec, opening versus dismissing an attempt can be described informally as a choice between immediate access and self-regulation. For Structured, task features can be ordered from flexible (inbox or all-day) to more committed (timed, recurrent, or otherwise structured). These descriptions motivate variables but do not identify preferences, strategies, or equilibria.

Results Across Datasets

DS5: a post-assignment response summary, not a moderator. The commitment proxy is the proportion of outcome-bearing attempts not resolved by opening. Because it overlaps with the override rate and is measured after assignment, its only supported outcome is a descriptive response summary. It is neither an independently identified preference nor a treatment moderator.

Structured: no consistent commitment optimum. Pooled completion rises from 36.7% at score 0 to 79.0% at score 2, but does not continue upward. Within-person and censoring-restricted patterns peak elsewhere, so the apparent optimum is not consistent across analyses. The index counts recorded task features rather

than utility or quality and supports neither a causal trade-off nor adaptation after rescheduling. Full checks are in Table B.1.

Suitability

The score can organize descriptive comparisons but is not a payoff or a game. Formal game theory would require observed utilities, a strategic counterpart, and repeated interaction.

4.7 Individual-Based Simulations (ABM)

Concept and Empirical Status

Agent-based modeling examines how population patterns can emerge from heterogeneous agents, interaction rules, and an environment (Borrill & Tesfatsion, 2011; Macal & North, 2010). The implementations in this thesis simulate one independently parameterized trajectory per participant. Agents do not interact with one another or adapt to a shared environment. The work is therefore more accurately described as individual-based Monte Carlo simulation than as a conventional ABM of emergence. Parameters are taken from models already fitted to the same participants, so agreement is an in-sample consistency check rather than independent validation.

Results Across Datasets

DS4: the observation process is necessary. Simulations based only on each participant's fitted mean-reverting parameters do not reproduce the observed difference between daily and weekly relaxation estimates. The single outcome is diagnostic: finite-count observation noise is a necessary part of the specification, not evidence for two latent behavioral timescales.

Structured: episodic activity is necessary but insufficient. A static simulation produces a Fano factor near 1, and adding an on/off state raises it to about 3.4, still below the observed 6.0. Episodic activity therefore explains part, but not all, of the burstiness. Because parameters come from the same participants and there is no held-out test, this is model criticism rather than validation.

Suitability

These simulations identify missing observation and episodic-activity processes. They do not test conventional agent-based emergence because the simulated individuals do not interact or adapt to a shared environment.

4.8 System-Dynamics-Motivated Stock and Loop Analysis (SyD)

Concept

System dynamics represents system-wide change through stocks, flows, delays, and feedback loops (Kunc, 2016). A stock accumulates as $\text{Stock}(t) = \int_{t_0}^{t}[\text{Inflows}(s) - \text{Outflows}(s)]\,ds + \text{Stock}(t_0)$; a reinforcing loop amplifies a trend, a balancing loop corrects it. Unlike the other seven families, this one needs a stock that persists and is measured more than once, which is a data-availability requirement rather than a conceptual one — it rules the family out on datasets that satisfy every other family's needs.

Translation into the Two Domains

One Sec supplies repeated survey measures only in DS6, allowing exploratory pressure and self-regulation loop associations. Structured supplies an observable backlog stock. Task creation is an inflow, while completion and deletion are outflows. Rescheduling changes a task's scheduled state but does not by itself change the number of unresolved tasks. DS5 and DS4 have no repeated stock measure.

Results Across Datasets

DS6: no supported loop association. After controlling each two-wave change score for its baseline, all proposed pressure and self-regulation relationships remain negligible to weak ($|r| \leq 0.111$). The dataset therefore does not support the proposed loop direction. With only two waves these are panel associations, not causal feedback tests; complete results are in Table B.3.

Structured: backlog grows for everyone, and pooled loops mislead. For each non-censored task with entry week e_i and exit week x_i, backlog is

$$B_w \;=\; \Big|\, \{\, i \;:\; e_i \leq w \;\wedge\; (x_i > w \;\vee\; x_i = \emptyset)\,\} \,\Big|, \tag{4.16}$$

initialized at zero in each participant's own week 0 and therefore a known undercount.
The main result is that backlog rises by a median of about 1.7 recorded unresolved tasks per participant-week. Every fitted trajectory is positive, but right-censoring and unresolved tasks at the end of observation make that growth partly an observation-window result. The sign is not a welfare judgment.

How to read the backlog trajectories. Each line is one participant, and an upward segment means that more recorded tasks remain unresolved than in the previous participant-relative week. A steeper line can reflect more task creation, fewer recorded resolutions, or both; it is not by itself evidence of overload or poor planning. The shared zero at entry and unresolved tasks at the right edge make positive

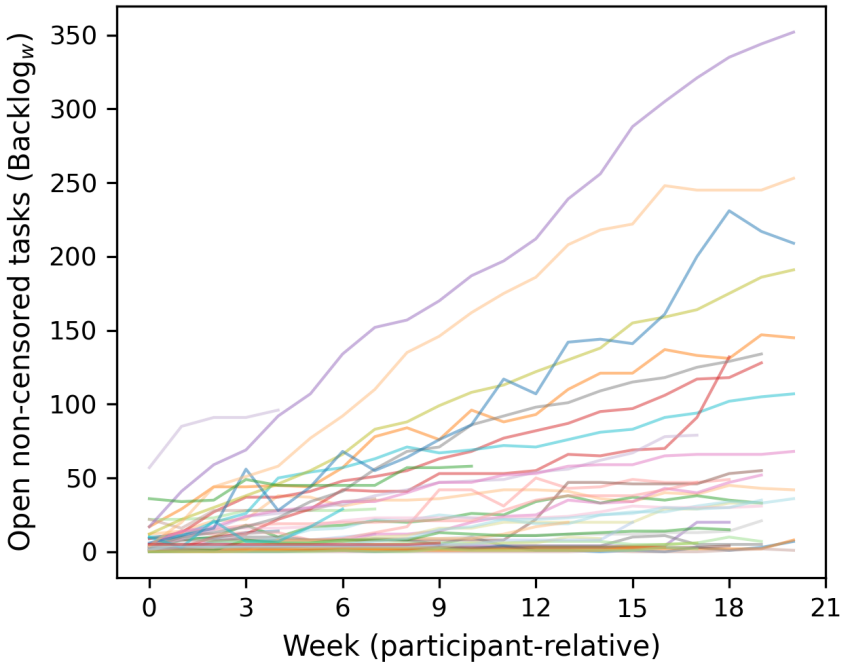


Figure 4.11: Weekly backlog stock against participant-relative week ($N = 47$ eligible participants), one line per participant. The backlog B_w of Equation 4.16 is the number of open non-censored tasks at week w, that is, tasks with a visible creation event that have not yet been completed or deleted.

slopes easier to produce, while a few high-volume participants stretch the vertical scale. The figure therefore demonstrates that a backlog stock can be reconstructed from the lifecycle data and that it usually accumulates within the observed window. It does not, without the loop checks below, explain why that accumulation occurs. The proposed explanations do not survive person-mean centering: large pooled correlations reduce to weak within-person relationships. Thus Figure 4.11 establishes an observable stock, not the mechanism producing it. Complete loop coefficients are in Table B.4.

Suitability

System dynamics is available only where repeated measurements or an open lifecycle supply a stock. It contributes an accumulation measure in Structured, but the proposed DS6 and Structured loops are unsupported after baseline or within-person adjustment.

4.9 Cross-Family Profiles and Redundancy

This section combines participant-level features from the preceding families and asks whether they recover low-dimensional structure beyond a single summary. Features were standardized, screened for near-zero variance and exact dependence, and compared in blended, behavior-only, and network-only sets. The reading key in

Table A.3 is especially important here: silhouette measures separation, bootstrap Jaccard measures resampling stability, and ARI measures agreement between two partitions. These answer different questions. Only the dataset-specific core feature sets described below determined cluster membership. Additional radar axes are descriptive summaries plotted after assignment; they did not determine the clusters. For visualization, all radar axes were subsequently min–max normalized to $[0, 1]$ within each analytical sample. The plotted values therefore show relative positions within a dataset, not absolute scores that can be compared across datasets.

Profile Structure by Dataset

DS5: a resampling-stable but feature-sensitive blended partition. After excluding participants with only one observed target app, the complete-case feature set was

$$\{\hat{\sigma}, H_{\text{emp}}, x_{\text{mean}}, \text{HHI}_{\text{net}}, \rho_{\text{self}}\}.$$

The main outcome is a two-profile blended partition that is reproducible under resampling (Jaccard 0.842) but changes when individual core features are removed. Because its inputs are post-assignment and membership is condition-associated, the profiles summarize observed response patterns. Complete sensitivity results are in Table B.5.

DS4: behavior dominates a related network partition. The network-only partition has near-chance agreement with the blended solution (ARI = 0.047), although the heatmap in Figure 4.14 shows that the separate label systems are still associated. The profiles therefore reflect primarily behavioral features, not a universal network–behavior geometry.

DS6: one constructed indicator dominates. The supplied `regime_changed` feature explains 93.4% of between-cluster separation. The solution therefore restates one input rather than discovering a multivariate profile; dropping it isolates only a small high-JSD tail.

Structured: a behavior-dominated, gap-confounded solution. A behavior-only analysis reproduces the selected partition exactly (ARI = 1.000), so network features do not drive it. However, the more volatile profile also has longer observation gaps, and its apparent backlog contrast disappears after adjustment. The small solution therefore partly captures intermittency, not a verified planner type.

Dataset-Specific Profile Geometry

The shared result is low dimensionality, not a common taxonomy. These are dataset-specific profiles of observed traces, with no evidence that membership persists across time or contexts.

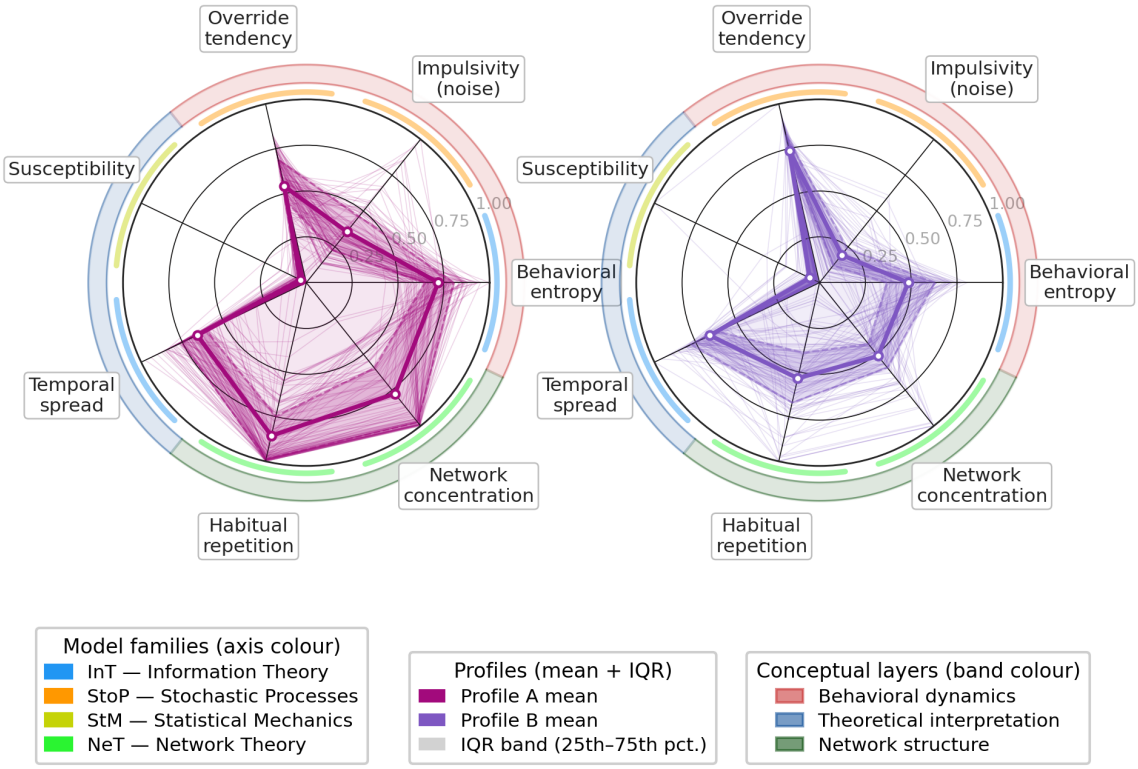


Figure 4.12: Min–max-normalized DS5 profile means for the five core response and transition features; additional displayed axes are secondary descriptive summaries. Profile A ($n = 112$) and Profile B ($n = 97$). Core axes: Behavioral entropy (H_{emp}, information theory), Impulsivity (noise; $\hat{\sigma}$, stochastic processes), Override tendency (mean daily override proportion x_{mean}, stochastic processes), Habitual repetition (ρ_{self}, network theory) and Network concentration (HHI_{net}, network theory). Secondary axes: Susceptibility (χ_{behav}, statistical mechanics) and Temporal spread (H_{hour}, information theory). Each axis is min–max normalised to $[0, 1]$ over the plotted population; the band is the interquartile range (IQR, 25th–75th percentile).

Why the DS5 profiles are not treatment moderators. The final DS5 profiles are derived entirely from behavior observed after randomized condition assignment, and membership is itself associated with condition. Stratifying the condition contrast by these profiles would therefore condition on a post-treatment variable and could introduce selection bias. Earlier interactions based on a different, network-only partition are not retained as evidence of personalized treatment response. A valid moderation analysis would require profiles fixed from pre-treatment data, applied without refitting, and evaluated against a prospectively specified outcome. The present profiles show heterogeneous post-assignment response patterns only.

Cross-family methodological findings. Three forms of non-independence recur. First, β_{behav}, T_{behav}, and H_{SDE} are deterministic transforms of $\hat{\sigma}$. Second, several regime labels threshold the same drift and variability estimates. Third, entropy bridges can use an inappropriate marginal population unless their support is checked explicitly. Agreement under several model-family names can consequently represent

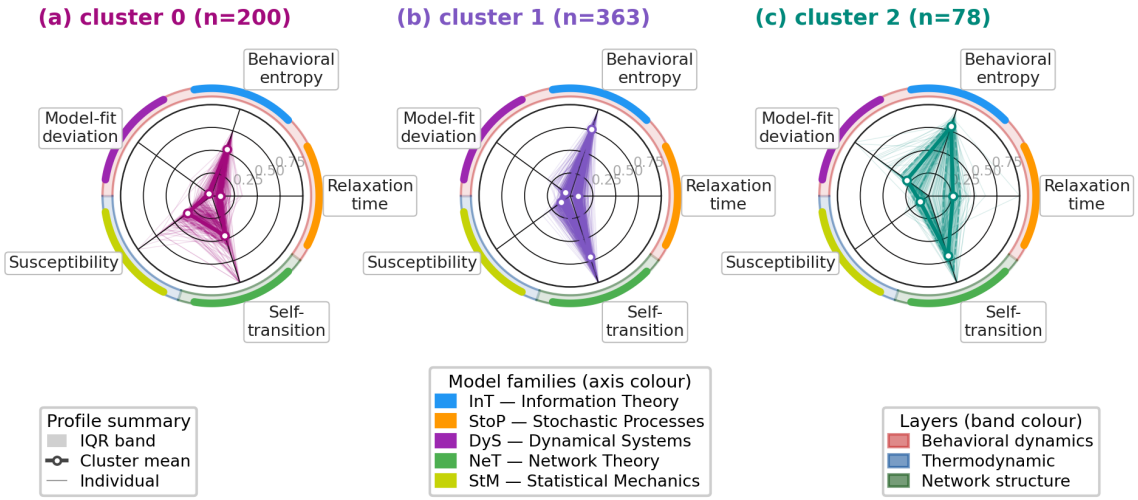


Figure 4.13: Min–max-normalized feature summaries for the selected DS4 blended $k = 3$ solution ($N = 641$), one panel per cluster. Axes: Relaxation time ($\hat{\tau} = 1/\hat{\theta}_{\mathrm{OU}}$, stochastic processes), Behavioral entropy (H_{emp}, information theory), Model-fit deviation ($|\bar{X} - \hat{\mu}_{\mathrm{OU}}|$, dynamical systems), Susceptibility ($\chi_{\mathrm{OU}} = \beta_{\mathrm{OU}}\, p(1-p)$ with $\beta_{\mathrm{OU}} = 2\hat{\theta}_{\mathrm{OU}}/\hat{\sigma}^2$, statistical mechanics) and Self-transition (ρ_{self}, network theory). Each axis is min–max normalised to $[0, 1]$ over all 641 participants; the band is the interquartile range (IQR, 25th–75th percentile).

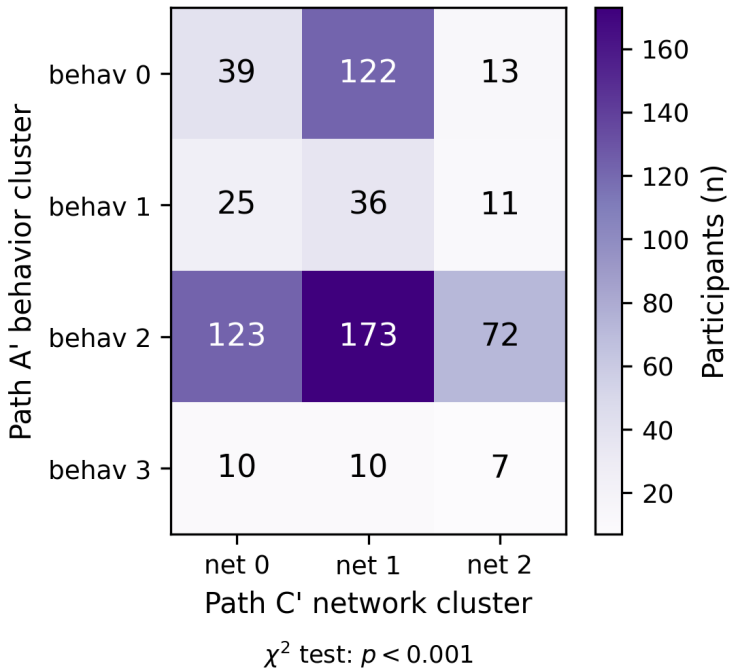


Figure 4.14: Joint distribution of the separately fitted behavior-only (rows) and network-only (columns) DS4 partitions ($N = 641$); each cell is the number of participants in that combination. The χ^2 test of independence between the two partitions gives $p < 0.001$.

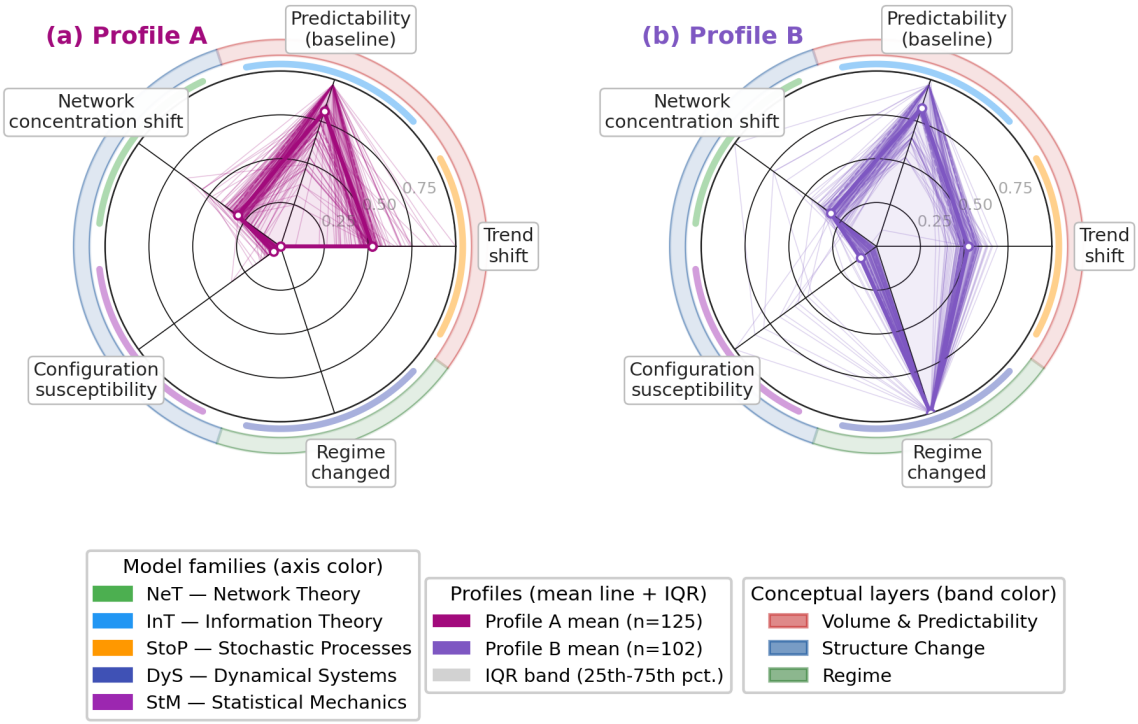


Figure 4.15: Min–max-normalized summaries for DS6 Profile A ($n = 125$) and Profile B ($n = 102$). Axes: Trend shift ($h_{\text{period}} = \hat{\mu}_{\text{intervention}} - \hat{\mu}_{\text{baseline}}$, stochastic processes), Predictability (baseline; the baseline empirical entropy H_{emp} of daily attempt counts in ten quantile bins, where higher values mean less predictable; information theory), Network concentration shift (the intervention-minus-baseline change in HHI_{net}, network theory), Configuration susceptibility (χ_i of Equation 4.2, statistical mechanics) and Regime changed (binary indicator that the dynamical-systems regime label differs between periods). Each axis is min–max normalised to $[0, 1]$ over all 227 participants; the band is the interquartile range (IQR, 25th–75th percentile).

a single underlying observation. Likewise, a simulation that under-reproduces observed dynamics identifies missing observation, session, or temporal-state structure in the tested specification; it does not show that the entire generative model family fails. Dependency checks and model criticism are thus central results of the framework rather than secondary diagnostics.

Answer to the profile subquestion. The derived features reveal person-level heterogeneity beyond group means, but the recovered structure is smaller, less robust to feature choice, and more dataset-dependent than the number of model families might suggest. DS5 produces a feature-sensitive blended partition; DS4 produces related but low-agreement behavioral and network partitions; Structured produces a small and partly confounded behavioral partition; and DS6 is dominated by a supplied indicator. The evidence therefore supports low-dimensional, dataset-specific profiles whose meaning depends on measurement design and explicit redundancy checks, not a universal profile taxonomy or dynamic user types.

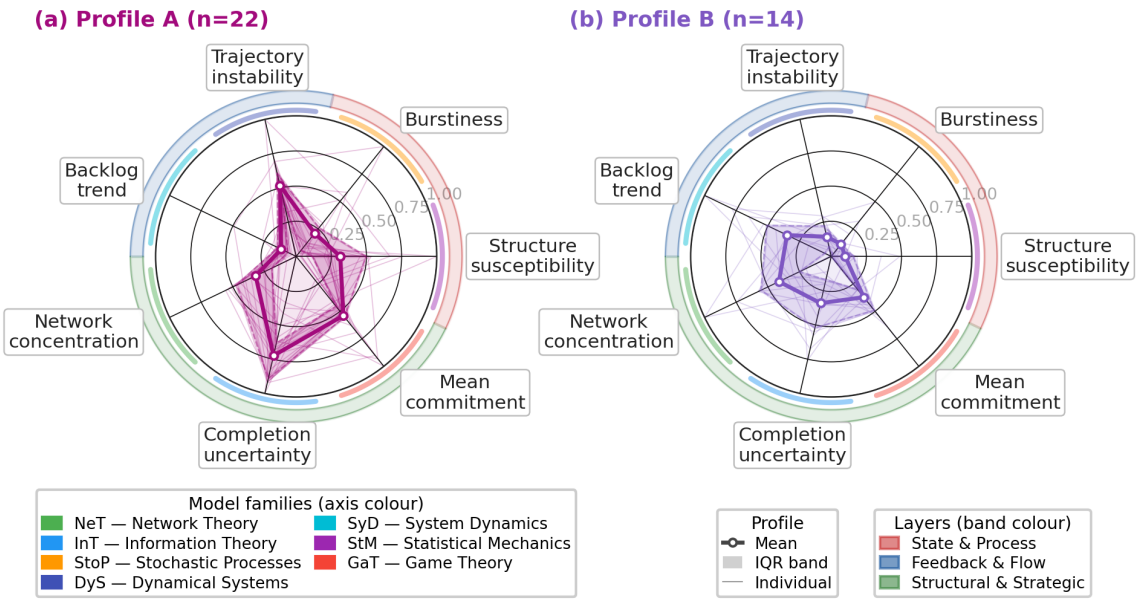


Figure 4.16: Min–max-normalized feature summaries for the two Structured profiles, Profile A ($n = 22$) and Profile B ($n = 14$), complete cases ($N = 36$). Profile A is the more volatile profile (higher burstiness, trajectory instability, structure susceptibility and completion entropy), Profile B the calmer one with a steeper backlog trend. Axes: Structure susceptibility (frequency-weighted variance of completion rate across the participant's three most frequent task configurations, statistical mechanics), Burstiness (Fano factor $F = \mathrm{Var}(N_t)/\mathbb{E}[N_t]$ of daily timed-task creations, stochastic processes), Trajectory instability (mean distance between consecutive standardized weekly state vectors, dynamical systems), Backlog trend (slope of the weekly backlog B_w, system dynamics), Network concentration ($\mathrm{HHI}_{\mathrm{net}}$, network theory), Completion uncertainty (entropy $H_{\mathrm{completion}}$ of the completed/deleted/unresolved task outcome, where higher values mean greater uncertainty; information theory) and Mean commitment (the participant's mean commitment score, game theory). Each axis is min–max normalised to $[0, 1]$ over the 36 plotted participants; the band is the interquartile range (IQR, 25th–75th percentile).

Table 4.1: Recoverable profile structure in the four behavioral datasets.

Dataset	Dominant structure	Secondary structure	Evidential interpretation
DS5	Blended response and transition summaries	No invariant secondary partition	Resampling-stable under bootstrap but feature-sensitive and condition-associated
DS4	Behavioral/process summaries	Network concentration	Separate partitions have low ARI but are statistically associated
Structured	Behavioral and intermittency summaries	Task-state network	Small, coupled solution; behavioral interpretation is confounded by observation gaps
DS6	Supplied regime-change indicator	High-JSD outliers	Marginal one-feature split, not a recovered multivariate profile

5

Overall Discussion and Conclusion

5.1 Answer to the Research Question

This thesis asked:

> *To what extent can eight CAS-inspired model families be operationalized as valid, non-redundant descriptions of heterogeneous digital trace data across behavioral domains, and what low-dimensional phenotype structure, if any, do they recover?*

The answer is conditional. Several families yield useful descriptions when their empirical objects are stated narrowly: increment summaries, entropy, transition concentration, configuration change, and a backlog stock. These features expose person-level heterogeneity that group means conceal. The data do not identify payoffs or equilibria, interacting adaptive agents, nonlinear attractors, or causal feedback loops. Several quantities under different family labels are also transforms or thresholds of the same estimate. The framework is therefore most defensible as a theory-guided approach to feature derivation and model criticism, rather than evidence for eight independent mechanisms or a unified CAS theory of digital behavior. The profile analyses recover low-dimensional, dataset-specific groupings rather than a universal taxonomy. DS5 yields a resampling-stable but feature-sensitive grouping. The other datasets recover weaker, partly confounded, or single-feature structures. No analysis tests whether membership persists within a person across time or contexts. These outputs are profiles of observed traces, not diagnostic or stable user types.

Exploratory and corrective contribution. The contribution is a graded answer to whether methods from physics, mathematics, and computational modeling can be mapped meaningfully onto sparse, heterogeneous digital traces. Across a bounded proportion, an unbounded count, and discrete task configurations, some families yield robust descriptors, some dependent analogies, and others expose missing data requirements; some proposed findings also become unidentifiable after correctness checks. The deliberate breadth functions as an initial screening design: it makes unexpected fits, principled exclusions, and future data requirements visible without claiming equal depth or definitive validation for all eight families. The correctness audit is part of that contribution: it identified wrong entropy marginals, algebraically dependent evidence, premature reporting gates, sampling-floor effects, window sensitivity, censoring, and pooled-versus-within-person discrepancies. Incorporating these checks turns a catalog of models into an account of when each behav-

ioral claim is justified. The framework states the ingredients each family needs, maps them to observable traces where possible, and marks where a descriptive translation no longer identifies a proposed mechanism. A limitation therefore need not mean either a weak theory or a generally poor dataset; it can reflect a mismatch between a question requiring payoffs, interactions, dense dynamics, or temporal ordering and data collected without those variables or resolutions. Negative or ambiguous results thereby become concrete requirements for future measurement and study design.
Table 5.1 condenses the final empirical role of each family. These roles are not rankings of theoretical quality. They state what the present operationalization and data can support: a descriptive quantity, a diagnostic analogy, a partial proxy, or a mechanism that remains unidentified.

Table 5.1: Final empirical role and claim boundary of each model family.

Model family	Supported contribution	Claim boundary
Statistical mechanics	Configuration displays; DS6's JSD summarizes condition-associated routine reorganization.	DS5 temperature and inverse temperature inherit $\hat{\sigma}$; no thermodynamic mechanism or phase transition is identified.
Dynamical systems	Checks whether the state geometry and fitted equation permit equilibrium or regime claims.	Constant-drift fits do not establish nonlinear attractors; several labels inherit threshold, endpoint, or window choices.
Stochastic processes	Drift, variability, relaxation, and count-dispersion summaries are broadly computable.	Interpretation depends on observation noise, boundaries, increment assumptions, and temporal resolution.
Network theory	Independent descriptions of ordered app and task-state transitions; the Structured analysis corrected the expected task pathway.	Logged succession is not interaction, strategy, or causality; vocabulary and window length constrain the graph.
Information theory	Portable uncertainty summaries and non-negativity or chain-rule checks that detect invalid bridges.	Estimates depend on discretization, support, sample size, and the correct marginal population.
Game theory	An ordinal commitment proxy organizes descriptive comparisons.	No utility, strategic counterpart, payoff structure, or equilibrium is observed.
Individual-based simulation	Forward simulation exposes missing observation and episodic-activity processes.	Agents do not interact; in-sample fitted inputs and targets do not validate emergence or a conventional ABM.
System dynamics	Backlog stocks and repeated-wave change descriptions where the data provide a persistent stock.	Observational or two-wave loop associations do not identify causal feedback.

5.2 What Was Learned From the Four Subquestions

5.2.1 Operationalization Requires Dataset-Specific Validity Conditions

The same conceptual family did not translate into the same estimator everywhere. A bounded daily override proportion in DS5 and DS4 carries binomial sampling variance; DS6's structurally constant outcome required a count state instead; Structured required task-lifecycle states and open-ended stocks. This re-grounding is a substantive result. A model family transfers only at the level of a question or principle, not by relabeling the same formula across incompatible observables.

The most portable families were those closest to measurement. Information-theoretic entropies, first-order transition summaries, and simple increment or count-dispersion statistics could be computed wherever suitable support existed. Even these required safeguards: correct marginal distributions, sufficient event counts, explicit discretization, session assumptions, and an observation model. Statistical-mechanics quantities were useful as configuration displays and analogies, but temperature and susceptibility constructions often inherited $\hat{\sigma}$ exactly. Dynamical labels similarly re-binned process estimates rather than identifying new dynamics.

The remaining families clarified what the datasets lacked. The commitment score was not a formal game because no utility or strategic counterpart was observed. The simulations contained heterogeneous individuals but no agent interaction or emergent environment. System-dynamics- motivated analyses produced a backlog stock and exploratory panel associations, but two-wave or observational correlations did not identify feedback. These are not demonstrations that game theory, ABM, or system dynamics are unsuitable for digital behavior. They show that the present data and implementations do not identify the mechanisms those families require.

5.2.2 Cross-Domain Transfer Was Partial Rather Than Literal

Transfer from One Sec to Structured was most successful for questions about variability, uncertainty, and ordered transitions. In each domain, count dispersion distinguished steady from episodic activity, entropy described the diversity of observed states, and transition networks showed concentration and recurrence. The behavioral meanings nevertheless changed: an app-opening attempt is a short friction episode, while a task lifecycle is open-ended and censored. A quantity with the same mathematical form did not automatically have the same construct interpretation.

This distinction is particularly important for system boundaries. The data record events produced by a coupled person–tool process. They do not directly observe interacting psychological components, adaptation rules, or emergence. Cross-domain reuse of a descriptor supports the portability of that descriptor, not the claim that both domains instantiate the same CAS mechanism.

The empirical conclusions are therefore also dataset-specific. Table 5.2 separates the strongest supported conclusion in each analyzed dataset from the design or measurement boundary that limits its interpretation.

Table 5.2: Dataset-specific conclusions and inferential boundaries.

Dataset	Strongest supported conclusion	Principal boundary
DS5	Randomized arms differ in their observed override distributions, and substantial person-level heterogeneity remains visible.	Drift and sampling-adjusted variability do not differ between arms; final profiles are post-assignment summaries, not treatment moderators.
DS4	Long series show that temporal resolution and finite event counts can reproduce apparently fast dynamics.	The cohort is naturalistic and has no randomized condition, so it supports no causal friction contrast.
DS6	Daily attempt volume falls, and the friction cohorts show more app-by-time configuration reorganization than control.	Condition is cohort-level, observation windows are unequal, and the logged outcome cannot distinguish opening from dismissal.
Structured	Planning counts are episodic and overdispersed; the task lifecycle is concentrated and supplies an observable backlog stock.	Heavy censoring prevents strong conclusions about an optimal commitment level, path dependence, or causal feedback.

5.2.3 Person-Level Structure Is Low-Dimensional and Conditional

The strongest person-level contribution is not a new set of user types. It is the demonstration that digital traces contain heterogeneous, low-dimensional combinations of behavioral and transition summaries, but that the recovered geometry depends on the feature set and dataset. In DS5, the blended solution is reproducible under resampling yet changes substantially when single core features are omitted and is associated with randomized condition. In DS4, the separate behavioral and network partitions have low agreement but remain statistically associated. These results argue against a universal geometry and show why resampling stability alone is insufficient for construct validity.

The weaker results are equally informative. DS6's clustering is mainly a binary input feature, and Structured's small solution partly reflects gaps between active weeks. High silhouette or bootstrap stability can coexist with a one-feature split or a measurement confound. Clustering diagnostics establish internal reproducibility under resampling; they do not establish construct validity, temporal stability, or psychological reality.

5.2.4 Non-Redundancy and Identifiability Are Part of the Result

Several apparent examples of cross-model convergence disappeared under dependency checks. H_{SDE}, behavioral temperature, and inverse temperature are monotone functions of $\hat{\sigma}$; some regime labels are deterministic thresholds of $\hat{\mu}$ and $\hat{\sigma}$; and DS4's statistical-mechanics entropy was numerically identical to its process entropy. Agreement among such quantities is arithmetic, not corroboration.

Other conclusions narrowed because the observation process was initially omitted. DS5's raw increment variability largely follows the binomial floor of daily proportions. DS4's apparently rapid relaxation and daily–weekly discrepancy can be reproduced by a slower latent process observed with counting noise. In DS6, equal-length within-participant windows reduce the raw regime-change rate only slightly, but the large endpoint-drift contrast is not reproduced by all-days slope estimates. Structured volatility incorporates gaps between observed weeks, and its backlog is censored; a time-valid within-participant test does not reproduce the small pooled path-dependence association. In each case, the measurement model is inseparable from the behavioral interpretation.

5.3 Limitations

First, the model-family selection was theory-guided but not systematic or exhaustive, and the operationalizations evolved during analysis. The reported inferential statistics are exploratory. Second, most constructs are behavioral proxies rather than measurements of internal psychological states (Jain et al., 2015; Oudin et al., 2023). No analysis observes motivations, payoffs, or the content viewed inside a platform.

Third, data structure restricts identification. DS5 is the only randomized condition comparison; DS4 is naturalistic; DS6 conditions are cohort-level and its periods are unequal; Structured is heavily left- and right-censored. Eligibility rules also produce different analytical populations across families. Cross-dataset differences may therefore reflect population, instrumentation, window length, or preprocessing as well as behavior.

Fourth, many temporal models are low-order approximations. Constant-drift and AR(1) fits do not test nonlinearity, and bounded proportions require observation and boundary models. First-order transition networks omit session boundaries and do not establish interaction or substitution mechanisms. The individual-based simulations lack agent interaction and held-out validation. System-dynamics-motivated correlations do not identify causal loops. The profile analyses are complete-case and partly data-contingent and have not been validated in an external cohort, tested for within-person temporal stability, or related to independent outcomes using held-out data. They should guide better-specified follow-up studies, not individualized intervention assignment.

5.4 Which Data Fit This Framework Best?

Tables 5.1 and 5.2 organize the findings by family and dataset. Table 5.3 adds the cross-cutting view: which datasets supplied the structure each family required, and what future designs must add.

Table 5.3: Coverage of the eight model families across the four datasets, including implemented analyses, structural exclusions, and combinations not attempted. *Excl.* marks a combination the dataset's design rules out structurally; *not attempted* marks a combination left out of scope rather than found infeasible. All other cells were executed and audited; see the cross-referenced section for the full result.

Family	DS5	DS4	DS6	Structured
Statistical mechanics (4.1)	dependent ($\propto \hat{\sigma}$)	identity (=StoP's H_{SDE})	descriptive (condition-assoc. JSD)	descriptive (persistent within window, null path-dep.)
Dynamical systems (4.2)	descriptive (low-noise regime)	dependent (tautological check)	descriptive (window-sensitive)	descriptive (classifier-order artifact)
Stochastic processes (4.3)	null (double null)	corrected artifact (resolution)	descriptive (level shift, no trend)	descriptive (strongly bursty)
Network theory (4.4)	descriptive (concen-trated, weak effect)	partial (via phenotyping only)	descriptive (weak, outlier-driven)	descriptive (corrected pathway)
Information theory (4.5)	descriptive (multidimen-sional)	identity (literal, not analogy)	descriptive (strong bridge + null)	descriptive (bridge-bug caught)
Game theory (4.6)	proxy (descriptive only)	not attempted	not attempted	proxy (pooled vs. within-person disagree)
Individual-based sim. (4.7)	not attempted	model-criticism (missing obs. process)	not attempted	model-criticism (underpro-duces)
System dynamics (4.8)	excl. (single wave)	excl. (single wave)	null (loop, adjusted)	descriptive (backlog + correction)

Coverage and evidential strength diverge. Structured permits all eight families and an observable backlog stock, but remains observational and censored. DS5 alone supports a randomized friction contrast; DS6 supports period and repeated-wave descriptions but only cohort-level condition associations; and DS4's long naturalistic

windows expose resolution artifacts. Thus family counts measure compatibility with the recorded data structure, not validation or theoretical quality.
Across the four datasets, one recurring limitation becomes apparent in Table 5.2: something a family needed was present in at most one or two of the four datasets, never in all of them at once. Generalizing from where each family stalled points to design properties that no single dataset analyzed here combined:

1. **Individual-level randomization, sustained.** Only DS5 randomizes, and only at intake; a design that keeps assigning or re-randomizing over the observation window would let condition effects be tested on drift and variability, not only on a pooled endpoint distribution.
2. **Three or more repeated waves, not two.** DS6's two waves were enough to show that a change score is not a feedback loop, not enough to identify one; system dynamics needs a stock measured often enough to separate a trend from a single transition.
3. **Session boundaries logged at source.** The One Sec event logs do not identify when app-access sessions begin or end. Structured records task-lifecycle events rather than app-access sessions. The session assumptions used for app-transition networks therefore cannot be tested where they are relevant.
4. **A state variable that is not double-bounded.** DS6's unbounded count was the only state in the thesis able to produce a *growing* regime; a proportion bounded on $[0, 1]$ forecloses part of the dynamical-systems state space before a single model is fitted.
5. **Observed incentives and real multi-agent interaction.** No dataset recorded a payoff, an opponent, or an interaction between users; game theory and agent-based modeling were a proxy and an individual-based simulation in this thesis for exactly that reason, and no amount of feature engineering on the present data changes it.
6. **Denser per-participant sampling.** The dynamical-systems analyses here remain low-order linear summaries or rule-based classifications. None estimates nonlinear dynamics. Testing a nonlinear model requires longer, more finely sampled individual series than the daily behavioral logs provide.

No single dataset needs all six properties. The relevant lesson is that no dataset here combines enough of them to identify every family: evidential reach depends on the match between a specific family's requirements and the study design.
To illustrate how these requirements could be combined in practice, consider a longitudinal One Sec study with repeated participant-level randomization and complete, time-stamped app-access and session records. Repeated surveys, contextual measures, and behavioral outcomes would allow changes in individual response patterns to be examined over time. Holding out later observation periods or an independent cohort would further permit prospective validation of the resulting models and profiles.

5.5 Priorities for Future Work

The data-collection requirements are stated once in Section 5.4. Within that better-designed evidence base, the analytical priorities are:

1. **Specify the observation process.** Model event counts underlying daily proportions, include bounded-state behavior, and compare alternative temporal resolutions before attributing variation to a latent behavioral process.
2. **Test dynamics rather than label them.** Use longer and denser series, nonlinear model comparison, residual diagnostics, change-point tests, and out-of-sample prediction before making claims about attractors, adaptation, or regime shifts.
3. **Validate profiles longitudinally.** Define and lock features in one dataset or time window, then test assignment, predictive value, and measurement invariance without refitting in later windows and independent cohorts. Continuous scores should remain primary even if clusters are reported.
4. **Replicate the targeted sensitivity results.** The null time-valid Structured path-dependence result should be tested with denser task histories and prespecified lags. DS6's matched-window result should be repeated in an independent cohort and compared across explicit change-point and observation models.

Linked physiology as a feasibility outlook. One additional analysis is retained here as a future-data demonstration rather than as a fifth empirical dataset. After data-quality exclusions, the linked One Sec–HealthKit material contained one usable participant, with 13,227 One Sec events and 741,932 physiological observations. The pipeline aligned the two sources into a common daily table, but none of fourteen exploratory physiology–behavior correlations survived the Bonferroni threshold for that test battery. This establishes technical linkage only: it cannot support population inference, profile validation, or a conclusion about physiological coupling. A cohort-scale replication with locked variables, lags, and a prespecified test family could instead use physiology as an external validation channel for the behavioral features developed here.

On-platform activity as a further data layer. The analyses in this thesis focus mainly on events at the boundary between a person and a digital tool: opening attempts, responses to friction, app transitions, and task lifecycles. The activity inside target apps remains unobserved. Subject to data access and participant consent, future work on TikTok or a comparable platform could link app-access events to chronological viewing records containing timestamps, viewing duration, content metadata, scrolling, interactions, and session endpoints. These records could describe what participants encounter after opening an app and how their actions develop across a session; brief self-reports could add experiences that event logs cannot reveal. This is a proposed extension, not an additional dataset or empirical finding. Transition networks and entropy could then describe the order and diversity of observed content categories, while sufficiently dense records with a well-understood observation process could support stochastic or dynamical summaries of continuation, interaction, and exit. Linking them to One Sec events could support exploratory tests of whether access friction is followed by different on-platform patterns. These would be new analyses, not conclusions from the datasets used here. Recommendation exposure also extends the system boundary: users' actions may affect later con-

tent selection, while selected content may be associated with later actions. Although this reciprocal relationship is compatible with a complex-systems perspective, observational logs cannot identify internal recommendation rules or causal feedback; those claims require more complete exposure information and, where feasible, an experimental or otherwise identification-oriented design. The value of this outlook is therefore limited but specific: it identifies platform content and recommendation exposure as an unobserved but measurable layer. Together with physiology, it forms one of two additional data layers that could extend the present person–tool description without altering the bounded interpretation of the reported results.

5.6 Conclusion

This thesis shows the value of using broad theory as a disciplined test of what heterogeneous digital traces can support. Simple process, uncertainty, transition, configuration, and stock summaries provide useful descriptions. Stronger claims about formal games, interacting-agent emergence, nonlinear attractors, and causal feedback require data that were not available here.
These corrections constitute substantive methodological findings rather than merely the absence of positive results. They identify where dependencies, sampling, censoring, and observation design change an apparent result. The next step is prospective validation with explicit observation processes, denser longitudinal sampling, locked features, and repeated or randomized measurements. Such designs can test whether the profiles predict later outcomes and whether richer mechanistic models add information beyond the descriptive quantities established here.

5.7 Code and Website Availability

The analysis code, preprocessing pipelines, and project documentation are available in the project repository:

https://github.com/sstrassbu/CAS_DigitalBehavior_ThesisRelease

To support science communication and explore alternative ways of presenting research, an accompanying interactive website presents the thesis and its findings in a more accessible and engaging format:

https://cas-digital-behavior-website.vercel.app/

Bibliography

Agrawal, A., & Jaiswal, D. (2012). When machine learning meets ai and game theory [CS229 course project]. *Stanford University*. https://cs229.stanford.edu/proj2012/AgrawalJaiswal-WhenMachineLearningMeetsAIandGameTheory.pdf

Beyens, I., Pouwels, J. L., van Driel, I. I., Keijsers, L., & Valkenburg, P. M. (2020). The effect of social media on well-being differs from adolescent to adolescent. *Scientific Reports*, *10*, 10763. https://doi.org/10.1038/s41598-020-67727-7

Böhmer, M., Hecht, B., Schöning, J., Krüger, A., & Bauer, G. (2011). Falling asleep with angry birds, facebook and kindle: A large scale study on mobile application usage. *Proceedings of the 13th International Conference on Human Computer Interaction with Mobile Devices and Services*, 47–56. https://doi.org/10.1145/2037373.2037383

Borrill, P. L., & Tesfatsion, L. (2011). Agent-based modeling: The right mathematics for the social sciences? In J. B. Davis & D. W. Hands (Eds.), *Elgar companion to recent economic methodology* (pp. 228–258). Edward Elgar. https://faculty.sites.iastate.edu/tesfatsi/archive/tesfatsi/ABMRightMath.PBLT.pdf

Bryan, C. J., Tipton, E., & Yeager, D. S. (2021). Behavioural science is unlikely to change the world without a heterogeneity revolution. *Nature Human Behaviour*, *5*, 980–989. https://doi.org/10.1038/s41562-021-01143-3

Bufano, P., Laurino, M., Said, S., Tognetti, A., & Menicucci, D. (2023). Digital phenotyping for monitoring mental disorders: Systematic review. *Journal of Medical Internet Research*, *25*, e46778. https://doi.org/10.2196/46778

Carmichael, T., Collins, A. J., & Hadžikadić, M. (Eds.). (2019). *Complex adaptive systems: Views from the physical, natural, and social sciences*. Springer.

Carmichael, T., & Hadžikadić, M. (2019). The fundamentals of complex adaptive systems. In T. Carmichael, A. J. Collins, & M. Hadžikadić (Eds.), *Complex adaptive systems: Views from the physical, natural, and social sciences* (pp. 1–16). Springer. https://doi.org/10.1007/978-3-030-20309-2_1

Cover, T. M., & Thomas, J. A. (2006). *Elements of information theory* (2nd ed.). Wiley. https://doi.org/10.1002/047174882X

Cox, A. L., Gould, S. J. J., Cecchinato, M. E., Iacovides, I., & Renfree, I. (2016). Design frictions for mindful interactions: The case for microboundaries. *Proceedings of the 2016 CHI Conference Extended Abstracts on Human Factors in Computing Systems*, 1389–1397. https://doi.org/10.1145/2851581.2892410

Daugman, J. (2020). Information theory [Lecture notes]. *University of Cambridge*. https://www.cl.cam.ac.uk/teaching/2021/InfoTheory/InfoTheoryNotes2020.pdf

Faigle, U. (2020). Mathematical game theory: A new approach [Preprint]. https://arxiv.org/abs/2012.01850

Farahani, F. V., Karwowski, W., & Lighthall, N. R. (2019). Application of graph theory for identifying connectivity patterns in human brain networks: A systematic review. *Frontiers in Neuroscience*, *13*, 585. https://doi.org/10.3389/fnins.2019.00585

Fisher, A. J., Medaglia, J. D., & Jeronimus, B. F. (2018). Lack of group-to-individual generalizability is a threat to human subjects research. *Proceedings of the National Academy of Sciences*, *115*(27), E6106–E6115. https://doi.org/10.1073/pnas.1711978115

Goodman, J. (2022). Stochastic calculus: Stochastic differential equations [Lecture notes]. *New York University*. https://math.nyu.edu/~goodman/teaching/StochCalc2022/materials/Section1.pdf

Gros, C. (n.d.). Chapter 9: Canonical ensemble [Statistical physics lecture notes; publication year not confirmed]. *Goethe University Frankfurt*. https://itp.uni-frankfurt.de/~gros/Vorlesungen/TD/9_Canonical_ensemble.pdf

Grüning, D. J., Riedel, F., & Lorenz-Spreen, P. (2023). Directing smartphone use through the self-nudge app one sec. *Proceedings of the National Academy of Sciences*, *120*(8), e2213114120. https://doi.org/10.1073/pnas.2213114120

Gunesch, R. (2005). Einführung in dynamische systeme [Lecture script]. *Universität Hamburg*. https://www.math.uni-hamburg.de/home/gunesch/Vorlesung/Einf_Dyn_Sys_SoSem2005/Skript/intro.pdf

Haliburton, L., Grüning, D. J., Riedel, F., Schmidt, A., & Terzimehić, N. (2024). A longitudinal in-the-wild investigation of design frictions to prevent smartphone overuse. *Proceedings of the 2024 CHI Conference on Human Factors in Computing Systems*, 1–16. https://doi.org/10.1145/3613904.3642370

Heino, M. T. J., Knittle, K., Noone, C., Hasselman, F., & Hankonen, N. (2021). Studying behaviour change mechanisms under complexity. *Behavioral Sciences*, *11*(5), 77. https://doi.org/10.3390/bs11050077

Hennig, P., Osborne, M. A., & Girolami, M. (2015). Probabilistic numerics and uncertainty in computations. *Advances in Neural Information Processing Systems*.

Higham, D. J. (2001). An algorithmic introduction to numerical simulation of stochastic differential equations. *SIAM Review*, *43*(3), 525–546. https://doi.org/10.1137/S0036144500378302

Holland, J. H. (1992). Complex adaptive systems. *Daedalus*, *121*(1), 17–30.

Hotz, H. (2006). A short introduction to game theory [Seminar handout]. *Ludwig-Maximilians-Universität München*. https://www.theorie.physik.uni-muenchen.de/lsfrey/teaching/archiv/sose_06/softmatter/talks/Heiko_Hotz-Spieltheorie-Handout.pdf

Jain, S. H., Powers, B. W., Hawkins, J. B., & Brownstein, J. S. (2015). The digital phenotype. *Nature Biotechnology*, *33*, 462–463. https://doi.org/10.1038/nbt.3223

Jaradat, Y., Masoud, M., Manasrah, A., Alia, M., Suwais, K., & Almanasra, S. (2025). Exploring the intersection of information theory and machine learn-

ing. *The International Arab Journal of Information Technology*, *22*(5), 845–858. https://doi.org/10.34028/iajit/22/5/1

Jensen, G., Ward, R. D., & Balsam, P. D. (2013). Information: Theory, brain, and behavior. *Journal of the Experimental Analysis of Behavior*, *100*(3), 408–431. https://doi.org/10.1002/jeab.49

Kapitel 3: Entropie – statistische zugänge. (n.d.). *Universität Freiburg*. Retrieved August 10, 2026, from https://physikdidaktik.uni-freiburg.de/wp-content/uploads/2024/02/T3_Entropie.pdf

Kawamura, H. (2010). Two models of spin glasses: Ising versus heisenberg. *Journal of Physics: Conference Series*, *233*, 012012. https://doi.org/10.1088/1742-6596/233/1/012012

Kunc, M. H. (2016). System dynamics: A behavioral modeling method. *Proceedings of the 2016 Winter Simulation Conference*, 53–64. https://doi.org/10.1109/WSC.2016.7822079

Levin, S. A. (1998). Ecosystems and the biosphere as complex adaptive systems. *Ecosystems*, *1*(5), 431–436. https://doi.org/10.1007/s100219900037

Ludde, C. (n.d.). Mechanik: Kapitel 3. *Goethe-Universität Frankfurt*. Retrieved August 10, 2026, from https://itp.uni-frankfurt.de/~luedde/Lecture/Mechanik/Intranet/Skript/Kap3/node5.html

Macal, C. M., & North, M. J. (2010). Tutorial on agent-based modelling and simulation. *Journal of Simulation*, *4*(3), 151–162. https://doi.org/10.1057/jos.2010.3

Maynard Smith, J. (1982). *Evolution and the theory of games*. Cambridge University Press. https://doi.org/10.1017/CBO9780511806292

Mitchell, M. (2009). *Complexity: A guided tour*. Oxford University Press.

Molenaar, P. C. M. (2004). A manifesto on psychology as idiographic science: Bringing the person back into scientific psychology, this time forever. *Measurement: Interdisciplinary Research and Perspectives*, *2*(4), 201–218. https://doi.org/10.1207/s15366359mea0204_1

Nahum-Shani, I., Smith, S. N., Spring, B. J., Collins, L. M., Witkiewitz, K., Tewari, A., & Murphy, S. A. (2018). Just-in-time adaptive interventions (JITAIs) in mobile health: Key components and design principles for ongoing health behavior support. *Annals of Behavioral Medicine*, *52*(6), 446–462. https://doi.org/10.1007/s12160-016-9830-8

Netz, R. R. (2016). Statistical physics and thermodynamics [Lecture script]. *Freie Universität Berlin*. https://www.physik.fu-berlin.de/en/einrichtungen/ag/ag-netz/lehre/past-semesters/Scripts/StatisticalPhysicsAndThermodynamics.pdf

Newman, M. E. J. (2010). *Networks: An introduction*. Oxford University Press.

Øksendal, B. (2003). *Stochastic differential equations: An introduction with applications* (6th ed.). Springer.

Onnela, J.-P., & Rauch, S. L. (2016). Harnessing smartphone-based digital phenotyping to enhance behavioral and mental health. *Neuropsychopharmacology*, *41*(7), 1691–1696. https://doi.org/10.1038/npp.2016.7

Oudin, A., Maatoug, R., Bourla, A., Ferreri, F., Bonnot, O., Millet, B., Schoeller, F., Mouchabac, S., & Adrien, V. (2023). Digital phenotyping: Data-driven

psychiatry to redefine mental health. *Journal of Medical Internet Research*, *25*, e44502. https://doi.org/10.2196/44502

Parkinson, J. A., Gould, A., Knowles, N., West, J., & Goodman, A. M. (2025). Integrating systems thinking and behavioural science. *Behavioral Sciences*, *15*(4), 403. https://doi.org/10.3390/bs15040403

Rahmstorf, S. (2006). Complex adaptive systems [Potsdam Institute for Climate Impact Research publication file]. https://publications.pik-potsdam.de/rest/items/item_24571_6/component/file_25355/content

Richardson, M. J., Dale, R., & Marsh, K. L. (2014). Complex dynamical systems in social and personality psychology: Theory, modeling, and analysis. In H. T. Reis & C. M. Judd (Eds.), *Handbook of research methods in social and personality psychology* (2nd ed., pp. 253–282). Cambridge University Press. https://doi.org/10.1017/CBO9780511996481.015

Roy, A. (2007). System dynamics: A practical approach for managerial problems. *Delhi Business Review*, *8*(2), 59–81. https://doi.org/10.51768/dbr.v8i2.82200706

Slantchev, B. L. (2005). Game theory: Elements of basic models [Lecture notes].

Smith, E. R., & Conrey, F. R. (2007). Agent-based modeling: A new approach for theory building in social psychology. *Personality and Social Psychology Review*, *11*(1), 87–104. https://doi.org/10.1177/1088868306294789

SmythOS. (n.d.-a). Agent-based modeling and game theory: Simulating strategic interactions in complex systems. Retrieved August 10, 2026, from https://smythos.com/managers/legal/agent-based-modeling-and-game-theory/

SmythOS. (n.d.-b). Agent-based modeling vs. system dynamics: Key differences and applications in complex systems. Retrieved August 10, 2026, from https://smythos.com/developers/agent-development/agent-based-modeling-vs-system-dynamics/

Stochastische prozesse i [Lecture script]. (n.d.). *Universität Leipzig*.

Strassburger, S., Schmiedmayer, P., & Grüning, D. J. (2026). *Exploring the utilization of established complex adaptive system-theories to model and understand digital behavior* [Article proposal for paper submission].

Szaszi, B., Goldstein, D. G., Soman, D., & Michie, S. (2025). Generalizability of choice architecture interventions. *Nature Reviews Psychology*, *4*, 518–529. https://doi.org/10.1038/s44159-025-00471-9

Teose, M., Ahmadizadeh, K., O'Mahony, E., Smith, R. L., Lu, Z., Ellner, S. P., Gomes, C. P., & Grøhn, Y. T. (2011). Embedding system dynamics in agent based models for complex adaptive systems. *Proceedings of the Twenty-Second International Joint Conference on Artificial Intelligence*, 2531–2538. https://doi.org/10.5591/978-1-57735-516-8/IJCAI11-421

Torous, J., Kiang, M. V., Lorme, J., & Onnela, J.-P. (2016). New tools for new research in psychiatry: A scalable and customizable platform to empower data driven smartphone research. *JMIR Mental Health*, *3*(2), e16. https://doi.org/10.2196/mental.5165

Torren-Peraire, D., Savin, I., & van den Bergh, J. (2024). An agent-based model of cultural change for a low-carbon transition. *Journal of Artificial Societies and Social Simulation*, *27*(1), 13. https://doi.org/10.18564/jasss.5291

Tsai, C. W., & Hung, Y.-J. (2025). Application of stochastic models for long-range sediment transport during extreme typhoon events. *Journal of Hydrology: Regional Studies*, *60*, 102463. https://doi.org/10.1016/j.ejrh.2025.102463

Tsironis, G. P. (2025). *Artificial intelligence and complex dynamical systems*. Springer. https://doi.org/10.1007/978-3-031-81946-9

Turner, G., Dalmaijer, E. S., Astle, D. E., & Orben, A. (2026). *Diverse behavioural-emotional profiles associated with self-reported social media addiction in adolescence*. https://doi.org/10.31234/osf.io/crxqp_v1

Turner, G., Gastelum, M. C. V., Anderson, I. A., Brufal, Z., Dillmann, S., Fassi, L., Gunschera, L. J., Monarca, I., Ramirez, O. P., Tentori, M., & Orben, A. (2026). *Relating smartphone App-Journeys to mental health: A novel network analysis approach* [PsyArXiv preprint]. https://doi.org/10.31234/osf.io/uytfr_v1

Wang, L., & Miller, L. C. (2020). Just-in-the-moment adaptive interventions (JITAI): A meta-analytical review. *Health Communication*, *35*(12), 1531–1544. https://doi.org/10.1080/10410236.2019.1652388

Watanabe, T., Masuda, N., Megumi, F., Kanai, R., & Rees, G. (2014). Energy landscape and dynamics of brain activity during human bistable perception. *Nature Communications*, *5*, 4765. https://doi.org/10.1038/ncomms5765

Witten, E. (2020). A mini-introduction to information theory. *La Rivista del Nuovo Cimento*, *43*(4), 187–227. https://doi.org/10.1007/s40766-020-00004-5

Wolschin, G. (2021). One- and two-dimensional ising model. *Universität Heidelberg*. https://www.thphys.uni-heidelberg.de/~wolschin/statsem21_3s.pdf

Wood, W., Quinn, J. M., & Kashy, D. A. (2002). Habits in everyday life: Thought, emotion, and action. *Journal of Personality and Social Psychology*, *83*(6), 1281–1297. https://doi.org/10.1037/0022-3514.83.6.1281

Wu, Y. (n.d.). Stochastic differential equations. *University of California, Los Angeles*. Retrieved August 10, 2026, from http://www.stat.ucla.edu/~ywu/research/documents/StochasticDifferentialEquations.pdf

Zhao, K., Karsai, M., & Bianconi, G. (2011). Entropy of dynamical social networks. *PLOS ONE*, *6*(12), e28116. https://doi.org/10.1371/journal.pone.0028116

A

Statistical Analysis and How to Read the Results

This appendix provides a common reading key for the numerical results in Chapter 4. Most reported quantities are not scores with a universal "good" and "bad" end. A high entropy can mean a broad repertoire or irregularity; a high self-loop share can mean behavioral persistence or a mechanical ceiling; and a falling app-use count can be an intended intervention response without showing why it occurred. Interpretation therefore requires five pieces of information: *what was calculated, from which observations, on what scale, relative to which reference, and with what claim boundary.* The Results chapter gives the dataset-specific comparison; Tables A.1, A.2, and A.3 give the shared scales and references.

A.1 Statistical Evidence

Continuous relationships are summarized with Pearson or Spearman correlations as appropriate; group contrasts use analysis of variance, rank-based alternatives, or contingency-table tests as reported with each result. Within-person or baseline-adjusted versions are preferred when pooled associations can mix variation within people with variation between people. Eligible sample sizes and effect-relevant group summaries are reported alongside p-values where available. No thesis-wide multiplicity correction is applied across the heterogeneous model-family–dataset analyses. Corrections are applied only within explicitly defined local test batteries; otherwise, reported p-values are nominal exploratory summaries rather than confirmatory evidence.

Table A.1: Plain-language reading key for the general statistical quantities reported in Chapter 4.

Quantity	Range or reference	What it measures	How it is read here
N or n	Positive count	Number of eligible participants, events, days, or paired observations; the unit is stated locally.	A large event count does not replace a sufficient participant count. Different eligibility rules can produce different N values within one dataset.

Quantity	Range or reference	What it measures	How it is read here
Mean and median	Variable's own scale	Two summaries of a distribution's center.	A large mean–median difference signals skew or outliers. It is not a formal test, but it can change which summary is representative.
p-value	$0 \leq p \leq 1$	Under the stated null model and its assumptions, the probability of a result at least as extreme as the observed one.	Smaller values are less compatible with that null. A p-value is not the probability that the null is true, and $1 - p$ is not the probability that the substantive explanation is true. The descriptive nominal reference is 0.05 unless a corrected threshold is stated; "not significant" means *not detected*, not proven equal.
ANOVA F	$F \geq 0$	Ratio of between-group variation to within-group variation. Its reference distribution also depends on the numerator and denominator degrees of freedom.	Larger values generally indicate clearer separation relative to within-group scatter, but there is no universal good/bad cutoff and F is not the size of the behavioral effect. Direction and magnitude must be read from the group summaries; p describes evidence against equal means. This F must not be confused with the Fano factor below.
Pearson r; Spearman ρ	-1 to $+1$	Linear association (r) or monotonic rank association (ρ).	The sign gives direction and the absolute value gives strength; 0 means no detected linear or monotonic relationship and ± 1 perfect alignment. As a deliberately rough reading aid, $\lvert r \rvert$ or $\lvert \rho \rvert < 0.1$ is described as little or negligible, 0.1–0.3 as weak, 0.3–0.5 as moderate, and > 0.5 as strong, always subject to the measurement design. Correlation is not causation.

Quantity	Range or reference	What it measures	How it is read here
Mann–Whitney or Wilcoxon test	Rank-based; statistic depends on sample size	Whether two independent groups, paired observations, or a sample and reference value differ in location without requiring a normal outcome.	The reported p-value is read as above. Group medians or distributions provide direction and practical magnitude; the test statistic itself is not a universal effect-size scale.
χ^2 or Fisher's exact test	$\chi^2 \geq 0$; Fisher reports a p-value	Whether two categorical variables are associated beyond the independence reference.	These tests establish neither direction nor causality. The contingency table is needed to understand which cells produce the association.
95% confidence interval	Outcome's scale	A repeated-sampling interval expressing estimator precision under the fitted model.	Narrower intervals are more precise. For a difference or correlation, an interval crossing zero is compatible with no signed effect at the corresponding level; it is not proof that the true value is zero.

Worked example. The DS6 result $F = 5.06$, $p = 0.0071$ compares sampling-floor-adjusted configuration change among three condition cohorts. The F value says that separation among the cohort means is large relative to the remaining within-cohort scatter; it does *not* mean a change of 5.06 units. If equal cohort means and the analysis-of-variance assumptions were true, a result at least this extreme would occur in about 0.71% of repeated samples. The surrounding means and pairwise comparisons provide the direction: the control cohort changed less than the two friction cohorts. The result supports a condition association. It does not imply a 99.29% probability that the hypothesis is true and, because DS6 condition is cohort-level rather than individually randomized, it does not by itself establish a causal effect.

A.2 Model-Specific Scales and Reference Points

Tables A.2 and A.3 collect the quantities that recur under several model families and in the profile analysis. *Higher* and *lower* below describe the observation, not its desirability. The local behavioral question determines whether either direction is favorable.

Table A.2: Ranges, reference points, and plain-language interpretations of recurring model-specific quantities.

Quantity	Range or reference	Origin in this thesis	Plain-language interpretation
Daily state X_t	0 to 1	Daily opened attempts divided by opened plus dismissed attempts in DS5 and DS4.	0 means all recorded outcome-bearing attempts were dismissed and 1 all were opened. It is an observed override proportion, not a direct score of self-control, dependence, or well-being.
Drift $\hat{\mu}$	Signed; state units per time step	Mean increment, endpoint change, or all-days slope, as stated locally.	Positive means the fitted series rises, negative means it falls, and near zero means no average direction was resolved. The value is only as reliable as the window and estimator; neither sign is universally good.
Diffusion or increment spread $\hat{\sigma}$	$\hat{\sigma} \geq 0$	Standard deviation of successive increments.	Larger values mean more observed day-to-day fluctuation. They can reflect behavioral variation, finite-count observation noise, gaps, or all three.
Sampling ratio R_σ	$R_\sigma \geq 0$; reference 1	Raw increment spread divided by the binomial sampling spread expected from daily event counts.	Around 1 means finite counts can explain the observed fluctuation; above 1 indicates excess spread relative to that reference. It is not a participant quality score.
Mean reversion $\hat{\theta}$ and relaxation $\hat{\tau}$	$\hat{\theta} > 0$ for mean reversion; $\hat{\tau} = 1/\hat{\theta} > 0$	AR(1)/Ornstein–Uhlenbeck approximation.	Larger θ or smaller τ means a faster fitted return toward the model-implied mean. Observation noise can make this return appear artificially fast.
Fano factor F_{Fano}	$F_{\text{Fano}} \geq 0$; Poisson reference 1	Count variance divided by count mean.	Near 1 is Poisson-like, above 1 is overdispersed or bursty, and below 1 is more regular than that reference. It describes dispersion, not why bursts occur, and is distinct from the ANOVA F-statistic.

Quantity	Range or reference	Origin in this thesis	Plain-language interpretation
Shannon entropy H	0 to $\log_2 K$ bits for K discrete categories	Probabilities of observed apps, hours, outcomes, states, or configurations.	0 means one category is observed with certainty; the ceiling means all K categories are equally frequent. Higher means greater diversity or unpredictability on that exact vocabulary, not better behavior. Gaussian *differential* entropy is different: it can be negative and has no fixed upper bound.
Jensen–Shannon divergence (JSD)	0 to 1 bit with base-2 logarithms	Difference between the same participant's two app-by-time distributions.	0 means identical distributions and 1 maximal separation with no overlap. Larger values mean more reorganization, not improvement or deterioration.
HHI concentration	$1/K$ to 1 for K represented categories	Sum of squared flow shares across apps or network source states.	Near 1 means flow is concentrated in one category; values nearer $1/K$ mean it is spread evenly. Comparisons require a comparable category vocabulary.
Self-loop or persistence share	0 to 1	Fraction of transitions returning to the same state, or adjacent periods retaining the same dominant label.	Higher means more repetition or stability. It can also be high mechanically when one state dominates almost all observations.
Mutual information $I(X;Y)$	0 to the smaller marginal entropy	Reduction in uncertainty about one categorical variable from knowing another.	0 means no dependence detected on the chosen discretization; larger values mean more predictive dependence. It does not identify a causal direction.

Table A.3: Ranges, reference points, and plain-language interpretations of derived and profile-analysis quantities.

Quantity	Range or reference	Origin in this thesis	Plain-language interpretation
Behavioral T, β, or χ proxy	Definition-specific	Exact transformations of $\hat{\sigma}$ and observed state occupancy in DS5; JSD is separately denoted χ in DS6.	In DS5, low T and high β restate lower fitted variability and are not independent evidence. There is no universal desirable value. DS6's χ is a different quantity and must be read on the JSD scale above.
Backlog B_w and slope	$B_w \geq 0$; slope signed	Number of observed created tasks not yet observed to exit by week w, and its fitted change over time.	A positive slope means the recorded backlog grows; a negative slope means it shrinks. Censoring can manufacture growth, so the slope is not automatically evidence of overload.
Commitment score	Integer 0 to 5	Temporal structure (inbox 0, all-day 1, timed 2), plus one point each for recurrence, subtasks, and a timed duration above the timed-task median.	Higher means more of the encoded task-structure features are present. It is an ordinal descriptive index, not utility, effort, task quality, or a payoff.
Standardized feature (z)	Center 0; one unit is one standard deviation	Each profile feature after subtracting its sample mean and dividing by its sample standard deviation.	Positive is above that analytical sample's mean and negative below it. Values from different datasets are not absolute-unit comparisons.
Silhouette score	-1 to 1	Within-cluster cohesion relative to nearest-cluster separation.	Values near 1 indicate clear separation, around 0 overlapping groups, and below 0 questionable assignments. Values around 0.21–0.30 in this thesis indicate weak separation even when a solution is reproducible.
Bootstrap Jaccard stability	0 to 1; thesis reference 0.75	Average membership overlap after resampling and refitting the clustering.	Near 1 means the same members tend to be grouped again. The thesis treats 0.75 as a practical stability threshold, not a universal law; stability does not prove substantive validity.

Quantity	Range or reference	Origin in this thesis	Plain-language interpretation
Adjusted Rand Index (ARI)	-1 to 1	Chance-adjusted agreement between two cluster partitions.	1 means identical membership, around 0 chance-level agreement, and negative values less agreement than expected by chance. Low ARI does not prove that the underlying feature families are statistically independent.

B

Detailed Empirical Results and Diagnostic Material

This appendix preserves the numerical audit trail and the figures or tables removed from the main Results chapter. The main chapter prioritizes the plain-language finding, its magnitude, its behavioral meaning, and its dataset-specific limitation. The material below supplies the full reported test statistics, sensitivity results, transition counts, and diagnostic visualizations. Relocation does not change evidential status: descriptive, provisional, null, dependent, and association-level findings retain the boundaries stated in Chapter 4.

B.1 Consolidated Statistical Results

Table B.1 collects the inferential and diagnostic values used in the main narrative. It is a reference table rather than a second set of findings. Exact values are read using the scales and cautions in Appendix A. Unless a local correction is stated explicitly, the p-values in this table are nominal; they should therefore be read as exploratory summaries, not as multiplicity-controlled confirmatory evidence.

Table B.1: Consolidated inferential and diagnostic statistics supporting Chapter 4.

Family and dataset	Analysis or comparison	Exact reported result	Narrow interpretation
StM, DS5	Behavioral-susceptibility proxy across randomized arms	$F = 0.742$, $p = 0.477$	No detected arm difference; the proxy is derived from fitted variability.
StM, DS5	Constructed behavioral temperature and inverse temperature	mean T: control 0.0196, default 0.0398, reintervention 0.0295; mean β: 144.86/43.78/84.19	The ordering exactly restates $\hat{\sigma}$ and is not independent thermodynamic evidence.
StM, DS6	Raw configuration change by cohort	control 0.028, default 0.070 ($p = 0.0011$ vs. control), intervention 0.052 ($p = 0.0075$ vs. control)	Both friction cohorts show greater app-by-time reorganization than control.

Table B.1 continued from the previous page.

Family and dataset	Analysis or comparison	Exact reported result	Narrow interpretation
StM, DS6	Configuration change after participant-specific sampling-floor subtraction	$F = 5.06$, $p = 0.0071$; mean floor ≈ 0.014 bits, observed mean ≈ 0.051	The cohort association remains after finite-sampling adjustment; it is not an individually randomized effect.
StM, Structured	Prior unresolved streak and structure added to the next task	pooled $r = -0.027$, $p = 0.006$; within person $r = 0.003$, asymptotic $p = 0.732$, stratified permutation $p = 0.707$	The pooled association disappears within person; no time-valid path dependence is detected.
StM, Structured	Configuration diversity and dominant-state persistence	mean entropy 2.068 bits; mean 10.96 configurations; persistence 0.953; 53/61 eligible	Several configurations are observed, but the dominant label has a timed-task ceiling.
DyS, DS5	Low-variability split and empirical increment entropy	Mann–Whitney $p = 1.3 \times 10^{-25}$; $r(\hat{\sigma}, H_{\text{emp}}) = 0.618$	The two spread summaries order participants similarly; the median split is not an independent attractor result.
DyS, DS5	Median-defined low-noise regime across arms	control 67.2%, default 29.6%, reintervention 54.1%; low-/high-noise entropy 1.783/2.328	Arm composition differs, but the regime is a thresholded diffusion estimate rather than an attractor.
DyS, DS4	Fitted fixed point compared with the empirical mean	real $r = 0.9925$; time-shuffled $r = 0.996$	Agreement is algebraic and survives destruction of temporal dynamics.
DyS, DS6	Drift under matched local-day windows	all-days $p = 0.625$; endpoint $p = 7.6 \times 10^{-5}$	The all-days trend remains null; the endpoint statistic is resolution-sensitive.
DyS, DS6	Deterministic-regime label and empirical entropy	baseline $p = 2.5 \times 10^{-6}$; intervention $p = 1.5 \times 10^{-4}$	The result restates the diffusion–entropy relationship used to create the label.

Table B.1 continued from the previous page.

Family and dataset	Analysis or comparison	Exact reported result	Narrow interpretation
DyS, Structured	Weekly volume trend, classifier ordering, and observation gaps	mean/median slope $-1.102/-0.026$; outlier -32.14; Wilcoxon $p = 0.389$; high-structure criterion 7/42, final label 2/42; volatility–gap $\rho = 0.499$, $p = 0.0008$	No sample-level trend is detected; the rare label is order-dependent and volatility partly reflects intermittent observation.
StoP, DS5	Endpoint and all-days drift across randomized arms	endpoint $F = 0.267$, $p = 0.766$; all-days $F = 0.144$, $p = 0.866$	Neither drift estimator detects an arm difference.
StoP, DS5	Raw increment variability across arms	means 0.176/0.261/0.215 (control/default/reintervention); $F = 23.144$, $p < 0.0001$	Recorded daily proportions differ in raw spread before observation noise is considered.
StoP, DS5	Variability relative to the binomial sampling floor	225/414 at or below the floor; $F = 0.026$, $p = 0.975$	The raw variability contrast disappears after sampling adjustment.
StoP, DS4	Raw and observation-corrected relaxation	median $\hat{\tau} = 0.63$ days; corrected $\hat{\theta} = 0.46$ day^{-1}, $\hat{\tau} \approx 2.2$ days	Finite daily counts make the fitted process appear too fast.
StoP, DS4	Daily versus weekly relaxation and observation-process simulation	real daily/weekly 0.660 days/0.985 weeks, $r = 0.316$; simulated 0.75 days/1.10 weeks, $r = 0.20$	One slow latent process observed at different resolutions reproduces the discrepancy.
StoP, DS6	Condition-associated change in daily attempt volume	control $50.0 \to 45.9$, default $43.8 \to 18.8$, intervention $41.9 \to 24.1$; $F = 25.42$, $p = 1.1 \times 10^{-10}$	The two friction cohorts show the larger level reduction.
StoP, DS6	Within-period drift	paired $p = 0.659$; matched-window all-days $p = 0.625$	The level changes, but no steady within-window trend is detected.
StoP, DS6	Count dispersion across unequal periods	median Fano $6.58 \to 3.34$; baseline window approximately half as long	Both periods are overdispersed, but the period contrast is not interpreted because variance precision differs.
StoP, Structured	Timed-creation and completion-count dispersion	median Fano 3.83/4.96; $F_{\text{Fano}} > 1$ for 97.7%/94.7%	Planning counts are strongly overdispersed relative to a Poisson process.

Table B.1 continued from the previous page.

Family and dataset	Analysis or comparison	Exact reported result	Narrow interpretation
StoP, Structured	Endpoint drift and rule-based stability sensitivity	median $\hat{\mu} = 0.000$; sign flips after removing one day in 40/81 series; regression trends in 10/43 and 12/38; classifier correlation -0.839	Near-zero endpoint drift does not establish stable planning, and the rare label is mechanically dependent.
NeT, DS5	Multi-app network metrics across randomized arms	HHI 0.719/0.656/0.727; self-loop 0.829/0.818/0.841; entropy 0.524/0.598/0.512 bits; group $p = 0.073/0.623/0.408$	Concentration and repetition are substantial, but no clear arm ordering is detected.
NeT, DS6	Volume change and concentration change	mean HHI $0.495 \rightarrow 0.502$; Pearson $r = -0.213$, $p = 0.0012$; Spearman $\rho = -0.093$, $p = 0.165$; leverage-trimmed $r = -0.062$, $p = 0.36$	Average concentration barely changes and the weak Pearson association does not survive robust checks.
NeT, Structured	Pooled lifecycle structure	timed→completed 5,756; moved→moved 4,760; self-loop share 39.3%	Direct completion dominates the expected moved pathway; succession does not identify a mechanism.
InT, DS5	Empirical and Gaussian differential entropy	empirical means 1.652/2.387/2.118 bits (control/default/reintervention); $r = 0.618$, $p = 5.0 \times 10^{-45}$	Friction cohorts have less concentrated daily states; the spread measures are not independent evidence.
InT, DS5	App and local-hour entropy diagnostics	app entropy 0 for 239/478; hour ceiling 4.585 bits, condition means 3.88–3.96	App diversity often has a one-app floor, while temporal diversity is high and similar across arms.
InT, DS6	Gaussian bridge and empirical entropy	baseline $r = 0.583$, $p = 6.9 \times 10^{-23}$; intervention $r = 0.719$, $p = 6.7 \times 10^{-39}$	The two spread summaries have a strong consistent ordering.
InT, DS6	Period information about app identity	$I(\text{period}; \text{app}) = 0.0003$ bits versus $H(\text{app}) = 1.884$ bits	Period removes virtually none of the pooled uncertainty about app identity.

Table B.1 continued from the previous page.

Family and dataset	Analysis or comparison	Exact reported result	Narrow interpretation
InT, Structured	Entropy dimensions and corrected dependence summaries	task type 0.200 bits; creation hour 2.887/4.585 bits; terminal status 0.960/1.585 bits; imbalanced binary MI 88.7%, three-class 34.5%	Task type is predictable and timing diverse; the largest normalized MI is an imbalance artifact.
GaT, Structured	Commitment proxy and completion/adaptation	pooled $r = -0.0054$; within person $r = 0.0633$; adaptation $r = 0.0113$, $p = 0.245$; censoring $\rho = 0.52$	No optimum or adaptation relationship is identified; censoring changes the composition of score levels.
ABM, Structured	Static and episodic simulations of count dispersion	observed Fano 6.011; static 1.019; on/off 3.377; rank $\rho = 0.848$	Episodic activity improves absolute dispersion but does not fully reproduce it; ranking is in-sample.
SyD, DS6	Baseline-adjusted loop associations	$\lvert r_{\text{partial}}\rvert \leq 0.111$, all $p \geq 0.138$; condition ANOVA $F = 1.225$, $p = 0.296$	None of the proposed two-wave loop associations is supported.
SyD, Structured	Weekly backlog accumulation and censoring check	slope minimum 0.0143, median 1.719; positive 47/47, positive after trimming 44/47; unresolved 27.1%	Backlog grows in the observed window, but censoring contributes and the sign is not a welfare judgment.
SyD, Structured	Pooled versus within-person loop associations	productive $0.946 \rightarrow 0.118$; overload $0.419 \rightarrow -0.179$; balancing $0.466 \rightarrow -0.108$	Large pooled values primarily reflect stable differences between participants.
Profiles, DS5	Final partition and sensitivity	silhouette 0.290, Jaccard 0.842; drop-feature ARI 0.310–0.506; condition $\chi^2 = 23.61$, $p = 7.5 \times 10^{-6}$	The solution is resampling-stable but overlapping, feature-sensitive, and post-treatment.
Profiles, DS4	Behavioral and network partitions	behavior-only ARI 0.664; network-only ARI 0.047; $\chi^2 = 31.4$, $p < 0.0001$	Low whole-partition agreement can coexist with categorical association.

Table B.1 continued from the previous page.

Family and dataset	Analysis or comparison	Exact reported result	Narrow interpretation
Profiles, DS6	Five-feature partition	silhouette 0.296, Jaccard 0.714; regime-change feature explains 93.4% of between-cluster variation	The supplied binary indicator dominates; no multivariate profile is recovered.
Profiles, Structured	Final and restricted partitions	silhouette 0.213, Jaccard 0.775; behavior-only ARI 1.000; network-only ARI 0.173; Fisher $p = 0.029$	The small solution is behavior-dominated and partly confounded by observation gaps.
Profiles, Structured	Burstiness and backlog growth after the profile sensitivity checks	$\rho = 0.48$, $p = 0.003$	The two summaries remain positively associated, but this does not establish a stable user type.

B.2 Statistical-Mechanics Distribution Diagnostic

The main chapter now uses a cohort comparison to visualize the DS6 result directly. The original pooled histogram is retained here because it shows the strongly skewed participant-level distribution and the high-value tail, although it cannot display the cohort contrast by itself.

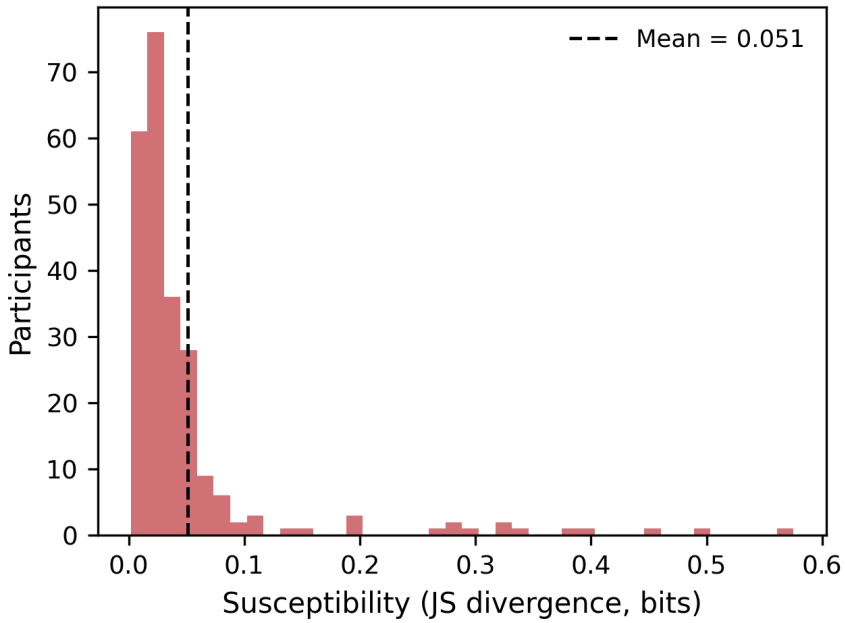


Figure B.1: Pooled distribution of the DS6 participant-level configuration change χ_i of Equation 4.2, the baseline-to-intervention Jensen–Shannon divergence in bits ($N = 238$ participants). The three condition cohorts are combined; Figure 4.2 displays their means separately.

B.3 Dynamical-Systems Diagnostics

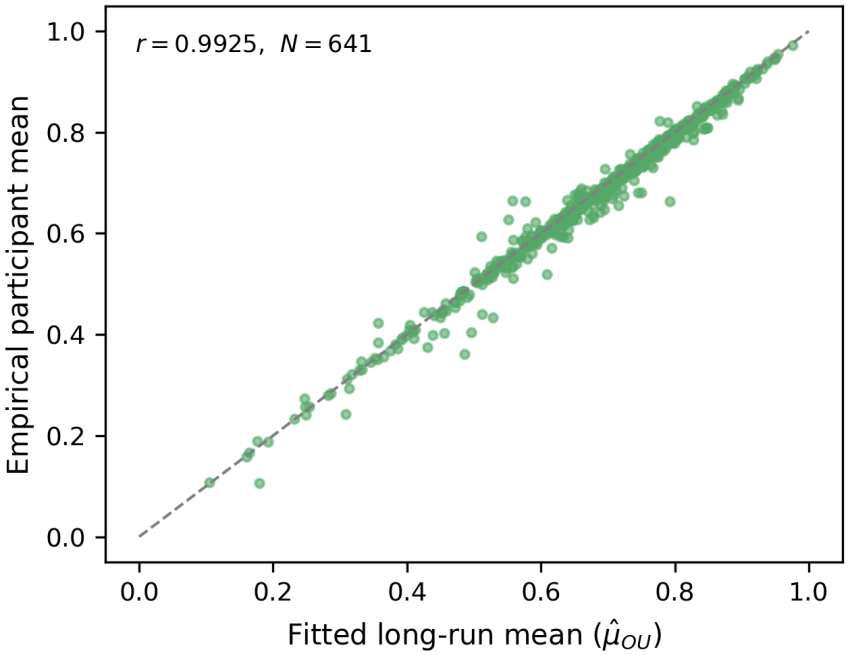


Figure B.2: DS4 fitted long-run mean $\hat{\mu}_{\mathrm{OU}}$ of the mean-reverting specification (Equation 4.9) against the participant's empirical mean daily override proportion ($N = 641$ participants with valid fits). The near-diagonal agreement is algebraic and is reproduced after destroying temporal order; it is not independent attractor validation.

Table B.2: DS6 regime transitions across the original unequal baseline-to-intervention windows ($N = 230$ classified in both periods); 126 (54.8%) retain the same label. The matched-window visualization in Figure 4.5 demonstrates the sensitivity of the destination labels.

	Intervention regime				
Baseline regime	Declining	Low-drift	Growing	Stochastic	Total
Declining	1	16	3	10	30
Low-drift	1	34	3	9	47
Growing	0	19	6	12	37
Stochastic	0	23	8	85	116
Total	2	92	20	116	230

B.4 Stochastic-Process Diagnostics

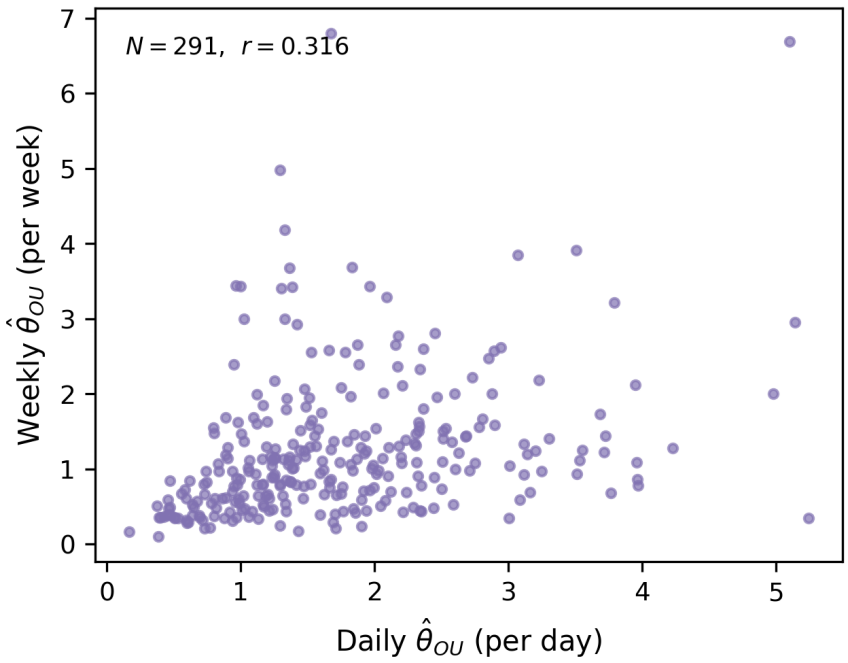


Figure B.3: DS4 relaxation estimates at daily and weekly resolution ($N = 291$ participants with valid fits at both resolutions): the mean-reversion rate $\hat{\theta}_{\mathrm{OU}}$ of Equation 4.9, estimated by AR(1) regression on daily and on weekly data (rates per day and per week). The corresponding observation-process simulation is summarized in Table B.1.

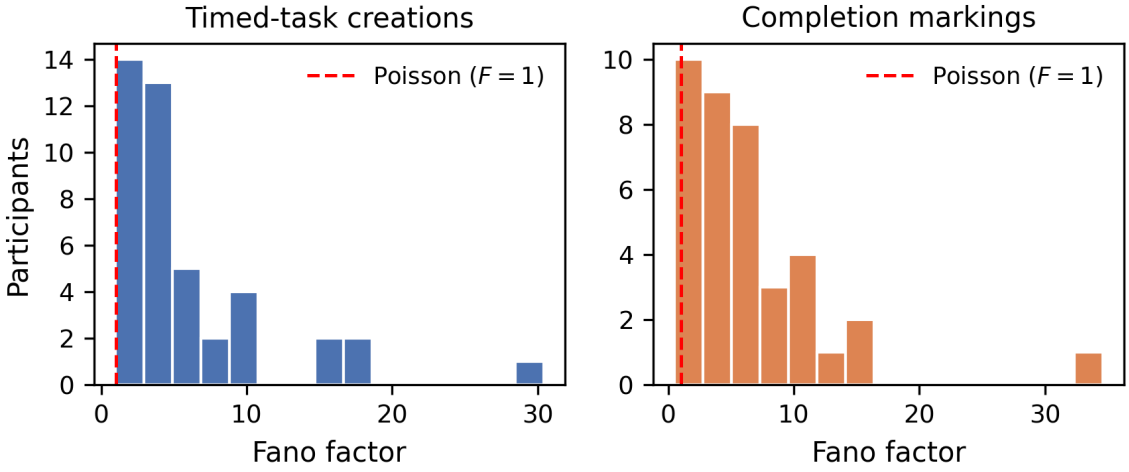


Figure B.4: Per-participant Fano factors $F = \mathrm{Var}(N_t)/\mathbb{E}[N_t]$ of daily counts (Equation 4.11) for timed-task creations ($N = 43$) and completion markings ($N = 38$). $F = 1$ is the Poisson reference, so values above it indicate bursty, overdispersed counts.

B.5 System-Dynamics Statistical Tables

Table B.3: DS6 system-dynamics loop tests. Only the baseline-adjusted partial correlation is treated as evidence; all three tests and the condition-level ANOVA on addiction-index change ($F = 1.225$, $p = 0.296$) are non-significant.

Loop	Behavioral flow	n	r_{raw}	r_{partial}	p_{partial}
1 — pressure reinforcement	mean daily volume (baseline)	180	−0.016	0.057	0.450
1 — pressure reinforcement	drift $\hat{\mu}$ (baseline)	180	−0.088	−0.111	0.138
2 — self-regulation	volume change (int. − base.)	178	0.077	0.093	0.217

Table B.4: The three proposed feedback loops tested pooled and again after person-mean centering. Only the within-participant column is treated as evidence.

Loop	Test	Predicted	Pooled r	Within-person r
Productive	$\text{completed}_w \rightarrow \text{created}_{w+1}$	positive	0.946	0.118
Overload	$B_w \rightarrow \text{created}_{w+1}$	negative	0.419 (opposite sign)	−0.179
Balancing	$B_w \rightarrow \text{reschedules}_w$	positive	0.466	−0.108 (unsupported)

B.6 Profile-Sensitivity Table

Table B.5: DS5 final-specification profile and feature-sensitivity checks. Stability is bootstrap Jaccard; ARI measures membership agreement with the five-feature solution.

Variant	Stability	Interpretation
Final five-feature solution	$J = 0.842$	$k = 2$, $N = 209$, silhouette 0.290
Drop H_{emp}	ARI $= 0.321$	Membership is sensitive to the increment-entropy feature
Drop HHI_{net}	ARI $= 0.506$	Only moderate agreement after removing flow concentration
Drop ρ_{self}	ARI $= 0.310$	Membership is sensitive to the self-transition feature
Add three secondary features	ARI $= 0.652$	Partial agreement with the extended feature set

C

Conceptual Review of the Complex Adaptive Systems Model Families

The main body introduces eight model families and states what each contributes operationally, but it does not develop them formally. This appendix provides that foundation. The models are drawn from mathematical, physical and computational traditions, and are reviewed here in their original conceptual and formal logic rather than in their behavioral translation.
For each family the review sets out the core concept, the theoretical framework, the mathematical basis, the key quantities, a typical implementation, and a core example from physics or from the field in which the model originated. The purpose is to establish the theoretical basis for the transfer without interrupting the shorter argument of the main text. The finalized translation into the two behavioral domains is given in Section 2.3, especially Table 2.2 and Figures 2.1–2.2.
The source material originated as a stand-alone theoretical review. It is integrated here as Sections C.1–C.8 so that the thesis retains one contents hierarchy, continuous page numbering, and one bibliography. The definitions and caveats in the main thesis govern its empirical interpretation across both smartphone use and task-planning behavior.

C.1 Statistical Mechanics (StM)

Core elements Statistical Mechanics (SM), or Statistical Physics, studies systems with many interacting components and seeks to explain macroscopic behavior from microscopic interactions. Rather than following one exact trajectory, it describes a system probabilistically through its possible *microstates*. These microstates are represented in *phase space*, and collections of possible system realizations are treated as *ensembles*. In the thermodynamic limit, fluctuations become small and stable macroscopic regularities emerge. (Netz, 2016)

Theoretical framework The relevant ensemble depends on how the system interacts with its environment. The *microcanonical ensemble* describes an isolated system with fixed energy, volume, and particle number. The *canonical ensemble* describes a system at fixed temperature that may exchange energy with a heat

bath. The *grand canonical ensemble* additionally allows particle exchange and is characterized by temperature and chemical potential. (Gros, n.d.; Netz, 2016)
Statistical-mechanical systems can also be interpreted through *energy landscapes*, in which local or global minima correspond to stable or metastable states and barriers determine how difficult transitions are. Temperature controls how strongly the system explores this landscape. At a critical temperature T_c, many systems undergo a phase transition from ordered to disordered behavior; at such critical points, systems are especially sensitive to perturbations. (Carmichael et al., 2019; Newman, 2010; Tsironis, 2025; Watanabe et al., 2014; Wolschin, 2021)
A further relevant concept is *hysteresis*, where the present state depends not only on current conditions but also on the path by which the system arrived there. This path dependence is important whenever systems retain memory of previous perturbations. (Tsironis, 2025)

Key quantities and formalism The central quantity is the Hamiltonian H, which represents the total energy of a microstate,

$$H(q,p) = T(p) + V(q) \tag{C.1}$$

where q denotes positions, p momenta, $T(p)$ kinetic energy, and $V(q)$ potential energy. Intuitively, the Hamiltonian defines the energy landscape on which the system moves. (Netz, 2016)
In the canonical ensemble, the probability of a state is given by the Boltzmann distribution,

$$P(s) = \frac{e^{-\beta H(s)}}{Z} \tag{C.2}$$

where $P(s)$ is the probability of state s, $\beta = \frac{1}{k_B T}$, k_B is the Boltzmann constant, T is temperature, and Z is the partition function. Intuitively, lower-energy states are more likely, while higher temperature makes the system explore more alternatives. (Gros, n.d.; Watanabe et al., 2014)
For energy levels $E_i(H) = E_i^0 - M_i H$ in an external field H, the partition function is

$$Z(H) = \sum_i e^{-\beta E_i(H)} = \sum_i e^{-\beta(E_i^0 - M_i H)} \tag{C.3}$$

which sums the Boltzmann weights over all states i, where E_i^0 is the zero-field energy of state i, M_i its magnetization, and H the external field. It links microscopic states to macroscopic observables. (Gros, n.d.; "Kapitel 3: Entropie – Statistische Zugänge", n.d.)
From it, the Helmholtz free energy follows as

$$F = -k_B T \ln Z \tag{C.4}$$

where F is the free energy. In equilibrium, systems tend to minimize F, balancing low energy against high entropy. (Gros, n.d.; Netz, 2016)
For equally probable accessible microstates, entropy can be expressed as

$$S = k_B \ln \Omega \tag{C.5}$$

where S is entropy and Ω is the number of accessible microstates. Along a reversible constant-volume path, its temperature dependence can also be written as

$$S(T) = S(0) + \int_0^T \frac{C_V(T')}{T'}\, dT' \tag{C.6}$$

where $C_V(T')$ is the heat capacity at constant volume and $S(0)$ permits residual entropy; additional entropy changes must be included if the path crosses a phase transition. Entropy measures how many different configurations are compatible with the system's macroscopic state. ("Kapitel 3: Entropie – Statistische Zugänge", n.d.; Netz, 2016)
In the canonical ensemble, the total heat capacity at constant volume is related to energy fluctuations by

$$C_V = k_B\beta^2(\langle E^2\rangle - \langle E\rangle^2), \qquad c_V = \frac{C_V}{N} \tag{C.7}$$

where C_V is the total heat capacity, c_V is the heat capacity per particle, N is the number of particles, and $\langle E\rangle$ is the mean energy. Large fluctuations often indicate that the system is near a transition. (Netz, 2016)
The susceptibility

$$\chi = \left(\frac{\partial M}{\partial H}\right)_T \tag{C.8}$$

measures how strongly magnetization M changes in response to an external field H at fixed temperature T. Intuitively, it quantifies how sensitive the system is to perturbation. (Tsironis, 2025)
Macroscopic observables can often be obtained from derivatives of $\ln Z$; for example,

$$\langle M\rangle = \frac{1}{\beta}\frac{\partial \ln Z}{\partial H} \tag{C.9}$$

where $\langle M\rangle$ is the mean magnetization. This shows that collective quantities can be derived from the partition function rather than from tracking every microscopic state directly. (Gros, n.d.)

Core example The prototypical example of statistical mechanics applied to collective behavior is the Ising model. It describes a system of discrete spins $s_i \in \{+1, -1\}$ located on lattice sites, where neighboring spins interact with coupling strength J. The Hamiltonian of the basic Ising model is

$$H = -J\sum_{\langle i,j\rangle} s_i s_j \tag{C.10}$$

(Wolschin, 2021)
Here, s_i denotes the spin state at site i, and J is the coupling constant. For $J > 0$, the model is ferromagnetic and favors aligned spins. The Ising model is important because it captures how local interactions can generate collective order and allows the derivation of a critical temperature T_c at which the system changes from a

disordered paramagnetic phase to an ordered ferromagnetic phase. (Tsironis, 2025; Wolschin, 2021)
The addition of an external field modifies the Hamiltonian to

$$H = -J \sum_{\langle i,j \rangle} s_i s_j - h \sum_i s_i \tag{C.11}$$

where h denotes the external field. (Kawamura, 2010)
Adding the field h transforms the model from a closed symmetric situation into one influenced by external parameters. In energy-landscape terms, this breaks the symmetry between competing states by making one well deeper and therefore more stable than the other. This changes the probabilities of the states and biases the system toward one direction of alignment. (Kawamura, 2010; Wolschin, 2021)

Implementation of StM A statistical-mechanical model is implemented by specifying a Hamiltonian H that defines the microscopic interactions. The key task is then to compute the partition function

$$Z = \sum e^{-\beta H_i} \tag{C.12}$$

where H_i is the energy of microstate i. (Netz, 2016)
From this, the free energy

$$F = -k_B T \ln Z \tag{C.13}$$

can be obtained. Macroscopic observables such as entropy, magnetization, or chemical potential are then derived from partial derivatives of the appropriate thermodynamic potential. Which quantities are fixed depends on the chosen ensemble. (Gros, n.d.; Netz, 2016)

C.2 Dynamical Systems (DyS)

Core elements Dynamical Systems (DyS) describe how a system's state changes over time. More generally, they provide a framework for studying coordinated temporal change in physical, biological, cognitive, and social systems. A central distinction is between *continuous* systems, which evolve continuously in time, and *discrete* systems, which evolve in separate time steps. Deterministic systems produce one trajectory from one initial condition, whereas stochastic variants additionally include noise. (Goodman, 2022; Richardson et al., 2014; Tsironis, 2025)

Theoretical framework Continuous-time systems are typically written as ordinary differential equations, while discrete-time systems are written as iterative maps. Most systems of interest in complex behavior are nonlinear, allowing for qualitatively rich dynamics. Important concepts are *fixed points*, where the system stops changing, and *attractors*, toward which trajectories converge. These may be point attractors, limit cycles, or more complex strange attractors. (Carmichael et al., 2019; Gunesch, 2005; Richardson et al., 2014)

Some deterministic systems exhibit *chaos*, meaning extreme sensitivity to initial conditions. A further key concept is *bifurcation*: a small change in a control parameter can cause a qualitative change in the number, type, or stability of attractors. In behavioral-change settings, such a bifurcation can be interpreted as the point at which enough tension, friction, or force is present for a system to leave a stable habit state and enter a different behavioral regime. (Richardson et al., 2014)

Key quantities and formalism Continuous-time dynamics are commonly written as

$$\frac{dx}{dt} = f(x(t), \mu) \tag{C.14}$$

where $x(t)$ is the state at time t, f defines the update rule, and μ is a control parameter. Intuitively, this equation says that change depends on the current state and on parameters shaping the regime of the system. (Gunesch, 2005)
Discrete-time dynamics are written as

$$f : X \to X, \qquad x_{n+1} = f(x_n) \tag{C.15}$$

where X is the state space, x_n the current state, and x_{n+1} the next state. This formulation is useful when change occurs in steps rather than continuously. (Gunesch, 2005)
A classical physical example is Newtonian mechanics, based on $F = ma$, which can be rewritten as a first-order dynamical system in phase space. For conservative systems, the total energy

$$H(x, v) = E_{kin}(v) + V(x) \tag{C.16}$$

is invariant along trajectories, where x is position, v velocity, $E_{kin}(v)$ kinetic energy, and $V(x)$ potential energy. This means the system moves within a constrained region of state space rather than arbitrarily. Such systems can also be formulated in the Lagrangian framework via the Euler–Lagrange equations. (Gunesch, 2005; Ludde, n.d.)

Core example The most classical physical example of a dynamical system is the Newtonian system of mechanics, based on the relation $F = ma$. Since acceleration is the second derivative of position, Newtonian dynamics can be reformulated as a system of first-order differential equations. Such systems are typically represented in *phase space*, where all relevant variables of the system are combined into a single state-space representation. For a classical mechanical system, this phase space consists of position and momentum coordinates. A phase-space trajectory therefore describes the complete temporal evolution or "living space" of the system, in the sense that only those states lying on the trajectory are dynamically reachable. (Gunesch, 2005; Ludde, n.d.)
In this framework, the total energy of the Newtonian system is given by Eq. C.16. For conservative systems, this total energy is invariant along the orbit, meaning that each trajectory lies on a curve for which H remains constant. (Gunesch, 2005)

Implementation of DyS Common implementations use ODEs and, for spatial models, PDEs. Numerical environments such as Python or Julia usually solve them through integration methods such as Runge–Kutta. (Tsironis, 2025)
In many applications, the goal is not only to compute trajectories but also to identify fixed points and determine their stability. This is done by linearizing the system locally and analyzing the eigenvalues of the Jacobian matrix, which tells us whether small perturbations decay or grow. Probabilistic numerical approaches, such as Gauss–Markov methods, can additionally represent numerical uncertainty. (Hennig et al., 2015; Newman, 2010)

C.3 Stochastic Processes (StoP)

Core elements Stochastic Processes extend deterministic dynamical models by explicitly incorporating randomness. While ODEs produce one trajectory from one initial condition, stochastic processes describe families of possible trajectories for random variables evolving over time. They are therefore useful when systems are partly noise-driven. (Goodman, 2022; Øksendal, 2003; "Stochastische Prozesse I", n.d.)

Theoretical framework A central concept is the *Markov property*, according to which the future depends only on the current state and not on the past history. The fundamental continuous stochastic process is *Brownian motion* or the *Wiener process*, whose increments are independent and normally distributed. For systems with long-range dependence, the Hurst exponent H is used, and processes with $H > 0.5$ are often modeled by *Fractional Brownian Motion*. ("Stochastische Prozesse I", n.d.; Tsai & Hung, 2025)
Because Brownian paths are continuous but non-differentiable, stochastic calculus is required. Two important variants are the *Itô integral* and the *Stratonovich integral*. (Wu, n.d.)

Key quantities and formalism A stochastic process is commonly represented by a random state variable X_t satisfying the SDE

$$dX_t = \mu(X_t)dt + \sigma(X_t)dW_t \tag{C.17}$$

where dX_t is the change in the state over a small time step dt, $\mu(X_t)$ is the drift, $\sigma(X_t)$ the diffusion amplitude, and dW_t the increment of Brownian motion. Intuitively, the drift describes the direction the system tends to move, while the diffusion term determines how widely trajectories spread around that trend. (Goodman, 2022)
The term dW_t can be understood as a random shock with mean zero and variance proportional to dt. Thus, the same initial state can generate many possible trajectories. (Goodman, 2022; Wu, n.d.)
For functions of stochastic processes, *Itô's Lemma* plays the role of the stochastic chain rule:

$$df = \left(\frac{\partial f}{\partial t} + a\frac{\partial f}{\partial x} + \frac{1}{2}b^2\frac{\partial^2 f}{\partial x^2}\right)dt + b\frac{\partial f}{\partial x}dW_t \tag{C.18}$$

where f is a function of the process, $\frac{\partial f}{\partial t}$ is its time derivative, $\frac{\partial f}{\partial x}$ and $\frac{\partial^2 f}{\partial x^2}$ are first and second derivatives with respect to the state variable x, a is the drift term, and b the diffusion term. The extra second-order term is the key correction that distinguishes stochastic from ordinary calculus. (Øksendal, 2003)
An alternative description is the *Fokker–Planck equation*, which tracks the evolution of the probability density rather than individual trajectories. (Tsai & Hung, 2025)

Core example A concrete physical example is sedimentation. Here, a particle in a fluid is influenced by gravity and slowly settles downward. In this case, the drift can be modeled as a constant downward velocity due to gravity, for example $\mu(X_t) = -v_g$, while the diffusion term may be written as $\sigma(X_t) = \sqrt{2D}$, where D is the diffusion coefficient derived from the Einstein relation. The resulting path of the particle can be interpreted as a random walk. (Tsai & Hung, 2025)
This example illustrates the conceptual value of SDEs: deterministic forces and stochastic fluctuations act together. Because noise is included, the model no longer predicts one unique path, but rather a distribution of possible particle trajectories. (Tsai & Hung, 2025)

Implementation of StoP Stochastic models are typically implemented by extending deterministic equations with an explicit noise term. Since analytical solutions are often unavailable, they are usually solved numerically, for example with the Euler–Maruyama method:

$$X_{n+1} = X_n + \mu(X_n)\Delta t + \sigma(X_n)\sqrt{\Delta t}\, Z_n, \qquad Z_n \sim \mathcal{N}(0,1) \tag{C.19}$$

where X_n is the current state, X_{n+1} the updated state, Δt the time step, and Z_n an independent standard-normal random variable. The square root is required because a Brownian increment over a step of length Δt has variance Δt, so it can be represented as $\sqrt{\Delta t}\, Z_n$. (Higham, 2001; Øksendal, 2003)
Because SDE solutions are random, repeated simulation is needed. Monte Carlo methods approximate distributions, mean behavior, and variability across many runs. (Tsai & Hung, 2025)

C.4 Network Theory (NeT)

Core elements Network Theory, or graph theory, studies systems through their pattern of relations rather than the properties of isolated parts. A network is represented as a graph $G = (V, E)$, where vertices V are the entities in the system and edges E are their interactions. Networks may be undirected, directed, or weighted. In this sense, network theory is especially useful when the main question is not what the elements are in isolation, but how their arrangement and interdependence shape the overall system. (Newman, 2010)

Theoretical framework The main aim of network theory is to characterize topology: how a system is organized, how efficiently influence or information can spread,

and which nodes occupy structurally important positions. More generally, the framework allows local interactions to be linked to global organization, studying aspects like clustering, community structure, and small-world effects. For this reason, *centrality* is one of the most important concepts in the framework. These measures are important because they capture different notions of importance; a node can be influential because it is highly connected, because it links otherwise separate clusters, or because it is globally well positioned within the whole system.
As illustrated in Fig. C.1, hubs can be understood as nodes with high centrality, although this importance may take different forms. *Hubs* are highly connected nodes that are often important for transport and resilience, while *leaves* are nodes connected to the rest of the network by only a single edge. Specifically, *degree centrality* is the simplest indicator of local importance, defined as the number of neighbors or direct connections a node has. *Betweenness centrality* identifies nodes that act as bridges or bottlenecks between otherwise weakly connected parts of the network by calculating the proportion of shortest paths that pass through them. *Closeness centrality* captures how near a node is to the rest of the network by measuring how quickly it can potentially access or reach other parts of the system; the more central a node is, the shorter its distance to all other nodes.
Further extending these concepts, *eigenvector centrality* defines importance recursively, whereby a node becomes important when it is connected to other important nodes. *PageRank* is a variant of eigenvector centrality originally used to rank web pages; while conceptually distinct, in undirected graphs it is often statistically similar to degree centrality. Regarding specialized roles, *connector hubs* link different parts of the network, whereas *provincial hubs* are highly central mainly within their own local neighborhood. Finally, the *participation coefficient* describes how a node's connections are distributed across different modules, determining whether it is confined to one community or spans several. (Farahani et al., 2019; Newman, 2010)

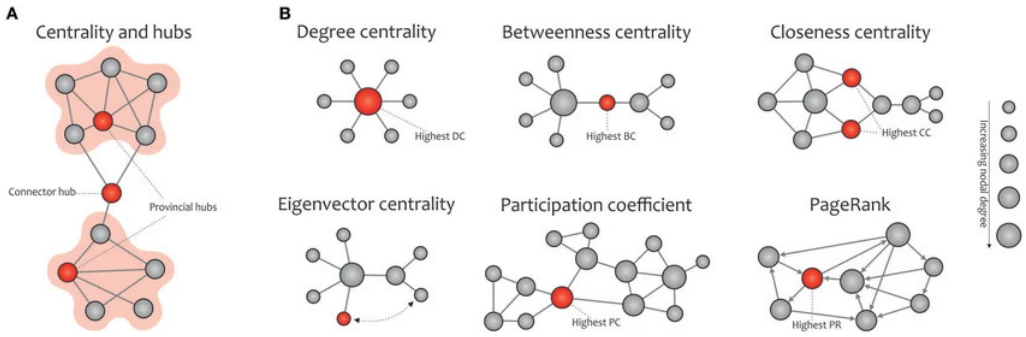


Figure C.1: Graphic illustration of hubs, degree centrality, betweenness centrality, closeness centrality, eigenvector centrality, PageRank, and participation coefficient in a hypothetical network sequence. Reproduced from Farahani et al., 2019, Figure 5 (CC BY 4.0).

Key quantities and formalism Networks are often encoded in an adjacency matrix A, where

$$A_{ij} = \begin{cases} 1, & \text{if there is an edge between vertices } i \text{ and } j, \\ 0, & \text{otherwise.} \end{cases} \tag{C.20}$$

Here, A_{ij} indicates whether nodes i and j are connected. For directed networks, $A_{ij} = 1$ indicates an edge from i to j. This formalism is important because it translates the full network structure into a form that can be analyzed mathematically and computationally. (Newman, 2010)
The degree of a node is

$$k_i = \sum_{j=1}^{n} A_{ij} \tag{C.21}$$

where k_i is the degree of node i and n is the number of nodes. This is one of the most basic and useful quantities because it gives the simplest measure of local importance: how many direct ties a node has. (Newman, 2010)
A second important formal quantity is the graph Laplacian,

$$L = D - A \tag{C.22}$$

where L is the Laplacian, D the diagonal degree matrix, and A the adjacency matrix. Intuitively, L captures how strongly a node differs from its neighborhood, which is why it is useful for studying diffusion, synchronization, and graph partitioning. (Newman, 2010)
Further important structural quantities are the clustering coefficient

$$C = \frac{(\text{number of triangles}) \times 3}{\text{number of connected triples}}, \tag{C.23}$$

where C measures transitivity, that is, the tendency of neighbors to also be connected. In the special case of a scale-free network, the tail of the degree distribution is often modeled as

$$p_k \sim k^{-\alpha}, \tag{C.24}$$

where p_k is the fraction of nodes with degree k and α is the scaling exponent. A power law is not a general property of networks and must be evaluated empirically. These quantities are important because they characterize whether the network is locally cohesive and whether connectivity is spread evenly or concentrated in a small number of hubs. (Newman, 2010)

Core example An empirical example already relevant to this project is the analysis of smartphone "app-journey" networks. In this approach, apps are represented as nodes, while transitions from one app to another within a smartphone usage session are represented as directed, potentially weighted edges. A phone session can therefore be modeled as a graph of behavioral transitions rather than as a simple measure of total screen time. Network descriptors such as density, modularity, and centrality then quantify structural properties of smartphone behavior. (Turner, Gastelum, et al., 2026) In such a model, centrality measures can identify apps that function as behavioral hubs, bottlenecks, or bridges between different usage clusters.

Implementation of NeT Networks are implemented as adjacency matrices or adjacency lists, depending on whether dense or sparse representations are more efficient. Centrality measures are then computed to identify structurally important nodes, and shortest-path methods such as BFS or Dijkstra's algorithm are used when distance-based measures are required. More generally, network analysis allows researchers to move from raw relational data to interpretable descriptors of structure, flow, and behavioral organization. (Newman, 2010)

C.5 Information Theory (InT)

Core elements Information Theory quantifies information and uncertainty in probabilistic terms. The less likely an event is, the more information its occurrence provides. Its core quantity is entropy, which measures uncertainty and is usually expressed in bits. Information gain can therefore be understood as uncertainty reduction after observation. (Daugman, 2020; Jaradat et al., 2025; Jensen et al., 2013; "Kapitel 3: Entropie – Statistische Zugänge", n.d.)
There is also a formal connection to statistical mechanics: Shannon entropy as a measure of uncertainty parallels Boltzmann entropy as a measure of disorder. ("Kapitel 3: Entropie – Statistische Zugänge", n.d.)

Theoretical framework Information Theory addresses how information is represented, compressed, transmitted, and transformed. At a theoretical level, it provides a language for asking how predictable a signal is, how much two signals share, and whether one process reduces uncertainty about another. (Daugman, 2020)
Shannon's Source Coding Theorem defines the lower bound for lossless compression, while the Channel Coding Theorem states that reliable transmission requires source entropy not to exceed channel capacity. More broadly, these ideas show that information is constrained: uncertainty cannot be removed for free, and signals cannot be transmitted arbitrarily well without sufficient capacity. (Daugman, 2020)
For modeling relations between variables, the main concepts are joint entropy, conditional entropy, mutual information, and transfer entropy. Together, these measures move from isolated uncertainty to relational structure: joint entropy captures total uncertainty in a combined system, conditional entropy captures what remains uncertain once another variable is known, mutual information captures shared information, and transfer entropy adds temporal directionality. (Jensen et al., 2013; Witten, 2020)

Key quantities and formalism The Shannon entropy of a random variable X provides a quantitative measure of uncertainty in a signal or behavioral variable. It is defined as

$$H(X) = -\sum_{x \in X} p(x) \log_2(p(x)). \tag{C.25}$$

Here, $p(x)$ is the probability of outcome x. Intuitively, entropy is high when many outcomes are plausible and low when the outcome is predictable. (Jensen et al., 2013)

The joint entropy is

$$H(X,Y) = -\sum_{x,y} p(x,y)\log_2(p(x,y)), \tag{C.26}$$

where $p(x,y)$ is the joint probability of outcomes x and y. It measures the total uncertainty in the combined system of X and Y rather than in each variable separately. The conditional entropy is

$$H(Y|X) = H(X,Y) - H(X), \tag{C.27}$$

which measures the uncertainty remaining in Y once X is known. This is useful when asking how informative one variable is for predicting another. (Jaradat et al., 2025; Witten, 2020)
The mutual information is

$$I(X;Y) = H(X) + H(Y) - H(X,Y). \tag{C.28}$$

It measures how much knowing one variable reduces uncertainty about the other. This makes it especially important in applications because it detects statistical dependence even when relationships are nonlinear and therefore not well captured by correlation alone. (Jensen et al., 2013)
A further useful measure is the Kullback–Leibler divergence,

$$D_{KL}(P||Q) = \sum p_i(\log p_i - \log q_i), \tag{C.29}$$

where P is the true distribution, Q the assumed distribution, and p_i and q_i their probabilities for outcome i. It quantifies how much information is lost when Q is used to approximate P. In practice, this makes it useful for model comparison, surprise, and prediction error. (Witten, 2020)
The quantity

$$H_{\mathrm{SDE}} = \frac{1}{2}\log_2\!\left(2\pi e\,\hat{\sigma}^2\right)$$

is the differential entropy of a Gaussian random variable with variance $\hat{\sigma}^2$, expressed in bits because the logarithm is taken to base 2. It quantifies the uncertainty, or spread, of a *continuous* random variable rather than a discrete one. More specifically, it is the standard entropy formula for a normal distribution

$$X \sim \mathcal{N}(\mu, \sigma^2).$$

For a Gaussian variable, the entropy depends only on the variance and not on the mean μ. Consequently, larger values of $\hat{\sigma}^2$ correspond to a wider distribution and therefore to higher entropy.
A standard reference for this result is *Elements of Information Theory* by Cover and Thomas, where the differential entropy of a Gaussian random variable is given in natural-logarithm form as

$$h(X) = \frac{1}{2}\log\!\left(2\pi e\,\sigma^2\right).$$

Expressing the logarithm in base 2 yields the equivalent entropy in bits,

$$h(X) = \frac{1}{2}\log_2\left(2\pi e\,\sigma^2\right).$$

In the present notation, the hat in $\hat{\sigma}^2$ indicates that the variance is estimated from data rather than known exactly. Accordingly,

$$H_{\mathrm{SDE}} = \frac{1}{2}\log_2\left(2\pi e\,\hat{\sigma}^2\right)$$

should be interpreted as an *estimated Gaussian differential entropy.* (Cover & Thomas, 2006)

Core example A simple illustrative example is a loaded die. If one outcome, such as the number 6, occurs with very high probability, then the result is only weakly surprising and requires relatively little information to describe. The entropy of the system is therefore low, and prediction is comparatively easy. By contrast, if all outcomes are equally likely, uncertainty is maximal and more bits are required on average to specify the result. In this way, entropy directly captures the relationship between uncertainty, predictability, and information content.

Implementation of InT Information-theoretic modeling starts by defining a probability distribution over possible states and estimating the corresponding probability mass function (PMF) from data. These relative frequencies provide the empirical probabilities needed for entropy-based quantities. (Daugman, 2020) The fundamental quantity is Shannon entropy (C.25). (Jensen et al., 2013; "Kapitel 3: Entropie – Statistische Zugänge", n.d.)
Beyond single variables, interaction is analyzed via mutual information, KL divergence, and transfer entropy. Optimization under constraints can be handled with Lagrange multipliers, while coding applications use methods such as Huffman coding. In machine learning, related ideas appear in cross-entropy loss functions. (Daugman, 2020; Jaradat et al., 2025; Witten, 2020)

C.6 Game Theory (GaT)

Core elements Game Theory examines decisions whose outcomes depend on the actions of others. It applies to economic, political, and evolutionary settings as well as to games in the everyday sense. A game specifies players, rules, strategies, outcomes, payoffs, available information, and possible chance events. Players are usually assumed to act rationally to maximize expected utility. (Hotz, 2006; Slantchev, 2005; SmythOS, n.d.-a)

Theoretical framework The main branches are *non-cooperative* and *cooperative* game theory. Normal-form games describe simultaneous choices via payoff matrices, whereas extensive-form games describe sequential decisions via game trees. *Evolutionary Game Theory* extends these ideas to populations in which strategy frequencies change over time. Across these branches, the central issue is strategic stability. (Faigle, 2020; Hotz, 2006; Slantchev, 2005; SmythOS, n.d.-a)

Key quantities and formalism A central solution concept is the Nash equilibrium:

$$u_i(s_1^*, \ldots, s_i^*, \ldots, s_n^*) \geq u_i(s_1^*, \ldots, s_i, \ldots, s_n^*) \tag{C.30}$$

where u_i is the payoff of player i, s_i^* is player i's equilibrium strategy, and s_i is any alternative strategy. Intuitively, no player can improve by unilaterally deviating. (Hotz, 2006)
For mixed strategies, the expected payoff is

$$U_i(\sigma) = \sum_{s \in S} \left(\prod_{j=1}^{n} \sigma_j(s_j) \right) u_i(s). \tag{C.31}$$

Here, $U_i(\sigma)$ is the expected payoff for player i, S is the set of strategy profiles, $\sigma_j(s_j)$ is the probability that player j chooses pure strategy s_j, and $u_i(s)$ is the payoff under profile s. The equation averages payoffs over all possible combinations of strategies. (Slantchev, 2005)
In Evolutionary Game Theory, strategy frequencies evolve according to the replicator equation

$$\dot{x}_i = x_i \left[(Ax)_i - x^T Ax \right], \tag{C.32}$$

where x_i is the proportion of the population using strategy i, $\dot{x}_i$ its rate of change, A the payoff matrix, $(Ax)_i$ the expected payoff of strategy i, and $x^T Ax$ the population's average payoff. Thus, strategies grow when they perform better than average. (Hotz, 2006)
Long-run stability can be formalized through the Evolutionarily Stable Strategy (ESS) conditions. For every mutant strategy $\mu \neq \sigma$, at least one of the following alternatives must hold:

1. $E(\sigma, \sigma) > E(\mu, \sigma)$
2. $E(\sigma, \sigma) = E(\mu, \sigma)$ and $E(\sigma, \mu) > E(\mu, \mu)$

where σ is the resident strategy, μ a mutant strategy, and $E(a, b)$ the payoff of strategy a against strategy b. These alternatives express that a rare mutant cannot successfully invade. (Maynard Smith, 1982)
In cooperative games, stability of joint allocations is captured by the Core:

$$x(N) = v(N) \quad \text{and} \quad x(S) \geq v(S) \quad \text{for all } S \subseteq N. \tag{C.33}$$

Here, N is the grand coalition, $v(N)$ its total value, S any subgroup, $v(S)$ that subgroup's value, and $x(S)$ the payoff assigned to it. The conditions mean that all value is distributed and no subgroup can do better by leaving. (Faigle, 2020)

Core example The Prisoner's Dilemma is the classical example used in game theory because it illustrates the tension between individual and collective rationality. In this game, two suspects are held in separate cells, each facing a classic dilemma: remain silent or confess. If both stay quiet, they receive a light 1-month sentence for a minor charge. If both confess, they each serve 6 months. However, if one betrays the other (defection) by confessing while their partner remains silent, the confessor is released immediately while the silent partner serves 1 year. (Slantchev, 2005)

The dilemma lies in the fact that, from the perspective of each individual player, defection is the dominant strategy, because it yields a better payoff regardless of the other player's action. However, if both players follow this individually rational logic, they reach an outcome that is collectively worse than mutual cooperation. The Prisoner's Dilemma therefore demonstrates that rational individual choice does not necessarily lead to socially optimal outcomes. (Agrawal & Jaiswal, 2012)
In iterated versions of the game, where the same players interact repeatedly, the simple *Tit-for-Tat* strategy has proven particularly successful. This strategy starts by cooperating and then copies the opponent's previous move in each subsequent round. Although Tit-for-Tat may lose in an individual round, it performs very well over the long run because it fosters cooperation while remaining resistant to exploitation. This illustrates that the success of a strategy depends strongly on the temporal and structural context in which the game is played. (Smith & Conrey, 2007)

Implementation of Game Theory Depending on the setting, games are solved by best-response analysis, backward induction, linear programming, or numerical fixed-point methods. In more complex systems, game-theoretic rules can also be embedded in Agent-Based Models or adaptive frameworks such as reinforcement learning. (Faigle, 2020; Hotz, 2006; SmythOS, n.d.-a)

C.7 Agent-Based Modeling (ABM)

Core elements Agent-Based Modeling (ABM) represents a system as a collection of autonomous interacting agents and studies how macro-level patterns emerge from micro-level behavior. Agents are typically characterized by autonomy, heterogeneity, local interaction, and bounded rationality. (Borrill & Tesfatsion, 2011; Smith & Conrey, 2007; SmythOS, n.d.-b)

Theoretical framework ABM is especially useful when system behavior cannot be derived analytically and must instead be explored by simulation. The model is built bottom-up: collective structure is not imposed but emerges from repeated local interactions. Simple rules can therefore generate unintended large-scale outcomes. (Borrill & Tesfatsion, 2011; Smith & Conrey, 2007)
ABMs are usually rule-based and may incorporate concepts such as social opinion dynamics, behavioral thresholds, or social learning. (Torren-Peraire et al., 2024)

Key quantities and formalism Unlike differential-equation models, ABMs are usually not defined by one global equation. Their formal structure lies in the specification of agents, states, environments, and update rules. The environment may be represented as a grid, spatial landscape, or network, and random-number seeds are often part of the formal setup because the model is typically stochastic. In intuitive terms, the "mathematics" of ABM lies in explicitly defining who interacts with whom, under what rules, and how those local updates accumulate into collective patterns. (Borrill & Tesfatsion, 2011)

Core example A core example of ABM is the emergence of residential segregation from simple individual rules. If agents follow a local decision rule such as relocating whenever too many neighbors differ from them, this can generate highly segregated spatial patterns at the macro level, even though each individual agent follows only a simple and locally motivated rule. This illustrates the central logic of ABM: complex collective outcomes can emerge from simple decentralized decision processes without requiring any global planner or collective intention. (Borrill & Tesfatsion, 2011; Smith & Conrey, 2007)

Implementation of ABM ABM implementation begins with a theoretical question, followed by construction of a digital environment and specification of agent attributes, behavioral rules, and initial conditions. The model is then simulated over many time steps and repeated across random seeds to generate a distribution of outcomes. Validation often relies on comparing emergent macro-patterns with empirical data, and results are commonly inspected through visualizations such as spatial plots or heatmaps. (Borrill & Tesfatsion, 2011; Carmichael & Hadžikadić, 2019; Macal & North, 2010)

C.8 System Dynamics (SyD)

Core elements System Dynamics (SyD) is a top-down modeling approach for understanding how system-wide behavior emerges over time from stocks, flows, and feedback loops. In contrast to ABM, it focuses on aggregate structure rather than individuals and adopts an endogenous perspective in which dynamics arise primarily from the system's internal organization. (Roy, 2007; SmythOS, n.d.-b)

Theoretical framework The main conceptual tools are *Causal Loop Diagrams* for qualitative feedback structure and *Stock and Flow Diagrams* for quantitative modeling. Stocks are accumulations, flows are rates of change, and feedback loops may be reinforcing or balancing. Their interaction can generate growth, saturation, oscillation, and collapse. Nonlinearity is often represented through table or policy functions. (Parkinson et al., 2025; Richardson et al., 2014; Roy, 2007)

Key quantities and formalism System Dynamics models are commonly written as integral or differential equations. A stock evolves as

$$Stock(t) = \int_{t_0}^{t} [\text{Inflows}(s) - \text{Outflows}(s)]\, ds + \text{Stock}(t_0) \tag{C.34}$$

where $Stock(t)$ is the amount accumulated at time t, $Stock(t_0)$ the initial amount at time t_0, and Inflows(s) and Outflows(s) the rates entering and leaving the stock at time s. Intuitively, a stock is like a reservoir whose level changes as inflows and outflows accumulate over time. (Kunc, 2016)
Equivalently, change can be written as

$$\frac{dX}{dt} = (F_{gen} + F_{in}) - (F_{des} + F_{out}) \tag{C.35}$$

where X is the stock, F_{gen} and F_{in} are internally generated and incoming flows, and F_{des} and F_{out} are destructive and outgoing flows. This formalizes the idea that behavior is produced by the balance of reinforcing and balancing processes. (Kunc, 2016; Teose et al., 2011)

Core example A typical System Dynamics representation models a system in terms of interacting stocks and flows, for example a population stock that increases through births and decreases through deaths, or a financial stock that increases through income and decreases through expenditure. In such cases, the central analytical question is not the behavior of individual actors, but how the overall internal feedback structure generates the observed macro-level dynamics over time. In this sense, System Dynamics is especially suited for explaining system-wide growth, stabilization, and policy-sensitive change through endogenous structure. (Kunc, 2016; Roy, 2007)

Implementation of SyD System Dynamics models are built by first conceptualizing the problem, then translating feedback hypotheses into stock-and-flow structures and equations. Because closed-form solutions are rare, they are usually solved numerically with iterative integration methods such as Euler or Runge–Kutta. Model evaluation typically examines whether the internal feedback structure reproduces known temporal patterns and how sensitive results are to parameter changes. (Kunc, 2016; Roy, 2007; Teose et al., 2011; Tsironis, 2025)

DEPARTMENT OF PHYSICS AND ASTRONOMY
CHALMERS UNIVERSITY OF TECHNOLOGY
Gothenburg, Sweden
www.chalmers.se



CHALMERS
UNIVERSITY OF TECHNOLOGY